

**Design, Synthesis, and Evaluation of Novel, Multifunctional
Dimethyltyrosine-Tetrahydroisoquinoline Opioid Peptidomimetics**

by

Deanna Montgomery

A dissertation submitted in partial fulfillment
of the requirements for the degree of
Doctor of Philosophy
(Medicinal Chemistry)
in The University of Michigan
2019

Doctoral Committee:

Professor Henry I. Mosberg, Chair
Associate Professor Emily M. Jutkiewicz
Professor Scott D. Larsen
Associate Professor Peter J. H. Scott

Deanna Montgomery

dmontg@umich.edu

ORCID iD: [0000-0002-6181-3131](https://orcid.org/0000-0002-6181-3131)

© Deanna Montgomery 2019

Acknowledgments

I am immensely grateful to the countless people who directly and indirectly impacted this work, which was completed at times in isolation but never without a community of support. I cannot express gratitude enough to these people who inspired, encouraged, enabled, and endured my journey to and through graduate school.

To Chris Schweiger who helped me discover my love of chemistry, to Karen Torraca and John Rowley who fostered it, and to Mark Kurth who gave me my first taste of medicinal chemistry and changed my mind about graduate school:

To Hank Mosberg who took a chance on me and provided an environment for me to rediscover the love of medicinal chemistry that I was afraid I had lost, whose unceasing support, guidance, and positivity were paramount to the completion of this journey:

To my carefully chosen dissertation committee members – Emily Jutkiewicz, Scott Larsen, and Peter Scott – whose insights, advice, and support shaped both my work and my development as a scientist:

To the others who contributed scientifically to this work, both directly – Mason Baber, Ira Pogozeva, John Traynor, Jess Anand, Nick Griggs, Thomas Fernandez, Josh Hartman, Ashley Sanchez-Santiago, Jack Twarozynski, Lennon DeLong, Ashley Brinkel, and others – and indirectly – Kate Kojiro, Larisa Yeomans, Tony Nastase, Sean Henry, Jeff Zwicker, Evan Schramm, and others – for their assistance with idea generation, data collection and analysis, and seemingly endless troubleshooting:

To the American Chemical Society Division of Medicinal Chemistry Pre-doctoral Fellowship, the American Foundation for Pharmaceutical Education Pre-doctoral Fellowship, and Rackham Graduate School for financial support:

To the innumerable others whose behind-the-scenes work made every day of this work possible:

To Dave Rogawski, Nicole Michmerhuizen, Joe Iafrate, Chris Wahl, Ryan Hayes, Heather George, Cherie Dotson, George Garcia, and others who provided personal and professional advice and support in a time of transition, without which I would not have completed this journey:

To my RELATE family - Elyse, Brandon, Stephanie, Joe, Nick, Patsy, Isabel, and Fatima – from whom I have learned much and among whom I have found true belonging and community:

To Graduate Christian Fellowship, Zion Lutheran Church, George and Mary Lindquist, and the other groups and people who provided community, fellowship, and friendship which made this undertaking bearable:

To my parents who, for me and from me, have learned much about both chemistry and the doctoral process, whose never-ending love and support surrounded me every step of the way:

To many, many other family members, friends, colleagues, and mentors, without whom none of this would have been possible:

I offer my deepest and sincerest thanks.

Table of Contents

Acknowledgements	ii
List of Figures	vi
List of Schemes	vii
List of Tables	ix
List of Abbreviations	xi
Abstract	xiv
Chapter 1: Introduction	1
1.1 History of Opioids	1
1.2 Opioid Receptors	3
1.2.1 Discovery	3
1.2.2 Structure	4
1.2.3 Function	7
1.3 Opioid Ligands	9
1.3.1 Endogenous Opioid Ligands	9
1.3.2 Selective Opioid Ligands	10
1.3.3 Multifunctional Opioid Ligands	10
Chapter 2: Introduction of Substitution on the Tetrahydroisoquinoline Aromatic Ring of Dimethyltyrosine-Tetrahydroisoquinoline Opioid Peptidomimetics	13
2.1 Introduction	13
2.2 Benzyl Scan Around the Tetrahydroisoquinoline Aromatic Ring	16
2.3 Substituted 7-Benzyl Pendant Analogues	19
2.4 Conclusions	24
Chapter 3: Further Exploration of the Structure-Activity Relationships of 7-Substituted Dimethyltyrosine-Tetrahydroisoquinoline Opioid Peptidomimetics	26
3.1 Introduction	26
3.2 Substituted 7-Benzyl Pendant Analogues	28

3.3	Pyridyl 7-Position Pendant Analogues	33
3.4	Aliphatic 7-Position Pendant Analogues	34
3.5	Naphthyl 7-Position Pendant Analogues	34
3.6	Nitrogen Scan of 7-Position 1-Naphthyl Pendant	36
3.7	Bicyclic Aliphatic 7-Position Pendant Analogues	38
3.8	Conclusions	40
Chapter 4: Exploration of Non-Pendant Regions of Dimethyltyrosine-Tetrahydroisoquinoline Opioid Peptidomimetics		42
4.1	Introduction	42
4.2	Substitution of Dimethyltyrosine with Tyrosine	42
4.3	Exploration of Linker Length in 7- and 8-Substituted Analogues	45
4.4	Carbonyl-Containing Linker Modifications	49
4.5	Aniline Linker Analogue	53
4.6	Conclusions	55
Chapter 5: Conclusions and Future Directions		57
5.1	Summary	57
5.2	Additional Analogues	59
5.3	Combination of Substitution at the 3-Position and 7-Position of Tiq	62
5.4	Future <i>in Vivo</i> Testing	62
5.5	Conclusion	63
Chapter 6: Experimental Section		64
6.1	Chemistry	64
6.1.1	General Procedures	65
6.1.2	Procedures and Characterization for Compounds Contained in Chapter 2	69
6.1.3	Procedures and Characterization for Compounds Contained in Chapter 3	86
6.1.4	Procedures and Characterization for Compounds Contained in Chapter 4	115
6.2	<i>In Vitro</i> Pharmacology	132
6.3	Computational Modeling	134
References		136

List of Figures

Figure 1. Stages of the Opium Poppy	1
Figure 2. Structure of Morphine	2
Figure 3. Structures of Ketocyclazocine and SKF-10,047	4
Figure 4. Comparison of Tertiary Structure of the Opioid Receptors	6
Figure 5. Illustration of GPCR-mediated G protein activation	8
Figure 6. Structures of Leu- and Met-enkephalin	10
Figure 7. Drug Cocktail vs. Bivalent Ligand vs. Multifunctional Ligand	12
Figure 8. Structure of TIPP[ψ]	14
Figure 9. Dimethyltyrosine-Tetrahydroisoquinoline Carboxylic Acid Scaffold	14
Figure 10. Dimethyltyrosine-Tetrahydroisoquinoline Scaffold	15
Figure 11. Compounds 4a , 4b , and 4c Docked in the KOR Orthosteric Site	19
Figure 12. Compounds 7a , 7d , and 7g Docked in the KOR Orthosteric Site	24
Figure 13. Structure of Proposed Acetylated Aniline Analogue	59
Figure 14. Structures of Proposed Heterocyclic Bicycle Pendant Analogues	60
Figure 15. Structures of Proposed Two-Carbon Linker Analogues	61
Figure 16. Structures of Proposed Unsaturated Two-Carbon Linker Analogues	61
Figure 17. Structures of Proposed Heteroatom Linker Analogues	61
Figure 18. Structures of Proposed 3- and 7-Substituted Analogues	62

List of Schemes

Scheme 1. Synthesis of Benzyl Pendant Dmt-Tiq Analogues 4a-4d	17
Scheme 2. Synthesis of Substituted 7-Benzyl Pendant Dmt-Tiq Analogues 7a-7f and 7h	20
Scheme 3. Synthesis of Substituted 7-Benzyl Pendant Dmt-Tiq Analogues 7g and 7i	21
Scheme 4. Synthesis of 7-Substituted Dmt-Tiq Analogues 12a-12z	30
Scheme 5. Synthesis of Tyrosine Analogues 13a-13d	43
Scheme 6. Synthesis of 7-Phenyl and 7-Phenethyl Pendant Dmt-Tiq Analogues 15a and 15b	46
Scheme 7. Synthesis of 8-Phenyl and 8-Phenethyl Pendant Dmt-Tiq Analogues 17a and 17b	47
Scheme 8. Synthesis of Amide Linker 7-Substituted Dmt-Tiq Analogue 18	50
Scheme 9. Synthesis of Amide Linker 7-Substituted Dmt-Tiq Analogue 23	51
Scheme 10. Synthesis of Ketone Linker 7-Substituted Dmt-Tiq Analogues 25a-25d	51
Scheme 11. Synthesis of Aniline Linker 7-Substituted Dmt-Tiq Analogue 28	54
Scheme 12. Synthesis of 4a-4d	69
Scheme 13. Synthesis of 7a-7f and 7h	75
Scheme 14. Synthesis of 7g and 7i	83
Scheme 15. Synthesis of 12a-12z	86
Scheme 16. Synthesis of 13a-13d	115

Scheme 17. Synthesis of 15a and 15b	118
Scheme 18. Synthesis of 17a and 17b	120
Scheme 19. Synthesis of 19	123
Scheme 20. Synthesis of 23	124
Scheme 21. Synthesis of 25a-25d	126
Scheme 22. Synthesis of 28	130

List of Tables

Table 1. Binding, Potency, and Efficacy Data for Benzyl Pendant Dmt-Tiq Analogues 4a-4d	18
Table 2. Binding, Potency, and Efficacy Data for Substituted 7-Benzyl Pendant Dmt-Tiq Analogues 7a-7i	22
Table 3. Comparison of Pharmacological Data for 4c at Rat and Human Opioid Receptors	28
Table 4. Binding, Potency, and Efficacy Data for Substituted 7-Benzyl Pendant Dmt-Tiq Analogues 12a-12i	32
Table 5. Binding, Potency, and Efficacy Data for Pyridyl 7-Position Pendant Dmt-Tiq Analogues 12j and 12k	33
Table 6. Binding, Potency, and Efficacy Data for Aliphatic 7-Position Pendant Dmt-Tiq Analogues 12l-12n	34
Table 7. Binding, Potency, and Efficacy Data for Naphthyl 7-Position Pendant Dmt-Tiq Analogues 12o and 12p	36
Table 8. Nitrogen Scan of 7-Position 1-Naphthyl Pendant on the Dmt-Tiq Scaffold: Binding, Potency, and Efficacy Data for Analogues 12q-12v	38
Table 9. Binding, Potency, and Efficacy Data for Bicyclic Aliphatic 7-Position Pendant Dmt-Tiq Analogues 12w-12z	40
Table 10. Substitution of Dimethyltyrosine with Tyrosine in Benzyl Pendant Dmt-Tiq compounds: Binding, Potency, and Efficacy Data for Analogues 13a-13d	45
Table 11. Modification of Linker Length in 7-Substituted Dmt-Tiq Compounds: Binding, Potency, and Efficacy Data for Analogues 15a and 15b	48
Table 12. Modification of Linker Length in 8-Substituted Dmt-Tiq Compounds: Binding, Potency, and Efficacy Data for Analogues 17a and 17b	49

Table 13. Binding, Potency, and Efficacy Data for Amide Linker 7-Substituted Dmt-Tiq Analogues 19 and 23	52
Table 14. Binding, Potency, and Efficacy Data for Ketone Linker 7-Substituted Dmt-Tiq Analogues 25a-25d	53
Table 15. Binding, Potency, and Efficacy Data for Aniline Linker 7-Substituted Dmt-Tiq Analogue 28	55

List of Abbreviations

[³⁵S]GTPγS	[³⁵ S]guanosine 5'-O-[γ-thio]triphosphate
6Cl-HOBt	1-hydroxy-6-chloro-benzotriazole
BCA	bicinchoninic acid
BH₃ SMe₂	borane dimethylsulfide
BINAP	2,2'-bis(diphenylphosphino)-1,1'-binaphthyl
Bn	benzyl
Boc	tert-butyloxycarbonyl
Boc₂O	di-tert-butyl dicarbonate
Boc-Tyr-OH	Boc-protected L-tyrosine
Br	bromo
CBr₄	carbon tetrabromide
CD₃OD	deuterated methanol
CDCl₃	deuterated chloroform
CH₃CO₂K	potassium acetate
CHO	Chinese hamster ovary
clogP	calculated partition coefficient
DAMGO	[D-Ala ² ,N-MePhe ⁴ ,Gly-ol]enkephalin
DCM	dichloromethane
diBoc-Dmt	di-Boc-protected 2',6'-dimethyl-L-tyrosine
DIEA	diisopropylethylamine
DMEM	Dulbecco's Modified Eagle's Medium
DMF	dimethylformamide
DMSO	dimethylsulfoxide
Dmt	2',6'-dimethyl-L-tyrosine
Dmt-Tic	Dimethyltyrosine-tetrahydroisoquinoline carboxylic acid
Dmt-Tiq	Dimethyltyrosine-tetrahydroisoquinoline
dns	does not stimulate
DOR	delta opioid receptor
DPDPE	[D-Pen ² ,D-Pen ⁵]enkephalin
EC₅₀	half maximal effective concentration

EDTA	ethylenediaminetetraacetic acid
GDP	guanidine diphosphate
GPCR	G protein-coupled receptor
GTP	guanidine triphosphate
HCl	hydrochloric acid
HEPES	4-(2-hydroxyethyl)-1-piperazineethanesulfonic acid
HPLC	high performance liquid chromatography
HRMS	high resolution mass spectrometry
K₂CO₃	potassium carbonate
KH₂PO₄	monosodium phosphate
K_i	inhibitory constant
KOR	kappa opioid receptor
LC-MS	liquid chromatography-mass spectrometry
Me	methyl
MgCl₂	magnesium chloride
MOR	mu opioid receptor
Na₂HPO₄	disodium phosphate
NaCl	sodium chloride
NaOtBu	sodium tert-butoxide
nd	no data
NH₄Cl	ammonium chloride
NMR	nuclear magnetic resonance
Pd(dppf)Cl₂	bis(diphenylphosphino)ferrocene]palladium(II) dichloride
Pd₂(dba)₃	Tris(dibenzylideneacetone)dipalladium(0)
PDB	Protein Data Bank
Phe	L-phenylalanine
PPh₃	triphenylphosphine
PyBOP	(benzotriazol-1-yl-oxytripyrrolidinophosphonium hexafluorophosphate)
SAR	structure-activity relationships
SEM	standard error of the mean
S_N2	bimolecular nucleophilic substitution
TFA	trifluoroacetic acid
THF	tetrahydrofuran
Tic	1,2,3,4-tetrahydroisoquinoline carboxylate
TIPP[ψ]	H-Tyr-Tic-psi[CH ₂ NH]Phe-Phe-OH

Tiq	1,2,3,4-tetrahydroisoquinoline
Tris	Tris(hydroxymethyl) aminomethane
Tyr	L-tyrosine
U69,593	(+)-(5 α ,7 α ,8 β)-N-Methyl-N-[7-(1-pyrrolidiny)-1-oxaspiro[4.5]dec-8-yl]-benzeneacetamide
UV	ultraviolet
Zn	zinc

Abstract

The opioid receptors modulate a wide variety of physiological and behavioral functions, including pain, mood, and reward. There are three main types of opioid receptors – kappa (KOR), mu (MOR), and delta (DOR), and many agonists and antagonists for these receptors have been developed. Because of the complex pharmacology of this system, selective opioid ligands have limited therapeutic potential; however, multifunctional opioid compounds, those which act simultaneously at more than one type of receptor, have shown clinical promise. It has been well-demonstrated that minor changes in the chemical structure of an opioid ligand can result in drastic changes in the associated pharmacological profile. Therefore, selective opioid scaffolds represent a rational starting point for the development of multifunctional opioid ligands. The dimethyltyrosine-tetrahydroisoquinoline (Dmt-Tiq) scaffold is well-known in the creation of DOR antagonist selective peptides, and many such compounds have been reported. However, the constraints of traditional peptide synthesis have limited the exploration of chemical space surrounding the tetrahydroisoquinoline (Tiq) core. This work reports the repurposing of this classically DOR selective scaffold in the creation of novel, multifunctional opioid peptidomimetics through the introduction of previously unexplored modifications. Installation of a 7-benzyl pendant on the Tiq aromatic ring introduced KOR agonism. Further exploration of the structure-activity relationships surrounding this pendant resulted in the development of compounds which exhibit a variety of multifunctional profiles. Ortho and meta substitution on the 7-benzyl pendant

or replacement of the benzyl ring with a bicyclic ring that mimics 1-naphthyl resulted in a KOR agonism and MOR partial agonism. This profile is being explored in the development of a treatment for cocaine addiction, for which there is currently no available therapeutic. Other modifications, including a tetrahydroisoquinoline or isoindoline pendant at the 7-position or replacement of the pendant linker with an aniline, led to a MOR agonist/DOR antagonist profile, which has potential for use as a treatment for pain with lower addiction potential than conventional opioids. Ultimately, the work presented here describes a library of novel Dmt-Tiq opioid peptidomimetics which display a variety of pharmacologically useful multifunctional profiles.

Chapter 1

Introduction

1.1 History of Opioids

“If the entire materia medica at our disposal were limited to the choice and use of only one drug, I am sure that a great many, if not the majority, of us would choose opium...”

-David I. Macht, Johns Hopkins University, 1915¹

Opioids have one of the longest known histories of any drug class. Medicinal, ritual, and/or recreational use of opium, a milky white substance derived from the poppy plant, *papaver somniferum*, (Figure 1) dates back to ancient Mesopotamia (circa 3400 BC). The Sumerians named the substance *gil* (“joy”) and the plant *hul gil* (“joy plant”), presumably as a result of opium’s euphoric effects. Over the next several thousand years, opium use spread throughout the known world - to Egypt, Greece, Persia, India, and eventually China, Europe, and the United States.²⁻⁴

Figure 1. Stages of the Opium Poppy

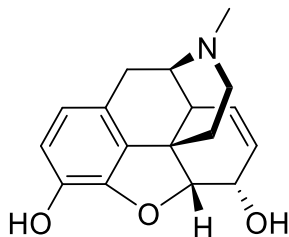


The three stages of *papaver somniferum*, the opium poppy – bud, flower, capsule (left to right)

This image by Alvesgaspar is licensed under [CC BY-SA 3.0](https://creativecommons.org/licenses/by-sa/3.0/).

In the early 1800s, Friedrich Wilhelm Adam Sertürner, a German pharmacist, isolated the primary active ingredient of opium (Figure 2). He named the substance morphine, after the Greek god of dreams, Morpheus, because of the observation that it caused sleep.² In 1827, Merck began commercial manufacture and sale of morphine, which was hailed as a miracle drug.⁵ The invention of the hypodermic needle by Alexander Wood in the 1850s gave morphine a further boost in popularity and dramatically transformed the medical field. Injections of morphine became known as “God’s Own Medicine,” and the drug became a medical mainstay, prescribed widely to treat pain, insanity, morning sickness, and a host of other conditions.⁴

Figure 2. Structure of Morphine



Chemical structure of morphine, the primary active ingredient of opium

It was not long, however, before doctors and patients came to realize the addictiveness of this wonder drug. The aftermath of widespread morphine use for treatment of battlefield ailments during the U.S. Civil War lent morphine addiction the nickname “soldier’s disease.”⁴ Opium and morphine addiction fueled the search for a non-addictive alternative and drove the discovery and development of new opioids as both therapeutics and chemical tools. As clinicians have sought new, less addictive treatments for pain, scientists have explored the mechanisms behind these drugs, ultimately leading to the booming field of modern opioid research.

1.2 Opioid Receptors

Widespread medicinal and recreational use of opium and morphine eventually led to mechanistic research that enabled discovery of the opioid receptors. Ever since, the opioid system has been intensely studied, and many biological functions of these receptors have been determined.

1.2.1 Discovery

“There is a long history of receptors in pharmacology, going back over a century, but the opiates were unique in that their receptor was identified without a known endogenous ligand.”

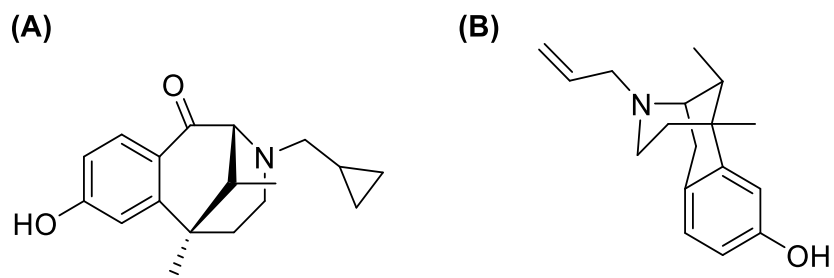
-Gavril W. Pasternak, Memorial Sloan-Kettering Cancer Center, 2014⁶

The existence of specific recognition sites in the brain for morphine and its analogues was widely accepted nearly a decade prior to biochemical evidence for the opioid receptors, due in part to the clear structure-activity relationships of the morphinan scaffold.^{7,8} In 1971, Goldstein et al. reported a method for measuring specific binding of radiolabeled levorphanol, an opioid agonist, in the presence of nonspecific interactions in brain tissue.⁹ Building on this work, three groups independently reported the first biochemical evidence for the existence of opioid receptors in 1973.^{10–12} Shortly following this evidence for opioid receptors came the discovery of endogenous opioid ligands.

The known existence of multiple endogenous opioids (see Section 1.3.1) led to postulation that more than one type of opioid receptor might exist.² In 1976, Martin et al. provided the first evidence for this assumption. By studying the physical and behavioral effects of morphine, ketocyclazocine, and SKF-10,047 administration on dogs, they identified three different receptors on which they believed these drugs to act. Two of these receptors, mu and kappa – named for the drugs used in the study which led to their initial discovery, *Morphine* and *Ketocyclazocine* (Figure 3) – are still recognized as

opioid receptors, while the third – sigma (SKF-10,047) is not.¹³ Later, knowledge of endogenous enkephalins led to identification of the third opioid receptor, delta – named for the inhibition of contractions in the mouse vas *Deferens* which led to its discovery.¹⁴ More recent work has focused on the elucidation of multiple opioid receptor subtypes, which have been proposed for decades, but existence of the three main opioid receptor types – the mu opioid receptor (MOR), the kappa opioid receptor (KOR), and the delta opioid receptor (DOR) – is uncontested.^{6,15}

Figure 3. Structures of Ketocyclazocine and SKF-10,047



(A) Chemical structure of ketocyclazocine (B) Chemical structure of SKF-10,047

1.2.2 Structure

“Recent opioid receptor crystal structures provide unprecedented molecular details of opioid ligand binding and specificity... there is still much to be learned about opioid receptor structure and dynamics before we can fully understand the molecular mechanisms underlying opioid function.”

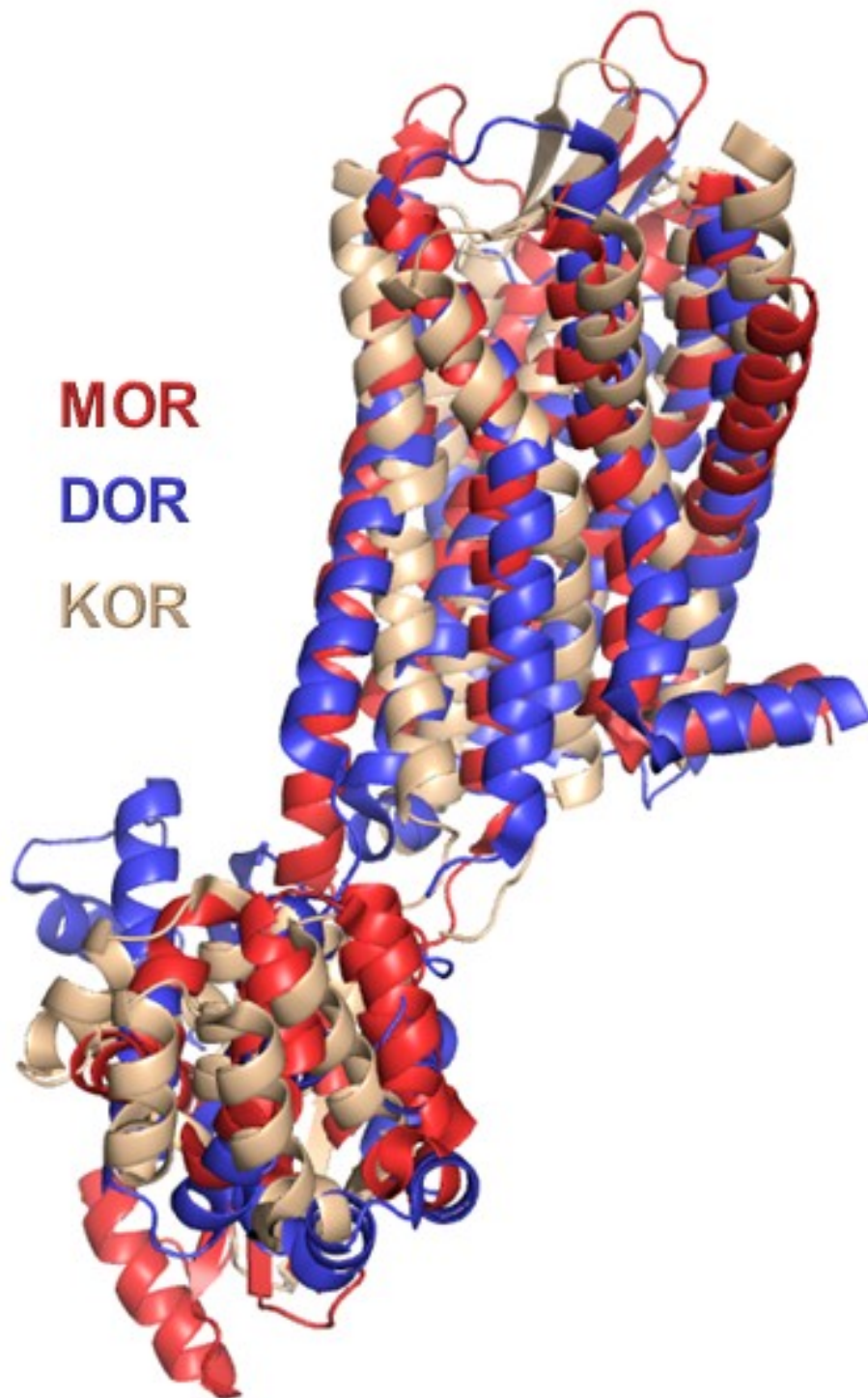
-Marta Filizola and Lakshmi A. Devi, Mount Sinai School of Medicine, 2013¹⁶

Despite the evidence for multiple opioid receptors, the structure of these receptors remained unknown until the 1990s. In 1992, two groups independently reported the cloning of cDNAs encoding the delta opioid receptor.^{17,18} This work revealed high sequence homology between DOR and other G protein-coupled receptors (GPCRs). Further work confirmed that all three opioid receptors are Class A GPCRs, characterized by seven transmembrane helices with an extracellular N-terminus and intracellular C-terminus. The three opioid receptors display 55-60% sequence identity

with closest homology within the transmembrane portion of the receptors which contains the orthosteric binding site.^{15,19}

Prior to the availability of crystal structures for the opioid receptors, homology models based on similar rhodopsin family GPCRs were commonly used.²⁰ In 2012, the first crystal structure was reported for each of the opioid receptors (KOR, PDB ID:4DJH;²¹ MOR, PDB ID:4DKL;²² DOR, PDB ID:4EJ4²³). A 2014 paper by Fenalti et al. which reported a high resolution crystal structure of DOR bound to naltrindole (PDB ID:4N6H) provided the first clear evidence in support of an allosteric sodium binding site, which had been suggested for decades.²⁴ To date, in addition to these antagonist-bound crystal structures, agonist-bound structures have been solved for KOR (PDB ID:6B73²⁵) MOR (PDB ID:5C1M²⁶). These structures are used extensively to study structural features of the opioid receptors and represent valuable tools in the structure-based design of opioid ligands.¹⁶

Figure 4. Comparison of Tertiary Structure of the Opioid Receptors



Comparison of the similar tertiary structure of the three major opioid receptors – MOR (red), DOR (blue), KOR (wheat) – based on the first reported crystal structure of each receptor (PDB IDs: 4DJH, 4DKL, 4EJ4)

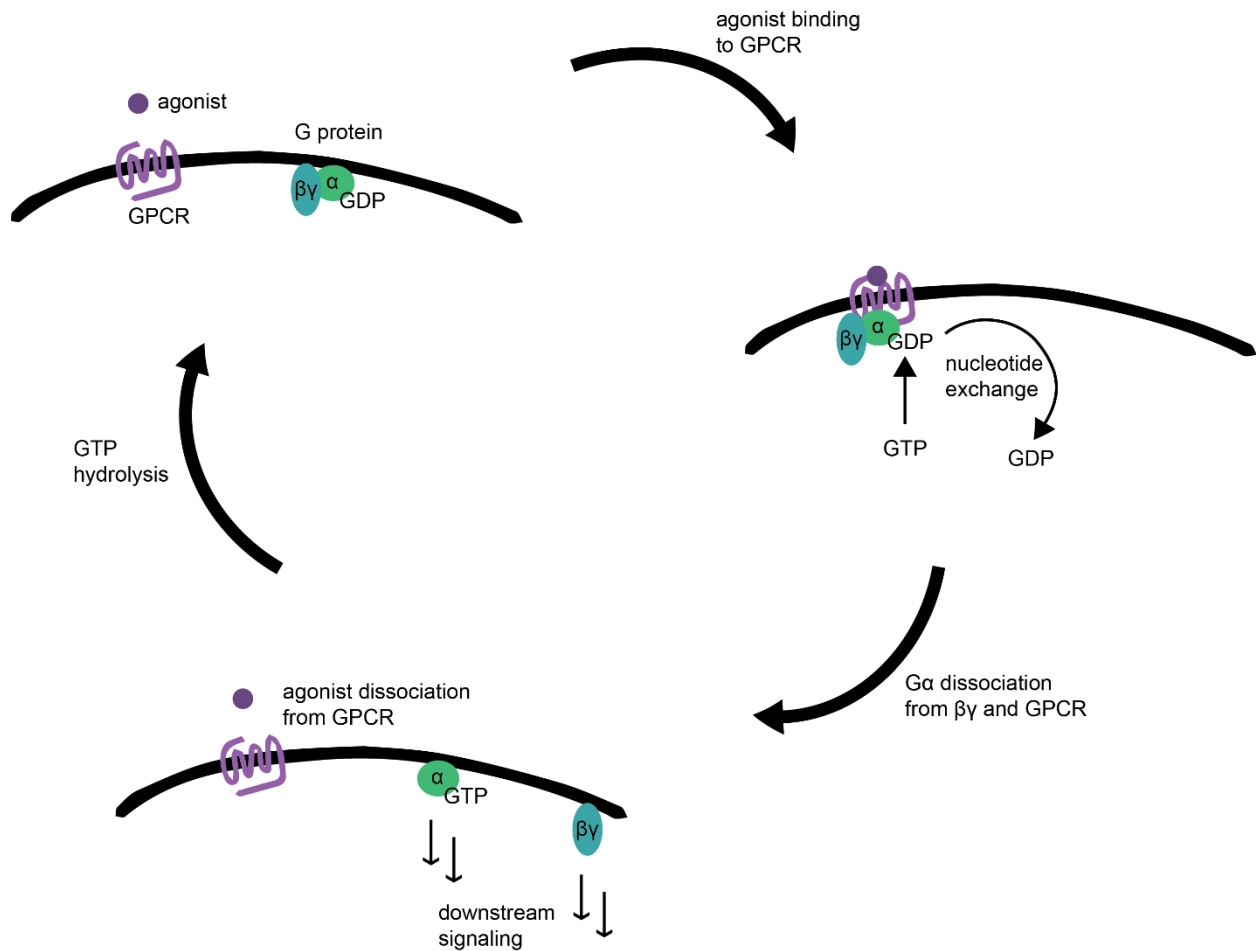
1.2.3 Function

“By untangling [multiple layers of complexity of opioid receptor function], basic research into the chemistry and pharmacology of opioid receptors is guiding the way towards deciphering the mysteries... that have plagued the field and is providing a platform for the development of more effective and safer opioids.”

-Rita J. Valentino and Nora D. Volkow, National Institute on Drug Abuse, 2018²⁷

As GPCRs, opioid receptors elicit biological effects primarily through interaction with heterotrimeric G proteins. In a 2015 review, Hanlon and Andrew summarize: “The GPCR cycle... is an elegant cellular solution for sensing a specific exogenous signal, transducing it to a signaling cascade, and then terminating the signal.”²⁸ The structure and function of these receptors have been comprehensively reviewed.²⁸⁻³² In brief, GPCR-mediated G protein activation, illustrated in Figure 5, is initiated upon agonist binding to the receptor. Subsequent activation of the GPCR causes a conformational change which results in activation of an associated G protein. Nucleotide exchange occurs at the α subunit of the G protein in which guanine diphosphate (GDP) is exchanged for guanine triphosphate (GTP). Upon GTP binding, the $G\alpha$ subunit dissociates from the GPCR and from the β and γ subunits of the G protein. The free G protein subunits then interact with downstream targets, resulting in GPCR signaling. Over time, the GTP attached to the $G\alpha$ subunit is hydrolyzed to GDP, resulting in an inactivated G protein and a completed cycle. GPCRs, including the opioid receptors, also have G protein independent signaling pathways. In particular, recent research has indicated a growing role of the interactions between opioid receptors and β arrestin.²⁷

Figure 5. Illustration of GPCR-mediated G protein activation



Upon agonist binding to a GPCR, nucleotide exchange occurs at an associated G protein. The α subunit of the G protein dissociates from the β and γ subunits of the G protein and the GPCR, and downstream signaling occurs.

These molecular and cellular effects and the ubiquitous expression of the opioid receptors throughout the peripheral and central nervous systems result in the involvement of the opioid system in a wide variety of biological and physiological processes. The most common and well-known clinical use of opioids is for pain management,^{33–35} but opioid receptors also play a role in many other functions including mood,^{36–38} reward,^{37,39} stress,³⁶ respiration,^{40,41} and gastrointestinal function.^{42–44}

Relevant functions of the opioid system will be discussed in more detail in later chapters.

1.3 Opioid Ligands

Opioid receptor function is modulated by endogenous and exogenous opioids, giving these ligands great potential as chemical and pharmacological tools and therapeutic agents for a wide assortment of indications. To date, thousands of endogenous, semi-synthetic, and synthetic opioid ligands have been discovered and developed. These molecules are widely used in the clinic and the laboratory.

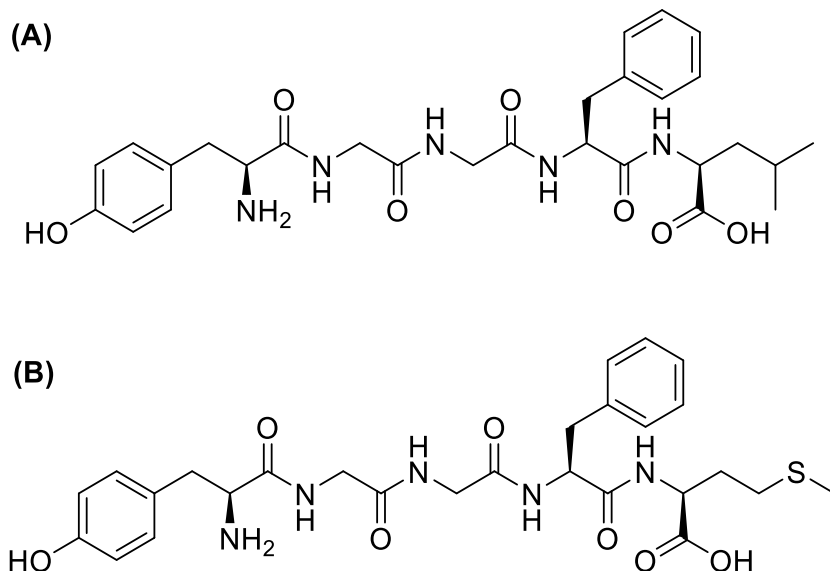
1.3.1 Endogenous Opioid Ligands

“Opioid peptides... are implicated in a wide variety of biological events...”

-Brigitte L. Kieffer, Ecole Supérieure de Biotechnologie de Strasbourg, 1995⁴⁵

Because of the long history of opium use and the early discovery of morphine, the postulation and discovery of opioid receptors predated the discovery of the associated endogenous ligands. It was not long after the discovery of the opioid receptors, however, that the search for these endogenous ligands began in earnest.⁶ The first identification of such ligands occurred in 1975 with two pentapeptides now known as Leu- and Met-enkephalin (Figure 6), named for the terminal leucine and methionine residues, respectively.⁴⁶ Since then, many other endogenous opioid ligands have been discovered, all of which are peptides, and their pharmacology and structure-activity relationships (SAR) have been well-studied. This work has been extensively reviewed,^{35,47-49} and as a result of this work, many novel opioid ligands have been developed.

Figure 6. Structures of Leu- and Met-enkephalin



(A) Chemical structure of Leu-enkephalin (B) Chemical structure of Met-enkephalin

1.3.2 Selective Opioid Ligands

Early progress in the discovery of synthetic opioids focused on the development of selective ligands for each receptor type. Before the complexity of opioid pharmacology was known, it was assumed that following the traditional drug discovery convention of using selectivity to minimize unwanted off-target side effects would lead to clinically useful compounds. While not always therapeutically relevant, selective agonists and antagonists for each opioid receptor have been useful tools in further elucidating the functions of each opioid receptor. Of note, this work uses DAMGO (MOR),⁵⁰ U69,593 (KOR),⁵¹ and DPDPE (DOR)⁵² as standard agonists at each receptor.

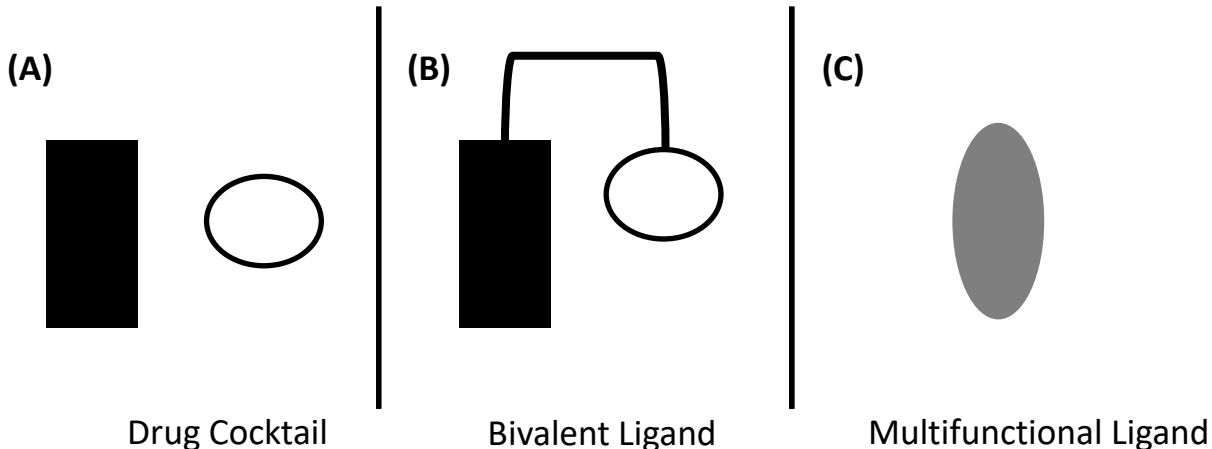
1.3.3 Multifunctional Opioid Ligands

More recently, the opioid field has shifted from synthesis of selective agonists and antagonists to multifunctional ligands, leaving room for the development of new

generations of opioids. Because of the complex pharmacology of the opioid system, unwanted effects often result from the same interaction of an opioid ligand with its target that causes the desired effect. The development of multifunctional ligands that simultaneously act at multiple opioid receptors represents one strategy for overcoming such undesired on-target effects.^{47,53–55}

The development of multifunctional ligands offers several advantages over the co-administration of multiple selective drugs. Drug cocktails, also known as combination therapies, complicate dosing regimens because of the differing pharmacokinetic properties of each active component. The more complex schedules, in turn, reduce patient compliance. Simultaneous administration of multiple drugs also increases the risk of drug-drug interactions and patient-to-patient variation in efficacy and adverse drug reactions. Multifunctional ligands, single compounds that act simultaneously at multiple targets, while often more difficult to develop, reduce this clinical complexity. These compounds can be divided into two main categories: (1) bivalent or bidentate ligands, in which two separate pharmacophores are linked by a flexible spacer and (2) multifunctional or mixed efficacy ligands, which contain a single set of binding elements that interacts with multiple targets (Figure 7).⁵⁵

Figure 7. Drug Cocktail vs. Bivalent Ligand vs. Multifunctional Ligand



(A) A drug cocktail containing two selective drugs with distinct pharmacophores (B) A bivalent ligand in which two separate pharmacophores are connected by a flexible linker to form a single molecule (C) A multifunctional drug in which multiple separate pharmacophores are merged into a single ligand which displays properties of each pharmacophore

This figure, used with permission, has been reproduced from reference 55.

This work focuses on the development of mixed efficacy ligands which interact with multiple opioid receptor types. The following chapters will describe the design, synthesis, and pharmacological evaluation of novel, multifunctional opioid ligands. These compounds have been designed from a well-known selective opioid scaffold. Structural modifications on this scaffold have led to the development of new opioids with a variety of potentially useful multifunctional profiles.

Chapter 2

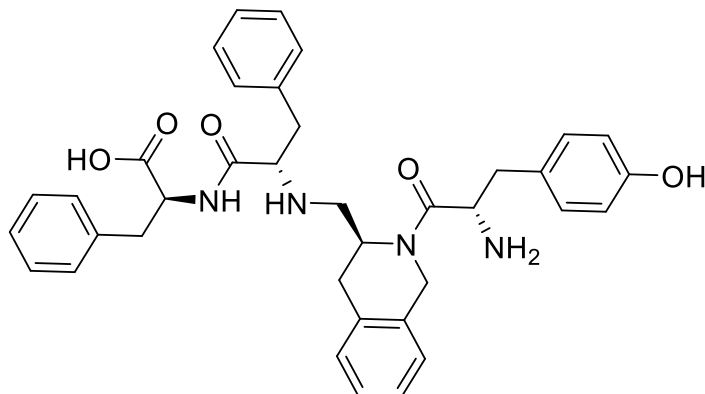
Introduction of Substitution on the Tetrahydroisoquinoline Aromatic Ring of Dimethyltyrosine-Tetrahydroisoquinoline Opioid Peptidomimeticsⁱ

2.1 Introduction

In the mid-1990s, the most selective opioid peptides known were the dermorphins (MOR agonists) and deltorphins (DOR agonists).⁵⁶ Structure-activity relationship (SAR) studies of these endogenous peptides, derived from amphibian skin, resulted in the identification of two residues – Tyr¹ and Phe³ – of their common N-terminal tripeptide sequence (Tyr-D-Xaa-Phe) which were essential for interaction with the opioid receptors.^{57–59} The incorporation of 1,2,3,4-tetrahydroisoquinoline carboxylate (Tic) at position 2 resulted in conformationally restricted tri- and tetrapeptides with varied opioid profiles.⁶⁰ Further work led to the development of TIPP[ψ], a stable and extraordinarily selective DOR antagonist and an important pharmacological tool (Figure 8).⁶¹

ⁱ Most of the work in this chapter was originally published in *ACS Chemical Neuroscience*.¹¹² The *in vitro* data presented here were acquired by Dr. Jessica P. Anand and Dr. Nicholas W. Griggs with assistance from Thomas J. Fernandez, Joshua G. Hartman, and Ashley A. Sanchez-Santiago under the supervision of Dr. John R. Traynor at the University of Michigan. Modeling studies were completed by Dr. Irina D. Pogozheva at the University of Michigan.

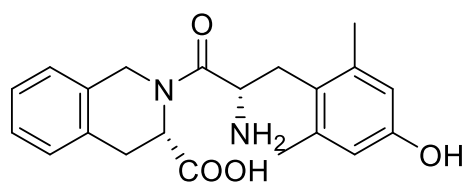
Figure 8. Structure of TIPP[ψ]



Chemical structure of TIPP[ψ], a selective delta opioid receptor antagonist

Subsequently, Phe³ was shown to be unnecessary for opioid activity by the shortening of this sequence to a series of Tyr-Tic dipeptides, the first opioid peptides with only two residues.⁶² Further conformational restriction by replacement of the tyrosine residue with 2',6'-dimethyltyrosine (Dmt) gave rise to exceptionally potent and selective DOR antagonists such as Dmt-Tic-OH.^{56,63} As a result, the dimethyltyrosine-tetrahydroisoquinoline carboxylic acid (Dmt-Tic) peptide scaffold (Figure 9) has been the basis for the creation of a host of additional DOR antagonists.^{64–66} Through further structural modifications, ligands with other pharmacological profiles have been developed from this originally DOR antagonist selective scaffold. These ligands include DOR agonists,⁶⁷ DOR inverse agonists,⁶⁸ and MOR antagonists.⁶⁹

Figure 9. Dimethyltyrosine-Tetrahydroisoquinoline Carboxylic Acid Scaffold

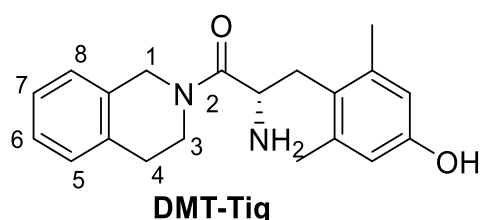


DMT-Tic

Chemical structure of the dimethyltyrosine-tetrahydroisoquinoline carboxylic acid (DMT-Tic) scaffold

Since relatively minor structural modifications often result in significant changes in the pharmacological profiles of opioid ligands, selective scaffolds such as Dmt-Tic also represent an important starting point for the creation and discovery of multifunctional compounds. The addition of a third aromatic center led to the development of DOR agonist and bifunctional DOR antagonist/MOR agonist ligands, depending on the spacer between Dmt-Tic and the third aromatic ring.⁷⁰ Bivalent compounds with Dmt-Tic linked to endomorphin-2 or morphine display various multifunctional profiles.^{71,72} Several monovalent MOR agonist/DOR antagonist compounds have also been reported based on the Dmt-Tic scaffold.^{73,74} Notably, the evaluation of Dmt-Tic ligands with modified C-termini suggests that the DOR selectivity observed in the original compounds in this series is primarily imparted by the negative charge of the C-terminal carboxylate.^{75,76} The removal or modification of this moiety results in a dimethyltyrosine-tetrahydroisoquinoline (Dmt-Tiq) core useful in the development of multifunctional ligands (Figure 10)

Figure 10. Dimethyltyrosine-Tetrahydroisoquinoline Scaffold



Dimethyltyrosine-tetrahydroisoquinoline (DMT-Tiq) scaffold with carbon numbering on the tetrahydroisoquinoline

Despite the plethora of Dmt-Tiq compounds that have been reported, modifications to this scaffold have been limited by the constraints of traditional peptide synthesis. As a result, substitution on the tetrahydroisoquinoline (Tiq) aromatic ring has been largely underexplored. In 2000, Pagé et al. reported a series of DOR antagonist

Dmt-Tiq compounds with substitutions at the 6-, 7-, and 8-positions of Tiq ranging from hydroxy and methoxy substituents to aryl rings.⁶⁶ In the same year, Santagada et al. published Dmt-Tiq compounds with small substituents at the 7-position of Tiq.⁷⁴ These analogues showed a similar DOR antagonist profile to the standard peptide. Overall, a severely limited range of substitutions has been reported at these positions, and for these compounds there remain gaps in the knowledge of their binding and efficacy. Given this gap, we set out to explore the structure-activity relationships between the aromatic region of Tiq within the Dmt-Tiq scaffold and its opioid profile by synthesizing novel Dmt-Tiq analogues with substitution on the Tiq aromatic ring.

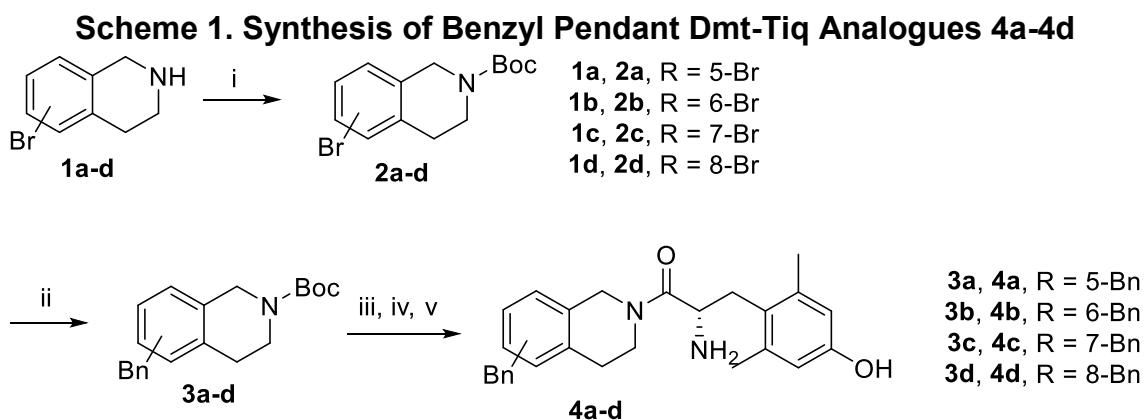
2.2 Benzyl Scan Around the Tetrahydroisoquinoline Aromatic Ring

To investigate the SAR of the tetrahydroisoquinoline aromatic region of the Dmt-Tiq scaffold, novel analogues were synthesized and evaluated for opioid activity. Initial exploration began with the installation of a benzyl pendant onto each available carbon of the Tiq aromatic ring. These pendants were larger than any substituents previously reported at these positions.

2.2.1 Synthesis

Analogues **4a-4d** were prepared according to the synthetic route shown in Scheme 1. Commercially available bromo-substituted tetrahydroisoquinolines **1a-1d** were Boc-protected, and the resulting bromides **2a-2d** were coupled with benzylboronic acid pinacol ester via Suzuki reaction to produce intermediates **3a-3d**. Deprotection of the tetrahydroisoquinoline nitrogen with hydrochloric acid, peptide coupling with diBoc-protected dimethyltyrosine, and subsequent deprotection with trifluoroacetic acid (TFA)

yielded peptidomimetics **4a-4d**. Detailed experimental procedures can be found in Chapter 6.



(i) Boc_2O ; (ii) benzylboronic acid pinacol ester, $\text{Pd}(\text{dppf})\text{Cl}_2$, K_2CO_3 , acetone/water; (iii) HCl , 1,4-dioxane; (iv) diBoc-Dmt, PyBOP, 6Cl-HOBt, DIEA, DMF; (v) TFA, DCM

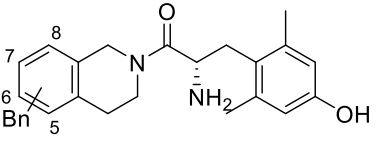
2.2.2 Pharmacological Evaluation

The binding and efficacy profile of each compound was determined individually at KOR, MOR, and DOR. Binding at each receptor was evaluated by competitive displacement of [^3H]diprenorphine, and efficacy and potency were determined by a [^{35}S]GTP γS binding assay. Reported percent stimulation values are from comparison to a standard agonist for each receptor and are used as a surrogate for efficacy. Detailed experimental procedures can be found in Chapter 6.

Each of these analogues (**4a-4d**) shows single to triple digit nanomolar binding at each of the opioid receptors (Table 1). At both KOR and MOR, **4c** binds tightest, followed by **4b** and **4d**, with **4a** having the lowest affinity for these two receptors. The binding profiles of these compounds at DOR differ from the other receptors, with all analogues displaying single digit nanomolar binding except for **4d**, which has much lower affinity for DOR. None of these compounds displays agonism at MOR or DOR; however, the efficacy profile at KOR differs widely. While **4a** and **4b** display no KOR

agonism, **4c** shows potent full (85%) agonism at KOR, and **4d** shows weak partial (46%) agonism at KOR. The compounds that bind best at KOR, **4c** and **4d**, also show the highest efficacy at this receptor.

Table 1. Binding, Potency, and Efficacy Data for Benzyl Pendant Dmt-Tiq Analogues 4a-4d



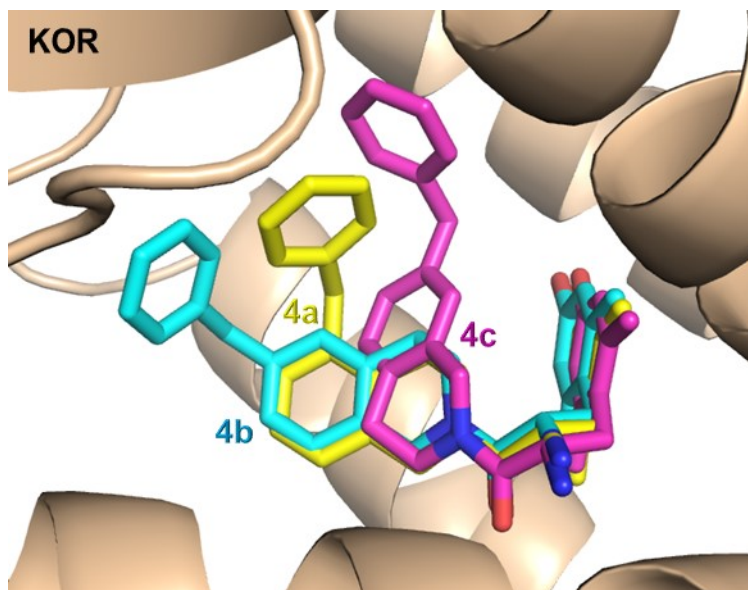
		K _i (nM)			EC ₅₀ (nM)			% Stimulation		
		KOR	MOR	DOR	KOR	MOR	DOR	KOR	MOR	DOR
4a	5-Bn	112 (13)	17 (5)	3.3 (0.2)	-	-	-	dns	dns	dns
4b	6-Bn	38 (5)	9.9 (1.6)	4.3 (0.6)	-	-	-	dns	dns	dns
4c	7-Bn	3.9 (0.8)	2.7 (0.8)	6.1 (2.1)	33 (6)	-	-	85 (8)	dns	dns
4d	8-Bn	26 (5)	4.1 (0.4)	185 (28)	319 (45)	-	-	46 (6)	dns	dns

Binding affinity (K_i) values determined by competitive displacement of [³H]diprenorphine in membrane preparations from CHO cells expressing human KOR or C6 cells expressing rat MOR or rat DOR. Potency (EC₅₀) and efficacy values determined by [³⁵S]GTPγS binding in the same membrane preparations. Efficacy expressed as percent stimulation versus standard agonist - U69,593 (KOR), DAMGO (MOR), or DPDPE (DOR). All values expressed as mean (SEM) of three or more separate assays run in duplicate. Bn = benzyl; dns = does not stimulate, average maximal stimulation <10% at concentrations up to 10 μM

2.2.3 Computational Modeling

To explore potential differences in binding between the various benzyl pendant Dmt-Tiq analogues, we employed a computational model of **4a**, **4b**, and **4c** docked to the inactive conformation of KOR (Figure 11). Whereas **4a** and **4b** are shown in a fashion typical of the binding of other Dmt-Tiq compounds to the opioid receptors, our model suggests that **4c** binds in a different conformation. The unique binding mode of **4c** likely allows for accommodation of this ligand by the active conformation of KOR which may explain the observed KOR agonism.

Figure 11. Compounds 4a, 4b, and 4c Docked in the KOR Orthosteric Site



Compounds **4a** (yellow), **4b** (cyan) and **4c** (magenta) docked to the inactive conformation of the KOR orthosteric site. The tetrahydroisoquinoline core of **4c** is oriented differently than that of **4a** and **4b**.

2.3 Substituted 7-Benzyl Pendant Analogues

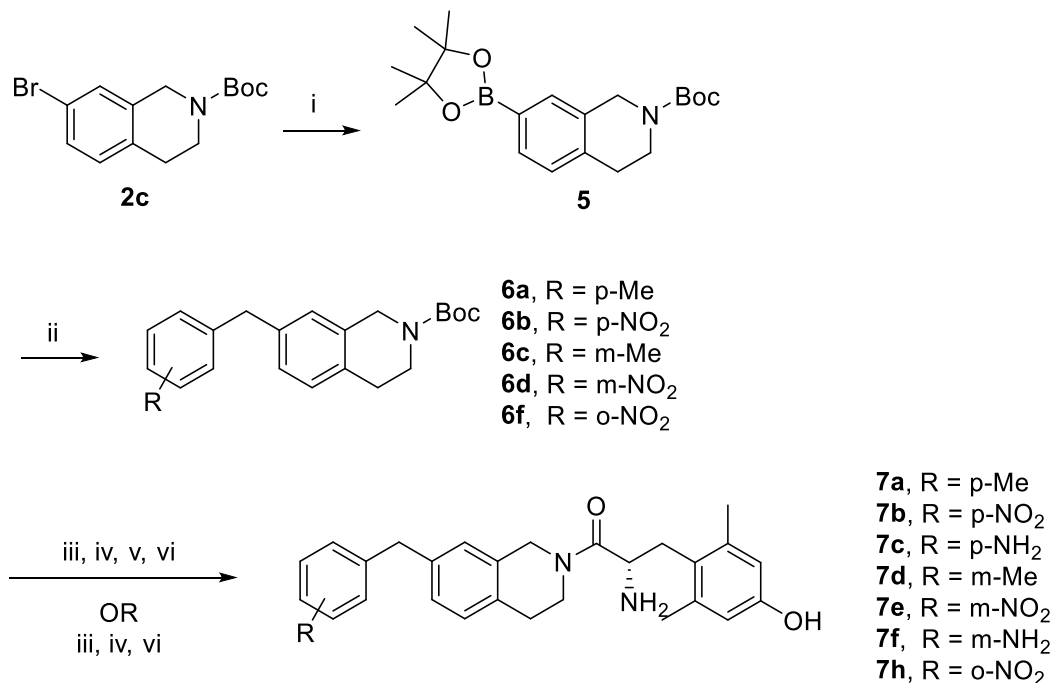
Based on the interesting profile of compound **4c** – potent full KOR agonism and high, non-specific opioid receptor binding affinity – we decided to use this compound as a starting point to further explore the SAR of this series. To investigate steric and electronic effects of 7-benzyl pendant substitutions on opioid binding and activity, we synthesized analogues of **4c** with various functional groups installed at each position of the phenyl ring. We introduced a methyl group at each position to test the steric effects of para, meta, and ortho substitutions. To further probe electronic effects at these positions, we used a nitro group (electron withdrawing, hydrogen bond accepting) and an amino group (electron donating, hydrogen bond donating).

2.3.1 Synthesis

Synthesis of Substituted 7-Benzyl Pendant Dmt-Tiq Analogues 7a-7f, 7h.

Analogues **7a-7f** and **7h** were prepared according to the synthetic route shown in Scheme 2. Common intermediate **5** was prepared from **2c**. Suzuki coupling of **5** with various substituted benzyl bromides yielded intermediates **6a-6d** and **6f**. Deprotection of the tetrahydroisoquinoline nitrogen with hydrochloric acid, peptide coupling with diBoc-protected dimethyltyrosine, and subsequent deprotection with trifluoroacetic acid yielded peptidomimetics **7a**, **7b**, **7d**, **7e**, and **7h**. For peptidomimetics **7c** and **7f**, reduction of the nitro group with zinc dust and ammonium chloride in acetone and water was performed prior to final deprotection. Detailed experimental procedures can be found in Chapter 6.

Scheme 2. Synthesis of Substituted 7-Benzyl Pendant Dmt-Tiq Analogues 7a-7f and 7h

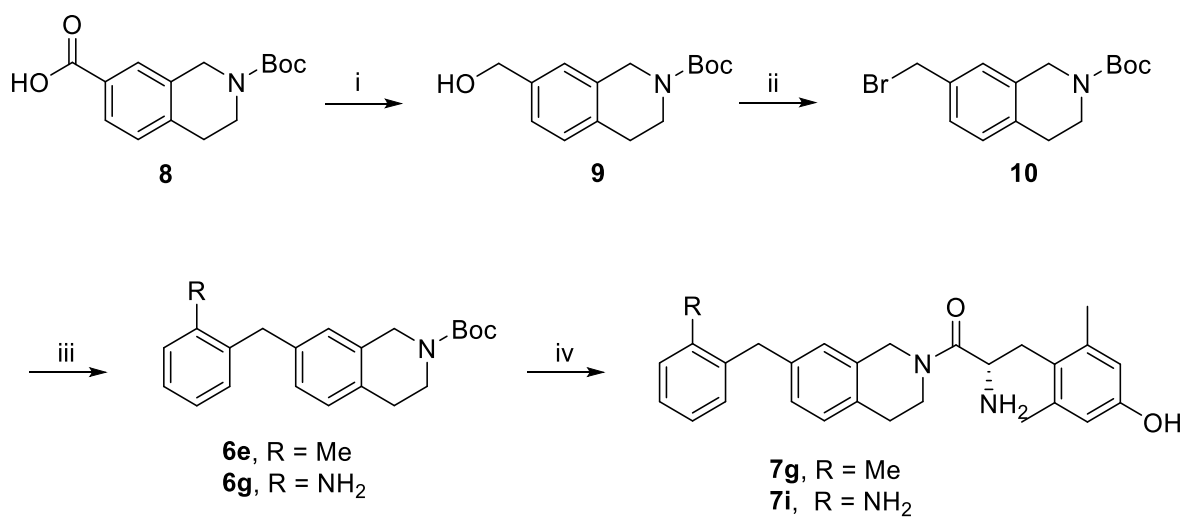


(i) bis(pinacolato)diboron, Pd(dppf)Cl₂, CH₃CO₂K, DMSO; (ii) substituted aryl boronic acid, Pd(dppf)Cl₂, K₂CO₃, 3:1 acetone:water; (iii) HCl, 1,4-dioxane; (iv) diBoc-Dmt, PyBOP, 6Cl-HOBt, DIEA, DMF; (v) Zn, NH₄Cl, acetone/water; (vi) TFA, DCM

Synthesis of Substituted 7-Benzyl Pendant Dmt-Tiq Analogues 7g and 7i.

Analogues **7g** and **7i** were prepared according to the synthetic route shown in Scheme 3. Commercially available **8** was reduced with borane dimethylsulfide to secondary alcohol **9** which was then converted to the corresponding secondary bromide **10** via Appel reaction. Suzuki coupling of **10** with 2-methylphenylboronic acid or 2-aminophenylboronic acid produced intermediate **6e** or **6g**. Deprotection of the tetrahydroisoquinoline nitrogen with hydrochloric acid, peptide coupling with diBoc-protected dimethyltyrosine, and subsequent deprotection with trifluoroacetic acid yielded peptidomimetic **7g** or **7i**. Detailed experimental procedures can be found in Chapter 6.

Scheme 3. Synthesis of Substituted 7-Benzyl Pendant Dmt-Tiq Analogues 7g and 7i

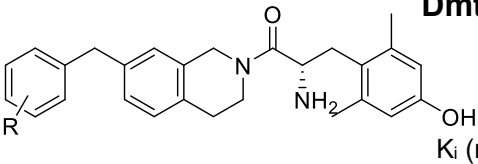


(i) BH₃ SMe₂, THF; (ii) CBr₄, PPh₃, DCM (iii) substituted aryl boronic acid, Pd(dppf)Cl₂, K₂CO₃, acetone/water; (iv) HCl, 1,4-dioxane; then diBoc-Dmt, PyBOP, 6Cl-HOBt, DIEA, DMF; then TFA, DCM

2.3.2 Pharmacological Evaluation

Table 2 shows binding and efficacy data for substituted 7-benzyl pendant Dmt-Tiq analogues **7a-7i**.

Table 2. Binding, Potency, and Efficacy Data for Substituted 7-Benzyl Pendant Dmt-Tiq Analogues 7a-7i



	R	K _i (nM)			EC ₅₀ (nM)			% Stimulation		
		KOR	MOR	DOR	KOR	MOR	DOR	KOR	MOR	DOR
4c	H	3.9 (0.8)	2.7 (0.8)	6.1 (2.1)	33 (6)	-	-	85 (8)	dns	dns
7a	p-Me	233 (41)	114 (22)	6.0 (1.2)	-	158 (49)	-	dns	23 (3)	dns
7b	p-NO ₂	22 (4)	2.6 (0.5)	2.9 (0.3)	424 (84)	-	-	33 (8)	dns	dns
7c	p-NH ₂	91 (7)	47 (10)	3.1 (0.4)	-	-	-	dns	dns	dns
7d	m-Me	2.7 (0.3)	3.1 (0.6)	3.0 (0.8)	80 (25)	42 (13)	-	83 (5)	30 (2)	dns
7e	m-NO ₂	2.5 (0.5)	3.1 (0.8)	2.5 (0.7)	97 (30)	-	-	76 (6)	dns	dns
7f	m-NH ₂	28 (4)	9.7 (2.4)	5.5 (0.9)	405 (65)	-	-	24 (3)	dns	dns
7g	o-Me	1.2 (0.2)	2.5 (0.3)	5.8 (1.1)	28 (7)	48 (16)	-	96 (9)	21 (4)	dns
7h	o-NO ₂	2.6 (1.0)	10 (2)	4.7 (1.5)	32 (6)	-	-	77 (2)	dns	dns
7i	o-NH ₂	25 (5)	2.1 (0.1)	9.0 (2.2)	471 (56)	116 (40)	-	96 (11)	27 (4)	dns

Binding affinity (K_i) values determined by competitive displacement of [³H]diprenorphine in membrane preparations from CHO cells expressing human KOR or C6 cells expressing rat MOR or rat DOR. Potency (EC₅₀) and efficacy values determined by [³⁵S]GTPγS binding in the same membrane preparations. Efficacy expressed as percent stimulation versus standard agonist - U69,593 (KOR), DAMGO (MOR), or DPDPE (DOR). All values expressed as mean (SEM) of three or more separate assays run in duplicate. dns = does not stimulate, average maximal stimulation <10% at concentrations up to 10 μM

Para substitutions (**7a-7c**) decrease KOR binding and result in a loss of KOR efficacy versus lead compound **4c** with no significant gain in MOR or DOR binding or

agonism. Analogues with a meta or ortho substituent (**7d-7i**) display binding profiles similar to that of parent **4c**, mostly in the single digit nanomolar range at KOR, MOR, and DOR, with the notable exception of meta and ortho amino analogues (**7f**, **7i**) which show an approximately tenfold decrease in binding affinity at KOR versus **4c**. Overall, however, small meta and ortho substitutions are accommodated by the orthosteric site of each opioid receptor. Meta substitutions (**7d-7f**) all retain some degree of KOR agonism. Methyl and nitro substitutions at the meta position (**7d**, **7e**) retain high (>75%) KOR efficacy while the amino analogue (**7f**) displays only partial (24%) KOR agonism. The meta methyl analogue (**7d**) also displays partial (30%) MOR agonism, while the nitro and amino analogues do not. Ortho substitutions (**7g-7i**) all retain high (>75%) KOR efficacy, suggesting that small substituents at this position are allowed by the active conformation of KOR. Methyl (**7g**) and amino (**7i**) analogues not only display higher KOR efficacy than lead compound **4c** but also introduce partial (21-27%) MOR agonism.

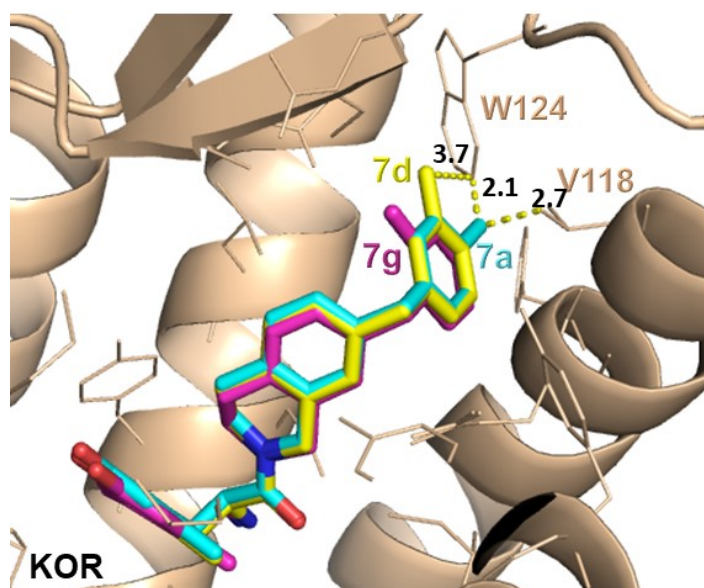
Overall, no strong trend is seen with electron withdrawing or electron donating groups on the 7-benzyl pendant. As such, the pharmacological profiles of these compounds are likely more influenced by steric, space-filling effects in the opioid receptor binding sites than specific, electronic interactions.

2.3.3 Computational Modeling

To further investigate interactions of this series of Dmt-Tiq compounds with the opioid receptors, we employed computational models similar to those previously developed^{77,78} and used^{79,80} by our group. Figure 12 shows each of the methyl-substituted analogues (**7a**, **7d**, **7g**) docked in the recent crystal structure of KOR in the

active conformation (PDB ID: 6B73).²⁵ The drastic decrease in KOR binding affinity and efficacy for para substituted analogues compared to lead compound **4c** is likely due to a lack of space in the KOR binding site. As shown, the para methyl group of **7a** causes a steric clash with V118 and W124 in the active configuration of KOR, suggesting that para substitutions are unfavorable for KOR agonism and binding. However, the meta and ortho methyl groups of **7d** and **7g** respectively are directed towards a different area of the binding site where there is space for them to be accommodated.

Figure 12. Compounds 7a, 7d, and 7g Docked in the KOR Orthosteric Site



Compounds **7a** (cyan), **7d** (yellow), and **7g** (magenta) docked in the orthosteric site of the active conformation of KOR. Dashed yellow lines represent distance, labeled in angstroms. The para methyl group of **7a** sterically clashes with V118 and W124 of KOR.

2.4 Conclusions

Several compounds in this series display KOR agonism and MOR partial agonism, a bifunctional profile which may be useful in the treatment of cocaine addiction.^{81–83} It has previously been demonstrated that KOR agonists have the potential to reduce cocaine self-administration in non-human primates.^{84,85} However, negative side effects such as dysphoria are associated with activation of KOR, so the

clinical utility of selective KOR ligands is limited. Since MOR agonists cause euphoria, it has been suggested that MOR partial agonism may mitigate dysphoria associated with KOR agonism, increasing the therapeutic potential of a KOR agonist.^{82,86–88}

Three compounds from this series (**7d**, **7g**, **7i**) show potential to be investigated for this purpose. Notably, the KOR potency and MOR potency of **7d** and **7g** are higher than that of **7i**, making them the most promising KOR/MOR ligands in this series. These compounds show little to no selectivity for KOR and MOR over DOR; however, there is evidence from our group and others to suggest that DOR antagonist activity may help mitigate the addictive potential of MOR agonists.^{89–95} Since none of the compounds reported here show agonism at DOR, this lack of selectivity may be beneficial for the development of a therapeutic for the treatment of addiction. The *in vivo* opioid activity of **4c**, **7d**, and **7g** is currently being evaluated.

In conclusion, the selective DOR antagonist Dmt-Tiq scaffold can be converted to multifunctional opioid peptidomimetics through the addition of 7-position pendants on the aromatic Tiq ring. The addition of a 7-benzyl pendant to the Tiq aromatic ring of Dmt-Tiq introduced strong KOR agonism. The introduction of ortho and meta substituents on the 7-benzyl pendant resulted in retention of KOR agonism and addition of partial MOR agonism, a profile which has shown promise for the treatment of cocaine addiction. This work provides a foundation for further exploration of the Tiq aromatic region of the Dmt-Tiq scaffold. The installation of additional 7-position pendants is described in Chapter 3.

Chapter 3

Further Exploration of the Structure-Activity Relationships of 7-Substituted Dimethyltyrosine-Tetrahydroisoquinoline Opioid Peptidomimeticsⁱⁱ

3.1 Introduction

The work described in Chapter 2 demonstrates that the classically delta opioid receptor (DOR) antagonist selective dimethyltyrosine-tetrahydroisoquinoline (Dmt-Tiq) scaffold can be used in the development of multifunctional opioid ligands. Specifically, the installation of a 7-position benzyl pendant on the tetrahydroisoquinoline (Tiq) core results in kappa opioid receptor (KOR) agonism, and the addition of ortho and meta substituents imparts a KOR agonist/mu opioid receptor (MOR) partial agonist profile. This initial work inspired further exploration of the structure-activity relationships (SAR) surrounding the 7-benzyl pendant.

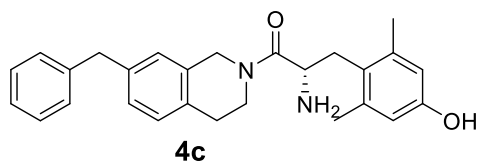
Building on our previous work, this study further explores installation of various 7-position pendants on the Tiq ring as a means of developing ligands with pharmacologically useful, multifunctional profiles. Previously, we reported ligands in this series that demonstrate KOR agonism and MOR partial agonism, a bifunctional profile which has shown promise for the treatment of addiction to cocaine and other drugs of abuse. Here, we further explore the SAR of this novel series of opioid ligands and report compounds with this and other multifunctional opioid profiles.

ⁱⁱ The work in this chapter is being submitted for publication. The *in vitro* data presented here were acquired by Dr. Jessica P. Anand with assistance from Jack J. Twarozynski, Joshua G. Hartman, Lennon J. DeLong, and Ashley C. Brinkel under the supervision of Dr. John R. Traynor at the University of Michigan. Compounds **12c**, **12d**, and **12f** were synthesized by Mason A. Baber under the direction of the author of this dissertation and the supervision of Dr. Henry I. Mosberg.

The importance of screening conditions in the collection and analysis of pharmacological data is often underappreciated. Compounds reported in Chapter 2 were all screened for binding, potency, and efficacy at human KOR and rat MOR and DOR. Based on the availability of cell lines expressing human MOR and DOR, respectively, we altered our screening paradigm. Rather than using C6 cells expressing rat MOR or rat DOR, membranes in the new screening method were prepared from Chinese hamster ovary (CHO) cells expressing human MOR or human DOR. The preparation of membranes containing human KOR from CHO cells was unchanged. Since the ultimate goal of this work is the development of novel opioids for therapeutic use in humans, we believe that the new screening paradigm provides data that gives a more accurate representation of the potential of these compounds to be developed for clinical use. As such, the activity of compounds reported in this chapter was evaluated solely at human opioid receptors.

Table 3 shows a direct comparison of data for compound **4c** from each of the two screening paradigms. The data for the old screening paradigm was originally reported in Chapter 2. As expected, the binding profile for this compound is similar across the receptors at both rat and human receptors. Notably, in the newer screening paradigm, **4c** exhibits partial agonism at both human MOR and human DOR. In both screening paradigms, compounds were evaluated at human KOR. The slight drop in potency at KOR is a result of variability in the assay over time.

Table 3. Comparison of Pharmacological Data for 4c at Rat and Human Opioid Receptors



Compound	Screening Paradigm	K _i (nM)			EC ₅₀ (nM)			% Stimulation		
		KOR	MOR	DOR	KOR	MOR	DOR	KOR	MOR	DOR
4c	old ^a	3.9 (0.8)	2.7 (0.8)	6.1 (2.1)	33 (6)	-	-	85 (8)	dns	dns
4c	new ^b	2.3 (0.3)	5.3 (0.5)	3.0** (1.1)	97 (24)	68 (15)	7.0** (2.0)	82 (6)	39 (4)	18** (4)

Comparison of data for compound 4c in old and new screening paradigms

^a Binding affinity (K_i) values determined by competitive displacement of [³H]diprenorphine in membrane preparations from CHO cells expressing human KOR and C6 cells expressing rat MOR or rat DOR. Potency (EC₅₀) and efficacy values determined by [³⁵S]GTPγS binding in the same membrane preparations.

^b Binding affinity (K_i) values determined by competitive displacement of [³H]diprenorphine in membrane preparations from CHO cells expressing human KOR, human MOR, or human DOR. Potency (EC₅₀) and efficacy values determined by [³⁵S]GTPγS binding in the same membrane preparations.

Efficacy expressed as percent stimulation versus standard agonist - U69,593 (KOR), DAMGO (MOR), or DPDPE (DOR). All values expressed as mean (SEM) of three or more separate assays run in duplicate unless otherwise indicated. **n=2; dns = does not stimulate, average maximal stimulation <10% at concentrations up to 10 μM.

3.2 Substituted 7-Benzyl Pendant Analogues

Based on the initial results from this series reported in Chapter 2, we believed ortho and meta substituents on a 7-benzyl pendant to be promising structural modifications for the development of KOR agonist/MOR partial agonist ligands from the Dmt-Tiq series. As such, a series of additional ortho and meta substitutions on the benzyl ring, including the *o*-,*m*-dimethyl analogue, were evaluated to confirm whether they would exhibit the anticipated profile (Table 4).

3.2.1 Synthesis

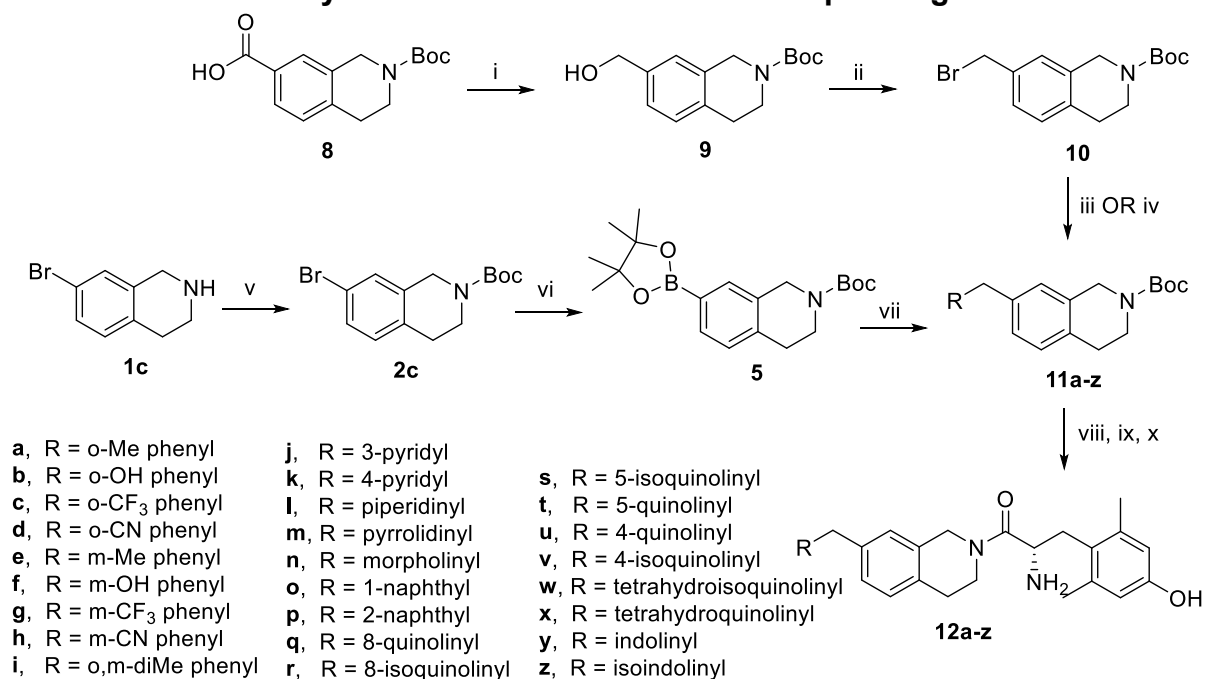
All compounds were prepared from commercial starting materials according to one of the synthetic routes shown in Scheme 4. In the first route, commercially available carboxylic acid **8** was reduced to the corresponding secondary alcohol (**9**) using borane

dimethylsulfide. An Appel reaction was performed to convert alcohol **9** to benzyl bromide **10**. The pendant was then attached via Suzuki coupling of **10** with the corresponding boronic acid or S_N2 reaction with the corresponding nucleophile. Intermediates **11a** and **11b** were prepared according to this route.

In the second route, Boc-protected **2c** was prepared from commercially available 7-bromotetrahydroisoquinoline (**1c**). This intermediate was converted to boronic ester **5**, and the appropriate pendant was attached by Suzuki coupling with the corresponding benzyl bromide. Intermediates **11c-11i** were prepared according to this route.

In each case, after the pendant was attached, the Boc group was removed from intermediate **11a-z** with acid, and the deprotected tetrahydroisoquinoline intermediate was coupled with diBoc-protected dimethyltyrosine. Finally, the Boc groups were removed to yield the final peptidomimetic (**12a-z**). Detailed experimental procedures for all compounds can be found in Chapter 6.

Scheme 4. Synthesis of 7-Substituted Dmt-Tiq Analogues 12a-12z



(i) BH₃ SMe₂, THF; (ii) CBr₄, PPh₃, DCM; (iii) substituted aryl boronic acid, Pd(dppf)Cl₂, K₂CO₃, 3:1 acetone:water; (iv) amine, K₂CO₃, DMF; (v) Boc₂O, microwave; (vi) bis(pinacolato)diboron, Pd(dppf)Cl₂, CH₃CO₂K, DMSO; (vii) substituted benzyl bromide, Pd(dppf)Cl₂, K₂CO₃, 3:1 acetone/water; (viii) HCl, 1,4-dioxane or TFA, DCM; (ix) diBoc-Dmt, PyBOP, 6Cl-HOBt, DIEA, DMF; (x) TFA, DCM

3.2.2 Pharmacological Evaluation

The binding and efficacy profile of each compound was determined individually at human KOR, MOR, and DOR. Binding at each receptor was evaluated by competitive displacement of [³H]diprenorphine, and efficacy and potency were determined by a [³⁵S]GTPγS binding assay. Reported percent stimulation values are from comparison to a standard agonist for each receptor and are used as a surrogate for efficacy. Detailed experimental procedures can be found in Chapter 6.

The results of the pharmacological evaluation of ortho and meta-substituted compounds **12a-12i** are shown in Table 4. Data for the previously reported 7-benzyl analogue, **4c**, are shown for comparison. Previously, this compound was evaluated at human KOR, rat MOR, and rat DOR. As discussed above, the profile shown here differs

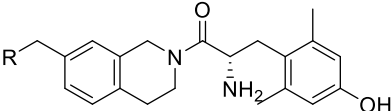
slightly from that previously reported because all subsequent compounds in this chapter were evaluated at human receptors.

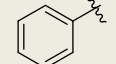
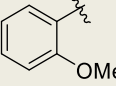
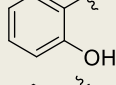
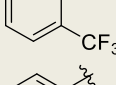
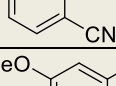
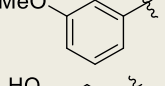
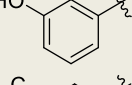
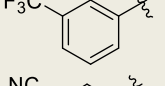
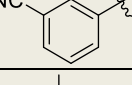
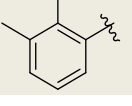
All ortho and meta substituted analogues reported here display single digit nanomolar or subnanomolar binding at all three opioid receptors. In general, ortho analogues show highest affinity for KOR compared to the other receptors, while most meta analogues show highest affinity for DOR. Each of these analogues retains moderate (54%) to high (89%) efficacy at KOR and low (29%) to high efficacy (81%) at MOR. Most analogues show no DOR agonism, but the ortho trifluoromethyl analogue (**12c**) shows weak partial DOR agonism. Potency for these compounds remains primarily in the double or triple digit nanomolar range. The balance of potencies varies for ortho analogues, while meta analogues and the disubstituted analogue are consistently more potent at MOR than KOR.

As expected, ortho and meta substitutions on the 7-benzyl pendant are favorable for the development of KOR/MOR ligands. Because di-substitution (**12i**) results in a notable drop in KOR potency, it shows no advantage over a single ortho or meta substituent. A few of the ligands in this series, including **12c**, show DOR agonism, which represents a problem for the development of a therapeutically useful KOR/MOR ligand because DOR agonism is associated with problematic side effects, including convulsions.^{38,96,97} DOR antagonism, on the other hand, may be beneficial for the development of a treatment for addiction since it has been shown to lower the addiction potential of MOR agonists.^{89,98,99} The strong MOR agonism of some compounds in this series (**12c**, **12f**) is also a concern for the development of a therapeutic, as this activity would likely impart greater abuse potential. The most promising compound in this series

for the development of a KOR agonist/MOR partial agonist for treatment of cocaine addiction, **12b**, shows high potency and efficacy at KOR, high potency and low efficacy at MOR, and is devoid of DOR agonism. This compound also has higher affinity for KOR and MOR than for DOR (eight-fold and two-fold, respectively), making it a promising candidate for further evaluation.

Table 4. Binding, Potency, and Efficacy Data for Substituted 7-Benzyl Pendant Dmt-Tiq Analogues 12a-12i



	R	K _i (nM)			EC ₅₀ (nM)			% Stimulation		
		KOR	MOR	DOR	KOR	MOR	DOR	KOR	MOR	DOR
4c		2.3 (0.3)	5.3 (0.5)	3.0** (1.1)	97 (24)	68 (15)	7.0** (2.0)	82 (6)	39 (4)	18** (4)
12a		3.1 (0.9)	3.7 (0.6)	2.7 (0.7)	130 (41)	92 (26)	-	72 (11)	37 (8)	dns**
12b		0.32 (0.01)	1.2 (0.1)	2.5 (0.3)	11 (1)	43 (13)	-	89 (6)	60 (5)	dns**
12c		2.6 (0.6)	4.3 (1.3)	4.9 (2)	173 (55)	53 (11)	368** (25)	81 (11)	76 (6)	24** (3)
12d		0.5 (0.1)	6.8 (0.2)	3.6 (0.8)	3.7 (0.8)	664 (515)	-	80 (9)	31 (9)	dns
12e		3.0 (0.9)	2.7 (0.6)	1.7 (0.4)	148 (38)	24 (3)	-	74 (4)	48 (6)	dns**
12f		0.8 (0.2)	0.6 (0.2)	1.4 (0.1)	148 (53)	18 (3)	-	83 (5)	81 (9)	dns**
12g		5.4 (1.1)	3.8 (1.3)	2.6** (0.1)	319 (115)	205 (96)	-	68 (8)	45 (3)	dns**
12h		5.9 (0.9)	3.4 (1.3)	1.5** (0.3)	287 (61)	53 (6)	-	60 (8)	29 (3)	dns**
12i		5.8 (1.2)	5.2 (1.4)	3.6 (0.6)	1028 (50)	380 (187)	-	54 (9)	34 (3)	dns**

Binding affinity (K_i) values determined by competitive displacement of [³H]diprenorphine in membrane preparations from CHO cells expressing human KOR, MOR, or DOR. Potency (EC₅₀) and efficacy values determined by [³⁵S]GTPγS binding in the same membrane preparations. Efficacy expressed as percent stimulation versus standard agonist - U69,593 (KOR), DAMGO (MOR), or DPDPE (DOR). All values expressed as mean (SEM) of three or more separate assays run in duplicate unless otherwise indicated. **n=2; dns = does not stimulate, average maximal stimulation <10% at concentrations up to 10 μM

3.3 Pyridyl 7-Position Pendant Analogues

Next, we explored the incorporation of nitrogen into the aromatic ring of the pendant. In place of the benzyl pendant, 3- and 4-pyridyl pendants were added at the 7-position of the tetrahydroisoquinoline ring with a methylene spacer (Table 5). Due to well-known synthetic difficulties,¹⁰⁰ the 2-pyridyl analogue was not successfully synthesized.

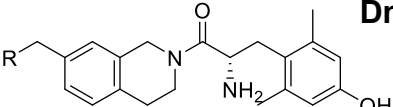
3.3.1 Synthesis

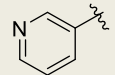
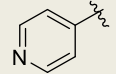
Compounds **12j** and **12k** were prepared according to the second synthetic route shown in Scheme 4. Detailed experimental procedures can be found in Chapter 6.

3.3.2 Pharmacological Evaluation

Evaluation of the pyridyl analogues revealed a loss in binding and a drastic loss of potency at KOR with low efficacy at MOR and no agonism at DOR. Introduction of a nitrogen to the 7-benzyl ring was not favorable for the development of a KOR/MOR ligand. Rather, these analogues are selective for DOR over KOR and MOR and display low potency and efficacy at KOR and MOR.

Table 5. Binding, Potency, and Efficacy Data for Pyridyl 7-Position Pendant Dmt-Tiq Analogues 12j and 12k



	R	K _i (nM)			EC ₅₀ (nM)			% Stimulation		
		KOR	MOR	DOR	KOR	MOR	DOR	KOR	MOR	DOR
12j		56 (0.9)	5.4 (0.3)	1.5 (0.2)	988 (277)	145 (30)	-	40 (7)	23 (1)	dns
12k		44 (12)	58 (3)	2.6 (1.0)	1177 (287)	179 (17)	-	44 (9)	28 (1)	dns

Binding affinity (K_i) values determined by competitive displacement of [³H]diprenorphine in membrane preparations from CHO cells expressing human KOR, MOR, or DOR. Potency (EC₅₀) and efficacy values determined by [³⁵S]GTPγS binding in the same membrane preparations. Efficacy expressed as percent stimulation versus standard agonist - U69,593 (KOR), DAMGO (MOR), or DPDPE (DOR). All values expressed as mean (SEM) of three or more separate assays run in duplicate. dns = does not stimulate, average maximal stimulation <10% at concentrations up to 10 μM

3.4 Aliphatic 7-Position Pendant Analogues

Non-aromatic pendants were also explored. Table 6 shows pharmacological data for analogues with saturated, cyclic amine pendants.

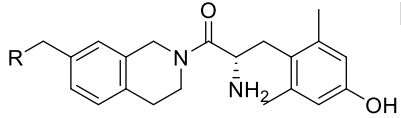
3.4.1 Synthesis

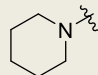
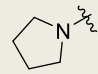
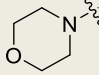
Compounds **12l-12n** were prepared according to the first synthetic route shown in Scheme 4. Detailed experimental procedures can be found in Chapter 6.

3.4.2 Pharmacological Evaluation

Replacement of the benzyl pendant with a saturated, cyclic amine pendant decreases MOR potency drastically and eliminates KOR agonism altogether (Table 6). Unlike many of the compounds reported here, these analogues do not show particularly useful opioid profiles.

Table 6. Binding, Potency, and Efficacy Data for Aliphatic 7-Position Pendant Dmt-Tiq Analogues 12l-12n



	R	K _i (nM)			EC ₅₀ (nM)			% Stimulation		
		KOR	MOR	DOR	KOR	MOR	DOR	KOR	MOR	DOR
12l		29 (11)	4.7 (0.9)	87 (15)	-	845 (97)	-	dns	34 (5)	dns
12m		69 (3)	5.7 (1.3)	175 (9)	-	639** (162)	-	dns	40** (22)	dns**
12n		43 (17)	12 (1)	5.6 (1.6)	-	1000** (204)	-	dns	24** (1.6)	dns

Binding affinity (K_i) values determined by competitive displacement of [³H]diprenorphine in membrane preparations from CHO cells expressing human KOR, MOR, or DOR. Potency (EC₅₀) and efficacy values determined by [³⁵S]GTPγS binding in the same membrane preparations. Efficacy expressed as percent stimulation versus standard agonist - U69,593 (KOR), DAMGO (MOR), or DPDPE (DOR). All values expressed as mean (SEM) of three or more separate assays run in duplicate unless otherwise indicated. **n=2; dns = does not stimulate, average maximal stimulation <10% at concentrations up to 10 μM

3.5 Naphthyl 7-Position Pendant Analogues

To test whether opioid activity could be maintained in the presence of larger pendants at the Tiq 7-position, we synthesized analogues with 1- and 2-naphthyl

pendants (Table 7). Though the high clogP (5.6) and associated insolubility of these compounds is a problem for the ultimate development of a therapeutic, they were prepared as useful probes to further explore what might be tolerated in this series. Based on our previous observations from ortho, meta, and para substitutions, we hypothesized that the 1-naphthyl pendant would be favorable for the development of a KOR agonist while the 2-naphthyl pendant would not. The 1-naphthyl pendant points in the same direction as ortho and meta substituents, where there is room for additional steric bulk to be accommodated in the active configuration of the KOR orthosteric site. The 2-naphthyl pendant, on the other hand, points in the direction of meta and para substituents, where it clashes with the receptor.

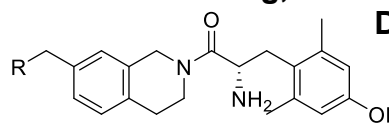
3.5.1 Synthesis

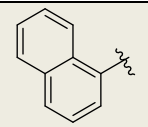
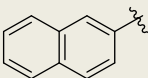
Compounds **12o** and **12p** were prepared according to the second synthetic route shown in Scheme 4. Detailed experimental procedures can be found in Chapter 6.

3.5.2 Pharmacological Evaluation

As expected, the 1-naphthyl analogue (**12o**) displays a KOR agonist/MOR partial agonist profile, while the 2-naphthyl analogue (**12p**) results in a drastic loss in KOR binding and a complete loss of KOR agonism. Both analogues show only weak potency at MOR, and **12o** shows even weaker potency at KOR than MOR. These results suggest that larger pendants can be accommodated as long as the added steric bulk points in the appropriate direction of the KOR binding site. However, optimizing for higher potency remains a challenge.

Table 7. Binding, Potency, and Efficacy Data for Naphthyl 7-Position Pendant Dmt-Tiq Analogues 12o and 12p



	R	K _i (nM)			EC ₅₀ (nM)			% Stimulation		
		KOR	MOR	DOR	KOR	MOR	DOR	KOR	MOR	DOR
12o		4.7 (0.5)	5.2 (1.0)	3.2 (0.6)	349 (112)	132 (76)	-	83 (14)	59 (1)	dns
12p		142 (23)	5.8 (1.6)	3.5 (0.7)	-	224** (84)	-	dns	43** (7)	dns

Binding affinity (K_i) values determined by competitive displacement of [³H]diprenorphine in membrane preparations from CHO cells expressing human KOR, MOR, or DOR. Potency (EC₅₀) and efficacy values determined by [³⁵S]GTPγS binding in the same membrane preparations. Efficacy expressed as percent stimulation versus standard agonist - U69,593 (KOR), DAMGO (MOR), or DPDPE (DOR). All values expressed as mean (SEM) of three or more separate assays run in duplicate unless otherwise indicated. **n=2; dns = does not stimulate, average maximal stimulation <10% at concentrations up to 10 μM

3.6 Nitrogen Scan of 7-Position 1-Naphthyl Pendant

Given the MOR/KOR profile of **12o**, a nitrogen scan was conducted to further explore the structure-activity relationships around the 1-naphthyl pendant. The introduction of a single nitrogen drops the clogP by approximately 1.5 units, making these analogues much more promising candidates for use in animal studies and clinical settings. Similar to the pyridyl analogues, synthetic difficulties prevented the synthesis and evaluation of the 1-isoquinoliny analogue.

3.6.1 Synthesis

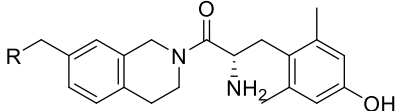
Compounds **12q-12v** were prepared according to the first synthetic route shown in Scheme 4. Detailed experimental procedures can be found in Chapter 6.

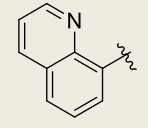
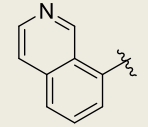
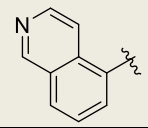
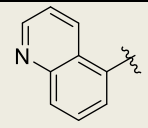
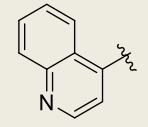
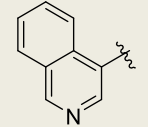
3.6.2 Pharmacological Evaluation

Overall, single digit nanomolar or stronger binding is observed at all three receptors for analogues in this series, and these compounds favor binding to DOR over MOR and KOR. The efficacy profiles of these analogues differ widely based on the

placement of the nitrogen. Only **12v** shows DOR agonism, and MOR and KOR activity ranges from no agonism to high efficacy across this series. Only **12t** displays the desired KOR agonist/MOR partial agonist profile. Notably, this compound is equipotent at KOR and MOR and is a promising candidate for further study. It is approximately three-fold selective for KOR and DOR over MOR which may lower the abuse potential of such a compound. **12u** displays no agonism at any of the receptors but high affinity for DOR, a profile similar to that of classic Dmt-Tiq compounds. Finally, **12v** has a potent KOR agonist/DOR partial agonist profile and is weakly selective for these two receptors over MOR. While interesting, this profile is likely clinically irrelevant. Ultimately, the addition of a single nitrogen to this ring results in compounds that show a wide range of multifunctional opioid profiles.

Table 8. Nitrogen Scan of 7-Position 1-Naphthyl Pendant on the Dmt-Tiq Scaffold: Binding, Potency, and Efficacy Data for Analogues 12q-12v



	R	K _i (nM)			EC ₅₀ (nM)			% Stimulation		
		KOR	MOR	DOR	KOR	MOR	DOR	KOR	MOR	DOR
12q		19 (2)	1.4 (0.3)	0.46 (0.08)	271** (13)	24 (4)	-	23** (3)	63 (8)	dns**
12r		2.7 (0.7)	1.8 (0.3)	0.69 (0.24)	65 (19)	24 (6)	-	42 (15)	36 (5)	dns**
12s		10 (1)	9.7 (1.4)	1.2 (0.2)	609 (226)	43 (21)	-	24 (3)	28 (8)	dns**
12t		1.5 (0.5)	4.6 (0.5)	1.2 (0.4)	58 (11)	54 (15)	-	69 (1)	31 (6)	dns**
12u		8.6 (0.4)	6.6 (1.0)	0.79 (0.25)	-	-	-	dns**	dns**	dns**
12v		0.73 (0.03)	1.4 (0.2)	0.30 (0.04)	14 (1)	-	19 (10)	71 (16)	dns**	39 (7)

Binding affinity (K_i) values determined by competitive displacement of [³H]diprenorphine in membrane preparations from CHO cells expressing human KOR, MOR, or DOR. Potency (EC₅₀) and efficacy values determined by [³⁵S]GTPγS binding in the same membrane preparations. Efficacy expressed as percent stimulation versus standard agonist - U69,593 (KOR), DAMGO (MOR), or DPDPE (DOR). All values expressed as mean (SEM) of three or more separate assays run in duplicate unless otherwise indicated. **n=2; dns = does not stimulate, average maximal stimulation <10% at concentrations up to 10 μM

3.7 Bicyclic Aliphatic 7-Position Pendant Analogues

Finally, bicyclic pendants with a saturated, cyclic amine attached to an aromatic ring were explored (Table 9).

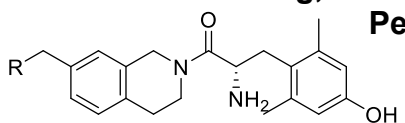
3.7.1 Synthesis

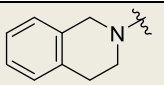
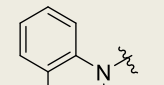
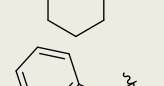
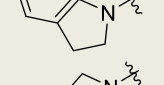
Compounds **12w-12z** were prepared according to the second synthetic route shown in Scheme 4. Detailed experimental procedures can be found in Chapter 6.

3.7.2 Pharmacological Evaluation

This subset of analogues displays two distinct profiles. **12x** and **12y** show balanced affinity and efficacy at KOR and MOR, while **12w** and **12z** display a loss in KOR binding and no KOR agonism. However, the latter two compounds show potent, moderate to high efficacy at MOR and strong binding but no agonism at DOR. This difference in profile is likely due to the placement of the second ring within the receptor binding site. As expected, those that would most closely mimic the 1-naphthyl pendant, **12w** and **12z**, exhibit a KOR agonist/MOR agonist profile. The binding and efficacy profile at KOR and MOR for these two compounds is remarkably balanced, though they are more potent at MOR (five-fold and two-fold, respectively). As discussed above, the higher MOR efficacy and potency of these compounds compared to others would likely impart greater addiction potential. On the other hand, those compounds which more closely mimic the 2-naphthyl pendant, **12w** and **12z**, show no KOR agonism, as expected. However, these analogues exhibit MOR agonism and DOR antagonism, a bifunctional profile being explored in the development of a less addictive treatment for pain.^{52,55,101} Both compounds display potent MOR agonism and selectivity for MOR and DOR over KOR (18-fold and 43-fold, respectively). In addition, **12z** shows balanced affinity at MOR and DOR, a quality previously explored by our group as a way to mitigate addiction potential.¹⁰² These compounds represent a starting point for further study for the development of a MOR agonist/DOR antagonist.

Table 9. Binding, Potency, and Efficacy Data for Bicyclic Aliphatic 7-Position Pendant Dmt-Tiq Analogues 12w-12z



	R	K _i (nM)			EC ₅₀ (nM)			% Stimulation		
		KOR	MOR	DOR	KOR	MOR	DOR	KOR	MOR	DOR
12w		42 (8)	0.6 (0.1)	2.3 (0.6)	-	8.2 (1.0)	-	dns	85 (9)	dns**
12x		7.1 (1.4)	7.2 (1.6)	6.6 (1.0)	375 (109)	73 (22)	-	67 (3)	65 (10)	dns**
12y		2.6 (0.6)	2.2 (0.6)	1.7 (0.5)	106 (20)	42 (10)	-	66 (8)	65 (5)	dns**
12z		65 (23)	1.5 (0.2)	1.3 (0.4)	-	27 (0.3)	-	dns	63 (10)	dns**

Binding affinity (K_i) values determined by competitive displacement of [³H]diprenorphine in membrane preparations from CHO cells expressing human KOR, MOR, or DOR. Potency (EC₅₀) and efficacy values determined by [³⁵S]GTPγS binding in the same membrane preparations. Efficacy expressed as percent stimulation versus standard agonist - U69,593 (KOR), DAMGO (MOR), or DPDPE (DOR). All values expressed as mean (SEM) of three or more separate assays run in duplicate unless otherwise indicated. **n=2; dns = does not stimulate, average maximal stimulation <10% at concentrations up to 10 μM

3.8 Conclusions

Further exploration surrounding the 7-position pendant on the tetrahydroisoquinoline ring of the classically DOR antagonist selective Dmt-Tiq scaffold revealed that this scaffold can be used to create novel opioid ligands with a variety of multifunctional profiles. We have further elucidated structure-activity relationships in this region and developed compounds with pharmacological profiles being explored for a variety of therapeutic uses.

As shown in Chapter 2, ortho and meta substitution on a 7-benzyl pendant on the Dmt-Tiq scaffold show promise for the development of a KOR agonist/MOR partial agonist ligand. The exploration of additional substituents at these positions revealed that this trend holds for a larger selection of ortho and meta substituents. However, the increased MOR potency and efficacy for some of these compounds is likely to impart

abuse potential, limiting the ability of certain analogues to be developed for clinical use. Replacement of one atom in the benzyl pendant ring with a nitrogen resulted in a drastic loss of KOR potency, and replacement of the benzyl ring with a saturated, cyclic amine resulted in abolishment of KOR agonism.

Naphthyl pendant analogues, though too lipophilic for use in animal or clinical studies, provided proof of concept that larger pendants may be tolerated if they fit into an available pocket of the KOR binding site. A nitrogen scan of the 1-naphthyl ring resulted in compounds with a vast array of multifunctional opioid profiles, including a promising KOR/MOR candidate (**12t**). Finally, the combination of a cyclic amine with an aromatic ring linked by a methylene to the 7-position of Tiq resulted in two distinct pharmacological profiles – balanced KOR/MOR agonism and MOR agonism/DOR antagonism.

In conclusion, ortho substituted analogues (especially **12b**) and select bicyclic pendant analogues (especially **12t**) show promise for the development of a KOR agonist/MOR partial agonist, a profile being investigated for the treatment of cocaine addiction. Two bicyclic pendant analogues, **12w** and **12z**, exhibit a balanced MOR agonist/DOR antagonist profile and have potential to be investigated as a treatment for pain with lowered addiction potential. These compounds are promising candidates for further development and *in vivo* investigation.

Chapter 4

Exploration of Non-Pendant Regions of Dimethyltyrosine-Tetrahydroisoquinoline Opioid Peptidomimeticsⁱⁱⁱ

4.1 Introduction

As discussed and demonstrated in previous chapters, small changes in ligand structure can result in drastic changes in opioids' pharmacological profiles. As a result, we sought to explore structure-activity relationships around areas of the repurposed dimethyltyrosine-tetrahydroisoquinoline (Dmt-Tiq) scaffold beyond the 7-position pendant on the tetrahydroisoquinoline (Tiq). The work discussed here includes minor alteration to the dimethyltyrosine (Dmt) portion of this scaffold as well as modification of the linker between the Tiq core and the pendant in the 7- and 8-positions.

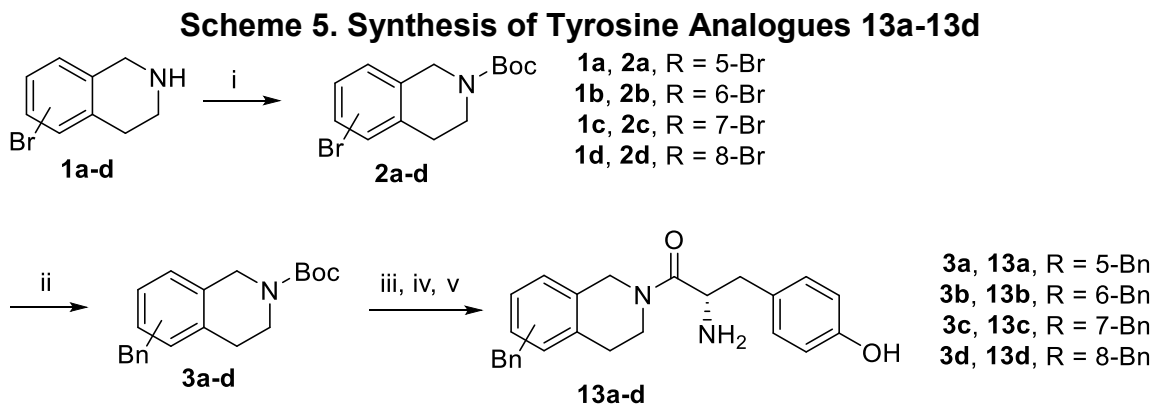
4.2 Substitution of Dimethyltyrosine with Tyrosine

The importance of dimethyltyrosine in the creation of opioid peptides and peptidomimetics is well-documented.¹⁰³ The use of this residue arose from modification of the tyrosine (Tyr) residue in opioid peptides modeled after endogenous opioids. We sought to explore the effects of removing this conformational restriction by trading the dimethyltyrosine residue for a tyrosine residue in this series. Tyrosine analogues have lower molecular weight and lower clogP, two favorable changes for increasing the "drug-likeness" of this series. In addition, the synthesis of tyrosine analogues is more time- and cost- effective, allowing them to be more easily translated into animal studies and clinical settings.

ⁱⁱⁱ Compounds **25a-25d** were synthesized by Mason A. Baber under the direction of the author of this dissertation.

4.2.1 Synthesis

Synthesis of dimethyltyrosine analogues (**4a-4d**) is described in Chapter 2. Tyrosine analogues (**13a-13d**) were prepared according to the synthetic route shown in Scheme 5. Commercially available bromo-substituted tetrahydroisoquinolines **1a-1d** were Boc-protected, and the resulting bromides **2a-2d** were coupled to benzylboronic acid pinacol ester via Suzuki reaction to produce intermediates **3a-3d**. Deprotection of the tetrahydroisoquinoline nitrogen with hydrochloric acid, peptide coupling with Boc-protected tyrosine, and subsequent deprotection with trifluoroacetic acid yielded peptidomimetics **13a-13d**. Detailed experimental procedures can be found in Chapter 6.



(i) Boc_2O ; (ii) benzylboronic acid pinacol ester, $\text{Pd}(\text{dppf})\text{Cl}_2$, K_2CO_3 , acetone/water; (iii) HCl , 1,4-dioxane; (iv) Boc-Tyr-OH , PyBOP , 6Cl-HOBt , DIEA , DMF ; (v) TFA , DCM

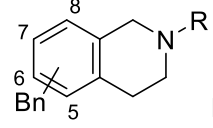
4.2.2 Pharmacological Evaluation

The binding and efficacy profile of each compound was determined individually at KOR, MOR, and DOR. Binding at each receptor was evaluated by competitive displacement of [^3H]diprenorphine, and efficacy and potency were determined by a [^{35}S]GTP γS binding assay. Reported percent stimulation values are from comparison to

a standard agonist for each receptor and are used as a surrogate for efficacy. Detailed experimental procedures can be found in Chapter 6.

Table 10 shows binding and efficacy data for benzyl pendant Dmt-Tiq compounds (also reported in Chapter 2) and their tyrosine analogues. First, we explored the substitution of tyrosine into the 5-benzyl Dmt-Tiq compound (**13a**). Surprisingly, this compound shows only a small (~4-fold) loss in binding at MOR compared to the parent Dmt analogue. It also displays low potency but high efficacy at MOR. Given this interesting result, we explored incorporating Tyr into the other benzyl pendant compounds in this series, hypothesizing that the methyl groups on the Tyr ring may not be necessary for opioid activity in this series. However, we observed drastically reduced binding across the opioid receptors for these analogues. The results shown in Table 10 confirm the importance of dimethyltyrosine for the opioid activity of this series.

Table 10. Substitution of Dimethyltyrosine with Tyrosine in Benzyl Pendant Dmt-Tiq compounds: Binding, Potency, and Efficacy Data for Analogues 13a-13d



	R	R	K _i (nM)			EC ₅₀ (nM)			% Stimulation		
			KOR	MOR	DOR	KOR	MOR	DOR	KOR	MOR	DOR
4a	5-Bn	Dmt	112 (13)	17 (5)	3.3 (0.2)	-	-	-	dns	dns	dns
4b	6-Bn	Dmt	38 (5)	9.9 (1.6)	4.3 (0.6)	-	-	-	dns	dns	dns
4c	7-Bn	Dmt	3.9 (0.8)	2.7 (0.8)	6.1 (2.1)	33 (6)	-	-	85 (8)	dns	dns
4d	8-Bn	Dmt	26 (5)	4.1 (0.4)	185 (28)	319 (45)	-	-	46 (6)	dns	dns
13a	5-Bn	Tyr	1400*	74 (6)	500** (12)	-	943** (225)	-	dns*	65** (1)	dns*
13b	6-Bn	Tyr	1250** (170)	6100** (2300)	8100	-	-	-	dns*	dns*	dns*
13c	7-Bn	Tyr	650*	1700*	1000*	-	-	-	dns*	dns*	dns*
13d	8-Bn	Tyr	2000*	3500** (600)	7200	-	-	nd	dns*	dns**	nd

Binding affinity (K_i) values determined by competitive displacement of [³H]diprenorphine in membrane preparations from CHO cells expressing human KOR or C6 cells expressing rat MOR or rat DOR. Potency (EC₅₀) and efficacy values determined by [³⁵S]GTPγS binding in the same membrane preparations. Efficacy expressed as percent stimulation versus standard agonist - U69,593 (KOR), DAMGO (MOR), or DPDPE (DOR). All values expressed as mean (SEM) of three or more separate assays run in duplicate unless otherwise noted. *n=1; **n=2; nd = no data; Bn = benzyl; Dmt = dimethyltyrosine; Tyr = tyrosine; dns = does not stimulate, average maximal stimulation <10% at concentrations up to 10 μM

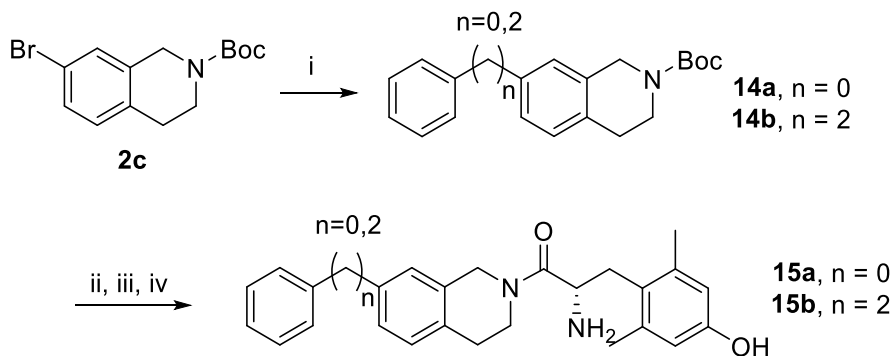
4.3 Exploration of Linker Length in 7- and 8-Substituted Analogues

Given the observed KOR agonism of 7-benzyl analogue **4c** and 8-benzyl analogue **4d**, reported in Chapter 2 and Table 10, we decided to explore the length of the linker between the Tiq core and these pendants. The linker was eliminated in the synthesis of phenyl analogues and extended by one methylene unit in the synthesis of phenethyl analogues.

4.3.1 Synthesis

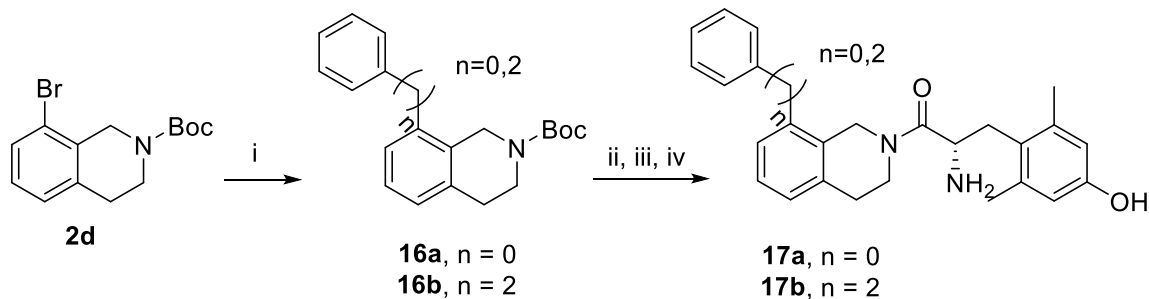
Synthesis of benzyl analogues (**4c**, **4d**) is described in Chapter 2. Phenyl (**15a**, **17a**) and phenethyl (**15b**, **17b**) analogues were prepared according to the synthetic routes shown in Scheme 6 and Scheme 7. Synthesis of intermediates **2c** and **2d** from commercially available bromo-substituted tetrahydroisoquinolines is described in Chapter 2. The appropriate Boc-protected bromotetrahydroisoquinoline was coupled to phenyl boronic acid or phenethyl boronic acid via Suzuki reaction to produce intermediates **14a**, **16a**, **14b**, or **16b**. Deprotection of the tetrahydroisoquinoline nitrogen with hydrochloric acid, peptide coupling with diBoc-protected dimethyltyrosine, and subsequent deprotection with trifluoroacetic acid yielded peptidomimetics **15a**, **15b**, **17a**, and **17b**. Detailed experimental procedures can be found in Chapter 6.

Scheme 6. Synthesis of 7-Phenyl and 7-Phenethyl Pendant Dmt-Tiq Analogues **15a** and **15b**



(i) phenyl boronic acid or phenethyl boronic acid, Pd(dppf)Cl₂, K₂CO₃, 3:1 acetone:water; (ii) HCl, 1,4-dioxane; (iii) diBoc-Dmt, PyBOP, 6Cl-HOBt, DIEA, DMF; (iv) TFA, DCM

Scheme 7. Synthesis of 8-Phenyl and 8-Phenethyl Pendant Dmt-Tiq Analogues **17a** and **17b**

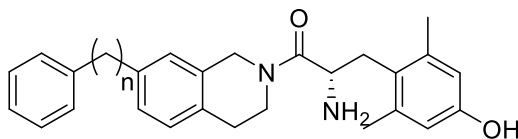


(i) phenyl boronic acid or phenethyl boronic acid, Pd(dppf)Cl₂, K₂CO₃, 3:1 acetone:water; (ii) HCl, 1,4-dioxane; (iii) diBoc-Dmt, PyBOP, 6Cl-HOBt, DIEA, DMF; (iv) TFA, DCM

4.3.2 Pharmacological Evaluation

Table 11 shows binding and efficacy data for 7-phenyl, benzyl, and phenethyl pendant Dmt-Tiq analogues **15a**, **4c**, and **15b**. Elimination of the linker (**15a**) results in a loss in binding across the opioid receptors, most drastically at KOR. This analogue also shows no KOR agonism. On the other hand, extension of the linker to two carbons (**15b**) maintains single digit nanomolar binding at each of the opioid receptors. This compound also displays a promising KOR agonist/MOR partial agonist profile. Of note, this compound shows equal affinity for KOR and MOR, but is slightly more potent at KOR. This compound represents a good starting point for further exploration of structure-activity relationships towards the development of a multifunctional KOR/MOR ligand. However, analogues of the 7-benzyl compound (**4c**) were selected for further exploration instead because they were more synthetically tractable.

Table 11. Modification of Linker Length in 7-Substituted Dmt-Tiq Compounds: Binding, Potency, and Efficacy Data for Analogues 15a and 15b

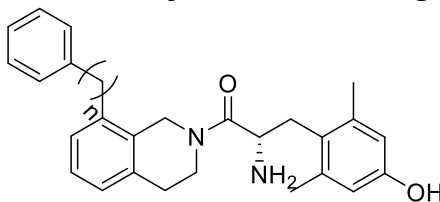


	n	K _i (nM)			EC ₅₀ (nM)			% Stimulation		
		KOR	MOR	DOR	KOR	MOR	DOR	KOR	MOR	DOR
15a	0	201** (24)	7.7 (4.2)	28 (5)	-	-	-	dns**	dns**	dns**
4c	1	3.9 (0.8)	2.7 (0.8)	6.1 (2.1)	33 (6)	-	-	85 (8)	dns	dns
15b	2	4.8 (1.0)	5.4 (1.9)	5.6** (1.4)	124 (11)	241 (53)	-	80 (8)	23 (1)	dns**

Binding affinity (K_i) values determined by competitive displacement of [³H]diprenorphine in membrane preparations from CHO cells expressing human KOR or C6 cells expressing rat MOR or rat DOR. Potency (EC₅₀) and efficacy values determined by [³⁵S]GTPγS binding in the same membrane preparations. Efficacy expressed as percent stimulation versus standard agonist - U69,593 (KOR), DAMGO (MOR), or DPDPE (DOR). All values expressed as mean (SEM) of three or more separate assays run in duplicate unless otherwise noted. **n=2; dns = does not stimulate, average maximal stimulation <10% at concentrations up to 10 μM

Table 12 shows binding and efficacy data for 8-phenyl, benzyl, and phenethyl pendant Dmt-Tiq analogues **17a**, **4d**, and **17b**. As in the 7-substituted series, elimination of the linker (**17a**) between the 8-position pendant and the Tiq core results in substantial loss of binding across the opioid receptors and no agonism. In this series, extending the linker by one carbon (**17b**) maintains KOR and MOR binding and increases DOR affinity; however, there is a notable loss of potency and efficacy at KOR. Ultimately, the 7-substituted series shows much more promise for the development of KOR/MOR ligands than the 8-substituted series.

Table 12. Modification of Linker Length in 8-Substituted Dmt-Tiq Compounds: Binding, Potency, and Efficacy Data for Analogues 17a and 17b



	n	K _i (nM)			EC ₅₀ (nM)			% Stimulation		
		KOR	MOR	DOR	KOR	MOR	DOR	KOR	MOR	DOR
17a	0	542 (117)	155 (36)	1850** (610)	-	-	-	dns**	dns**	dns*
4d	1	26 (5)	4.1 (0.4)	185 (28)	319 (45)	-	-	46 (6)	dns	dns
17b	2	25 (5)	3.5 (0.6)	30 (5)	559 (21)	-	-	20 (1)	dns**	dns**

Binding affinity (K_i) values determined by competitive displacement of [³H]diprenorphine in membrane preparations from CHO cells expressing human KOR or C6 cells expressing rat MOR or rat DOR. Potency (EC₅₀) and efficacy values determined by [³⁵S]GTPγS binding in the same membrane preparations. Efficacy expressed as percent stimulation versus standard agonist - U69,593 (KOR), DAMGO (MOR), or DPDPE (DOR). All values expressed as mean (SEM) of three or more separate assays run in duplicate unless otherwise noted. *n=1; **n=2; dns = does not stimulate, average maximal stimulation <10% at concentrations up to 10 μM

4.4 Carbonyl-containing Linker Modifications

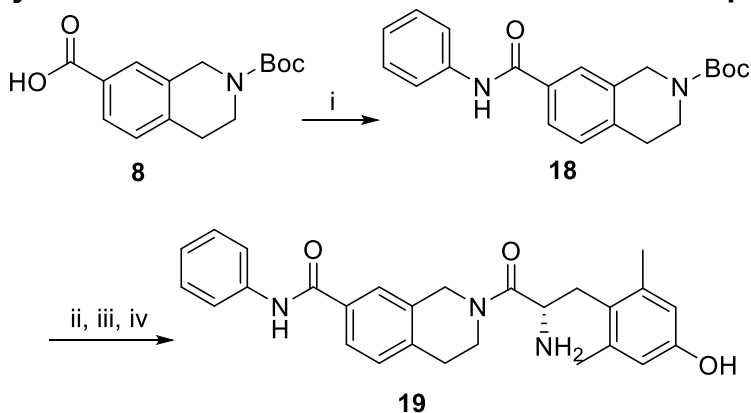
Based on the promising KOR/MOR profile of the 7-phenethyl analogue (**15b**), other analogues with two-atom linkers were synthesized. Due to the change in screening paradigm discussed in Chapter 3, these analogues were evaluated only at human opioid receptors. For this reason, the data shown in tables below cannot be directly compared to the data for **15b** shown in Table 13.

4.4.1 Synthesis

Synthesis of Amide Linker Analogue 19. Analogue **19** was prepared according to the synthetic route shown in Scheme 8. Commercially available carboxylic acid **8** was coupled to aniline to yield intermediate **18**. Deprotection of the tetrahydroisoquinoline nitrogen with hydrochloric acid, peptide coupling with diBoc-protected dimethyltyrosine,

and subsequent deprotection with trifluoroacetic acid yielded peptidomimetic **19**. Detailed experimental procedures can be found in Chapter 6.

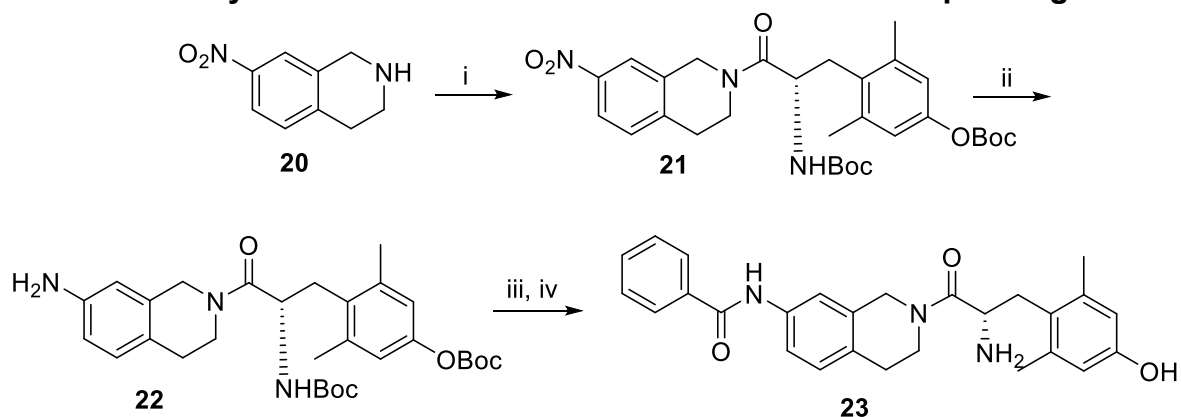
Scheme 8. Synthesis of Amide Linker 7-Substituted Dmt-Tiq Analogue 19



(i) aniline, PyBOP, DMF; (ii) HCl, 1,4-dioxane; (iii) diBoc-Dmt, PyBOP, 6Cl-HOBt, DIEA, DMF; (iv) TFA, DCM

Synthesis of Amide Linker Analogue 23. Analogue **23** was prepared according to the synthetic route shown in Scheme 9. 7-nitrotetrahydroisoquinoline (**20**) was coupled to diBoc-protected dimethyltyrosine to produce intermediate **21**, and the nitro group was reduced with zinc dust and ammonium chloride in acetone and water. Coupling of intermediate **22** to benzoic acid and subsequent removal of the Boc groups with trifluoroacetic acid yielded peptidomimetic **23**. Detailed experimental procedures can be found in Chapter 6.

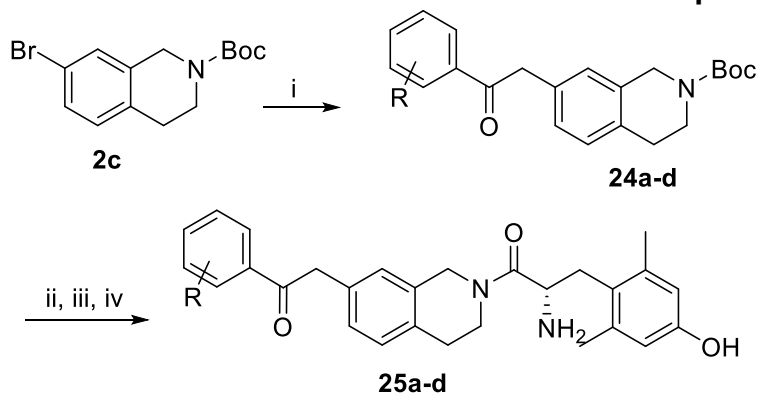
Scheme 9. Synthesis of Amide Linker 7-Substituted Dmt-Tiq Analogue 23



(i) diBoc-Dmt, PyBOP, DIEA, DMF; (ii) Zn, NH₄Cl, acetone/water; (iii) benzoic acid, PyBOP, DIEA, DMF; (iv) TFA, DCM

Synthesis of Ketone Linker Analogues 25a-25d. Analogues **25a-25d** were prepared according to the synthetic route shown in Scheme 10. Synthesis of intermediate **2c** from commercially available 7-bromotetrahydroisoquinoline is described in Chapter 2. Intermediates **24a-24d** were prepared from the palladium-catalyzed coupling of **2c** and substituted acetophenones. Deprotection of the tetrahydroisoquinoline nitrogen with hydrochloric acid, peptide coupling with diBoc-protected dimethyltyrosine, and subsequent deprotection with trifluoroacetic acid yielded peptidomimetics **25a-25d**. Detailed experimental procedures can be found in Chapter 6.

Scheme 10. Synthesis of Ketone Linker 7-Substituted Dmt-Tiq Analogues 25a-25d

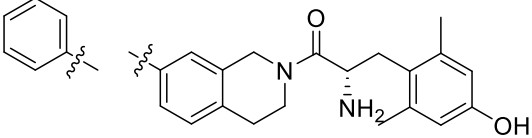


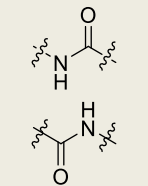
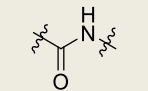
(i) substituted acetophenone, Pd₂(dba)₃, BINAP, NaOtBu, THF; (ii) HCl, 1,4-dioxane; (iii) diBoc-Dmt, PyBOP, DIEA, DMF; (iv) TFA, DCM

4.4.2 Pharmacological Evaluation

Table 13 shows pharmacological data for analogues of **15b** in which the two methylene units have been replaced by an amide. For both orientations of the amide, affinity is highest at MOR then DOR then KOR. These compounds (**19**, **23**) show no KOR or DOR agonism and partial agonism or no agonism at MOR.

Table 13. Binding, Potency, and Efficacy Data for Amide Linker 7-Substituted Dmt-Tiq Analogues 19 and 23

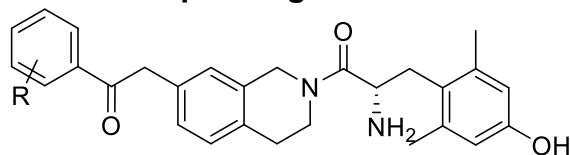


		K _i (nM)			EC ₅₀ (nM)			% Stimulation		
		KOR	MOR	DOR	KOR	MOR	DOR	KOR	MOR	DOR
19		294 (44)	5.5 (1.3)	11.3 (2.2)	-	193** (59)	-	dns	47** (6)	dns
23		64 (26)	7.5 (1.8)	14.5 (2.1)	-	-	-	dns	dns**	dns

Binding affinity (K_i) values determined by competitive displacement of [³H]diprenorphine in membrane preparations from CHO cells expressing human KOR, MOR, or DOR. Potency (EC₅₀) and efficacy values determined by [³⁵S]GTPγS binding in the same membrane preparations. Efficacy expressed as percent stimulation versus standard agonist - U69,593 (KOR), DAMGO (MOR), or DPDPE (DOR). All values expressed as mean (SEM) of three or more separate assays run in duplicate unless otherwise noted. **n=2; dns = does not stimulate, average maximal stimulation <10% at concentrations up to 10 μM

An analogue of **15b** with a two-atom linker containing a ketone adjacent to the aromatic ring of the pendant (**25a**) was also synthesized. A methyl scan was performed around the pendant aromatic ring (**25b-25d**). Data for these compounds are shown in Table 14. Overall, these compounds display single digit nanomolar binding across the opioid receptors and have highest affinity for DOR. All of the analogues in this series show agonism at KOR and MOR; however, each analogue is more potent and efficacious at MOR than KOR, a profile undesirable for the development of a KOR agonist/MOR partial agonist.

Table 14. Binding, Potency, and Efficacy Data for Ketone Linker 7-Substituted Dmt-Tiq Analogues 25a-25d



	R	K _i (nM)			EC ₅₀ (nM)			% Stimulation		
		KOR	MOR	DOR	KOR	MOR	DOR	KOR	MOR	DOR
25a	H	14 (3)	24 (9)	2.2*	1500 (300)	235 (74)	-	48 (6)	75 (10)	dns*
25b	p-Me	5.3 (1.6)	5.8 (1.9)	1.3 (0.2)	262** (4)	91** (61)	-	19** (1)	57** (0.5)	dns*
25c	m-Me	4.5 (0.7)	4.2 (1.3)	0.33** (0.04)	532 (189)	12.8** (5.4)	-	22 (4)	53** (2)	dns*
25d	o-Me	4.3 (1.4)	1.3 (0.3)	1.3** (0.2)	297 (152)	30** (18)	-	40 (4)	65** (3)	dns*

Binding affinity (K_i) values determined by competitive displacement of [³H]diprenorphine in membrane preparations from CHO cells expressing human KOR, MOR, or DOR. Potency (EC₅₀) and efficacy values determined by [³⁵S]GTPγS binding in the same membrane preparations. Efficacy expressed as percent stimulation versus standard agonist - U69,593 (KOR), DAMGO (MOR), or DPDPE (DOR). All values expressed as mean (SEM) of three or more separate assays run in duplicate unless otherwise noted. *n=1; **n=2; Me = methyl; dns = does not stimulate, average maximal stimulation <10% at concentrations up to 10 μM

4.5 Aniline Linker Analogue

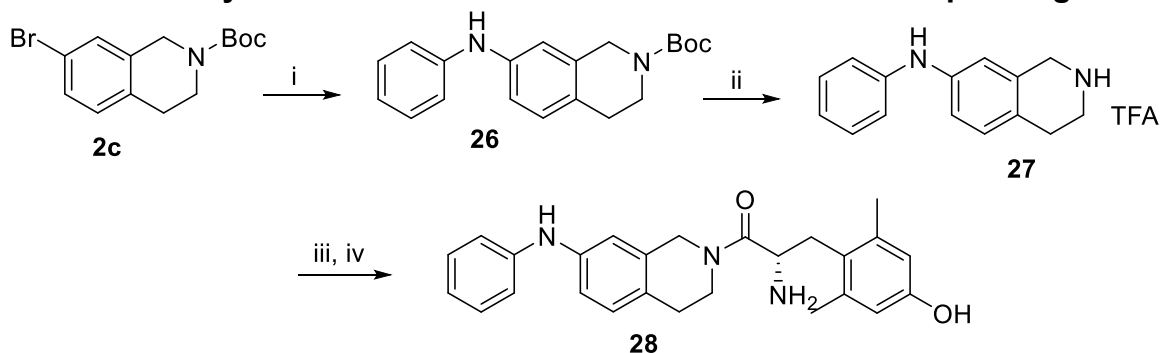
Substitution of the methylene linker in **4c** with a heteroatom allows for further exploration of the structure-activity relationships of this region. Though several possible heteroatoms may be incorporated, only the aniline analogue (**28**) was successfully synthesized. This compound was evaluated at human opioid receptors, and human receptor data for **4c** is shown in Table 15 for direct comparison.

4.5.1 Synthesis

Analogue **28** was prepared according to the synthetic route shown in Scheme 11. Synthesis of intermediate **2c** from commercially available 7-bromotetrahydroisoquinoline is described in Chapter 2. Intermediate **26** was prepared from the palladium-catalyzed coupling of **2c** and aniline. The Boc group was removed from the tetrahydroisoquinoline nitrogen with trifluoroacetic acid to yield TFA salt **27**.

Finally, peptide coupling with diBoc-protected dimethyltyrosine and subsequent deprotection with trifluoroacetic acid yielded peptidomimetics **28**. Detailed experimental procedures can be found in Chapter 6.

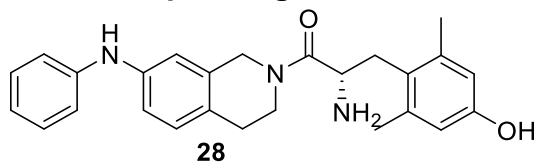
Scheme 11. Synthesis of Aniline Linker 7-Substituted Dmt-Tiq Analogue 28



4.5.2 Pharmacological Evaluation

Results of the pharmacological evaluation of **28** are shown in Table 15. The replacement of the methylene linker of **4c** with an aniline linker results in a loss of KOR binding and a complete loss of KOR agonism. However, **28** maintains single digit nanomolar binding at MOR and DOR and moderate potency and efficacy at MOR with no DOR agonism. As such, **28** represents a good starting point for the development of a MOR agonist/DOR antagonist ligand.

Table 15. Binding, Potency, and Efficacy Data for Aniline Linker 7-Substituted Dmt-Tiq Analogue 28



	X	K _i (nM)			EC ₅₀ (nM)			% Stimulation		
		KOR	MOR	DOR	KOR	MOR	DOR	KOR	MOR	DOR
4c	CH ₂	2.3 (0.3)	5.3 (0.5)	3.0** (1.1)	97 (24)	68 (15)	7.0** (2.0)	82 (6)	39 (4)	18** (4)
28	NH	70** (2)	3.3** (0.3)	6.0** (1.5)	-	22** (8)	-	dns	65** (4)	dns

Binding affinity (K_i) values determined by competitive displacement of [³H]diprenorphine in membrane preparations from CHO cells expressing human KOR, MOR, or DOR. Potency (EC₅₀) and efficacy values determined by [³⁵S]GTPγS binding in the same membrane preparations. Efficacy expressed as percent stimulation versus standard agonist - U69,593 (KOR), DAMGO (MOR), or DPDPE (DOR). All values expressed as mean (SEM) of three or more separate assays run in duplicate unless otherwise noted. **n=2; dns = does not stimulate, average maximal stimulation <10% at concentrations up to 10 μM

4.6 Conclusions

Despite unusual MOR activity of the 5-benzyl tyrosine analogue (**13a**), the synthesis of tyrosine analogues of benzyl pendant Dmt-Tiq compounds confirmed the necessity of the dimethyltyrosine residue for opioid binding and activity. Shortening and lengthening the linker between the tetrahydroisoquinoline core and the pendant in the 7- and 8-positions further elucidated the structure-activity relationships in this region. Analogues with 8-position pendants show little to no KOR agonism and are not useful in the development of opioid ligands with pharmacologically useful multifunctional profiles. On the other hand, 7-position pendant analogues show significant promise for the development of KOR agonist/MOR partial agonist ligands. Pharmacological data for the 7-phenyl analogue (**15a**) compared to the 7-benzyl (**4c**) and 7-phenethyl (**15b**) analogues confirms that a linker of some sort is necessary for KOR activity. Because of the high KOR efficacy and potency of the 7-benzyl analogue (**4c**) and the synthetic tractability of benzyl pendant analogues, this compound served as a lead compound for

the development of many multifunctional opioid ligands in this series, described in Chapter 2 and Chapter 3. The 7-phenethyl analogue (**15b**) shows a promising KOR agonist/MOR partial agonist profile and is a useful starting point for future exploration.

Modifications to the two-atom linker were explored through the synthesis of 7-substituted Dmt-Tiq compounds that mimic **15b**. Replacement of the two-carbon linker with an amide (**19**, **23**) eliminates KOR agonism, while incorporation of a ketone at the carbon adjacent to the pendant (**25a**) reverses the pharmacological profile. A methyl scan around the aromatic ring of the pendant (**25b-25d**) confirmed that this linker consistently imparts higher efficacy at MOR than KOR. Finally, replacement of the methylene linker with an aniline (**28**) results in a promising lead for the development of a MOR agonist/DOR antagonist compound. Ultimately, modification of the linker in 7-substituted Dmt-Tiq compounds results in the creation of novel opioids with a variety of multifunctional profiles, some of which have therapeutic potential.

Chapter 5

Conclusions and Future Directions^{iv}

5.1 Summary

For hundreds, if not thousands, of years, opioids have been important medicinal compounds. This class of drugs has been used widely in the treatment of pain and other conditions. Recent decades have seen a shift away from the development of selective opioids as the complex pharmacology of this system has been revealed. The advent of multifunctional opioid ligands, compounds which act simultaneously at more than one type of opioid receptor, has opened new doors for the development of useful chemical and pharmacological probes and therapeutics.

Because relatively minor structural modifications often result in significant changes in the pharmacological profiles of opioid ligands, selective scaffolds represent an important starting point for the creation and discovery of multifunctional compounds. The dimethyltyrosine-tetrahydroisoquinoline (Dmt-Tiq) scaffold is well-known in the opioid literature as the basis for a series of delta opioid receptor (DOR) antagonist selective peptides. Many Dmt-Tiq compounds have been reported, but the constraints of traditional peptide synthesis have previously limited the structural diversity of these analogues. Here, using synthetic methods often applied to the creation of small molecules, we introduced previously unexplored modifications to this scaffold to convert the pharmacological profile from selective to multifunctional.

^{iv} The *in vivo* studies discussed at the end of this chapter are being conducted by Bryan Sears under the direction of Dr. Emily M. Jutkiewicz.

The installation of a benzyl pendant at each position of the Tiq aromatic ring at the core of the Dmt-Tiq scaffold revealed that a 7-benzyl pendant could introduce kappa opioid receptor (KOR) agonism. As a result, the 7-benzyl Dmt-Tiq analogue (**4c**) was used as a lead compound to further explore structure-activity relationships (SAR) in this new series and create a variety of multifunctional opioid ligands. Further substitution on this pendant created compounds (**7d**, **7g**) that exhibit a KOR agonist/mu opioid receptor (MOR) partial agonist profile, which is being explored for the treatment of addiction to cocaine and other drugs of abuse.

These initial results led to further exploration of the SAR surrounding this new 7-position pendant on the Dmt-Tiq scaffold. Ortho and meta substituents on the benzyl ring reliably resulted in a KOR agonist/MOR partial agonist profile, with **12b** being one of the most promising compounds in this series because of its high affinity and potency for KOR and MOR. Other 7-position pendants imparted different profiles. Most notably, introduction of a tetrahydroisoquinoline pendant (**12w**) or isoindoline pendant (**12z**) resulted in a MOR agonist/DOR antagonist profile. These compounds have potential to be explored as a treatment for pain with lowered addiction potential.

Finally, we explored the SAR around non-pendant regions of this new series. Replacement of dimethyltyrosine with tyrosine resulted in a dramatic loss of opioid activity, consistent with previous results in opioid peptides and peptidomimetics. Modification of the linker between the 7-position pendant and the Tiq core revealed that a two-carbon linker imparts a KOR agonist/MOR partial agonist profile. Addition of a ketone in the linker adjacent to the aromatic ring of the pendant resulted in compounds that are more potent and efficacious at MOR than KOR. Introduction of an aniline linker

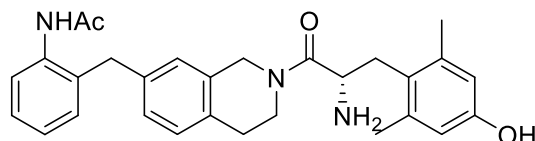
decreased KOR affinity and abolished KOR agonism, but this compound (**28**) may represent a promising lead for the development of a MOR agonist/DOR antagonist.

Ultimately, the work presented here describes novel structural modifications to the classically DOR antagonist selective Dmt-Tiq scaffold that result in the development of multifunctional opioid ligands with a variety of pharmacologically useful profiles.

5.2 Additional Analogues

The results reported in Chapters 2-4 introduce avenues for additional structural modifications to further evaluate the SAR of this novel series of Dmt-Tiq peptidomimetics. Based on the consistent results of ortho and meta substituents on the 7-benzyl pendant imparting KOR agonism and MOR partial agonism, further substitution at these positions should be explored. From a nearly endless list of possible substituents, ones with hydrogen bond donating groups at the ortho position may show the most promise for development of KOR/MOR ligands. As reported in Chapter 3, the ortho hydroxy analogue (**12b**) shows higher affinity for KOR than do similar analogues. Though we were not able to identify a specific interaction between this substituent and the receptor in our modeling studies, it is possible that a water-mediated hydrogen bond is responsible for this higher affinity. A proposed future analogue that also has a hydrogen bond donor, an acetylated aniline, at this position is shown in Figure 13.

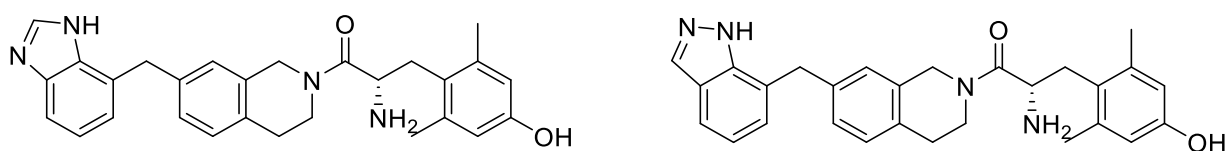
Figure 13. Structure of Proposed Acetylated Aniline Analogue



Proposed future analogue with a hydrogen bond donor, acetylated aniline, at the ortho position of the 7-benzyl pendant on the Dmt-Tiq scaffold

Additionally, bicyclic analogues which mimic the 1-naphthyl pendant show promise for the development of a KOR/MOR ligand. Select analogues in Chapter 3 with bicyclic pendants (**12o**, **12t**, **12x**, **12y**) show KOR agonism and MOR agonism and represent a starting point for further exploration. In particular, heterocyclic bicycle pendants show promise for the development of a KOR/MOR ligand with the desired pharmacological profile and improved pharmacokinetic properties due to the lower clogP of such analogues. Two of these possible analogues are shown in Figure 14. Initial attempts at synthesis of these analogues were unsuccessful, but a variety of alternative synthetic possibilities remain to be explored.

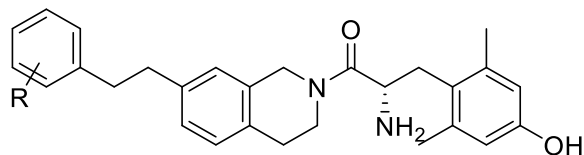
Figure 14. Structures of Proposed Heterocyclic Bicycle Pendant Analogues



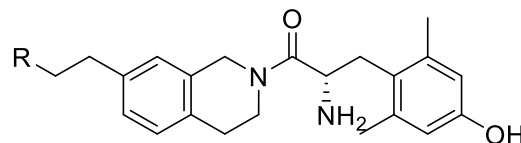
Proposed future analogues with heterocyclic bicycle pendants at the Tiq 7-position of the Dmt-Tiq scaffold

Linker modifications represent another promising area for exploration in this series. The 7-phenethyl Dmt-Tiq analogue (**15b**) displays a KOR agonist/MOR partial agonist profile. Analogues containing this two-carbon linker with a modified pendant represent a large possible area of exploration in the development of multifunctional opioid ligands. Synthetic difficulties prevented the synthesis of methyl-substituted analogues of **15b** in initial attempts, but future work could explore these and other substitutions on the aromatic ring as well as replacement of the aromatic ring with other pendants. A sample of these compounds is shown in Figure 15. Additionally, conformational restriction could be added through synthesis of **15b** analogues with unsaturated linkers. These proposed analogues are shown in Figure 16.

Figure 15. Structures of Proposed Two-Carbon Linker Analogues



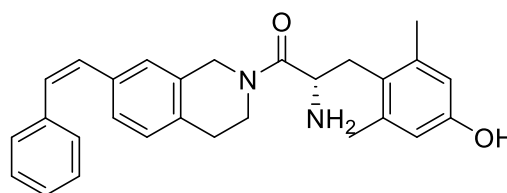
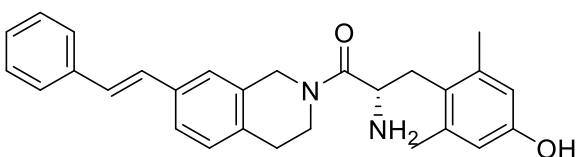
R = Me, OH, OMe



R = piperidine, pyrrolidine, thiophene

Proposed future analogues with two-carbon linker between the 7-position pendant and the Tiq core of the Dmt-Tiq scaffold

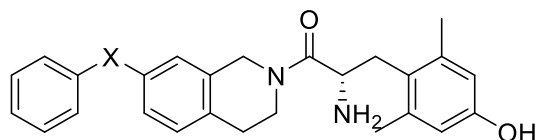
Figure 16. Structures of Proposed Unsaturated Two-Carbon Linker Analogues



Proposed future analogues with unsaturated two-carbon linker between the 7-position pendant and the Tiq core of the Dmt-Tiq scaffold

Further modification of the linker also represents a promising area of study. As reported in Chapter 4, replacement of the methylene linker of **4c** with an aniline linker resulted in a MOR agonist/DOR antagonist (**28**). The incorporation of other heteroatom linkers may result in this or other interesting multifunctional profiles. Some possible analogues with heteroatom linkers are shown in Figure 17.

Figure 17. Structures of Proposed Heteroatom Linker Analogues



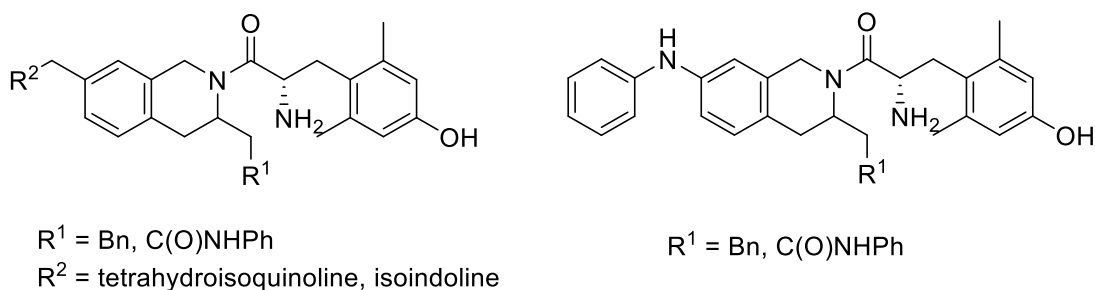
X = O, S, SO₂, SO₄

Proposed future analogues with heteroatom linkers between the 7-position pendant and the Tiq core of the Dmt-Tiq scaffold

5.3 Combination of Substitution at the 3-Position and 7-Position of Tiq

Previous reports in the literature have shown that modification at the 3-position of the tetrahydroisoquinoline ring of DMT-Tiq peptides can allow them to manifest binding and agonism at MOR.^{73,76,104} As a result, these compounds show promise for the development of a MOR agonist/DOR antagonist ligand. Some of the compounds we report here also show potential for the development of this profile. Thus, combining these substitutions represents a promising avenue for further exploration of the structure-activity relationships of Dmt-Tiq peptidomimetics with the goal of developing MOR/DOR ligands. In particular, compounds with 3-substitution and a tetrahydroisoquinoline or isoindoline pendant or an aniline linker at the 7-position would be interesting starting points for further development. Structures for these proposed compounds are shown in Figure 18.

Figure 18. Structures of Proposed 3- and 7-Substituted Analogues



Proposed future analogues with 3- and 7-substitution on the Tiq core of the Dmt-Tiq scaffold

5.4 Future *in Vivo* Testing

A variety of studies to examine the *in vivo* pharmacology of the novel opioid ligands reported here are already underway. Because kappa opioid receptor agonists have been reported to increase urination, the *in vivo* effects of **4c**, **7d**, and **7g** are being evaluated in mice in a micturition assay. The effects of administration of these compounds on the effects of other KOR agonists is also being examined. Other

promising candidates for *in vivo* evaluation include **12b**, **12t**, and **15b**. Compounds with promising *in vitro* and *in vivo* KOR/MOR profiles will be further screened for effects on cocaine self-administration,^{105,106} cocaine discrimination,¹⁰⁷ and conditioned place preference.^{108–110}

Compounds with promising MOR agonist/DOR antagonist profiles, including **12w**, **12z**, and **28** will be evaluated for *in vivo* antinociceptive properties in mice. These tests may include a warm water tail withdrawal assay, hot plate assay, or von Frey assay.¹¹¹ Candidates that demonstrate antinociception will be further evaluated *in vivo* to determine duration of action and development of tolerance.

5.5 Conclusion

In conclusion, the work reported here describes a new library of multifunctional dimethyltyrosine-tetrahydroisoquinoline opioid peptidomimetics. This series includes several promising KOR agonist/MOR partial agonist ligands, some of which are currently being evaluated *in vivo*. The profile demonstrated by these compounds shows promise in the development of a treatment for addiction to cocaine and other drugs of abuse. This collection of novel compounds also includes promising leads for evaluation and further development of a MOR agonist/DOR antagonist ligand, which may be useful as a pain treatment with lowered abuse and addiction potential. This work represents substantial progress in the investigation of underexplored regions of the Dmt-Tiq scaffold and opens new avenues for exploration of the structure-activity relationships of this series and the development of multifunctional opioid peptidomimetics.

Chapter 6

Experimental Section

6.1 Chemistry

Unless otherwise noted, all reagents and solvents were purchased from commercial sources and used without additional purification. DiBoc-DMT was prepared from commercially available dimethyltyrosine according to standard procedures.¹¹² Microwave reactions were performed in a CEM Discover SP microwave synthesizer in a closed vessel with maximum power input of 300 W. Column chromatography was carried out on silica gel cartridges using a Biotage Isolera One flash purification system. Before chromatographic purification, crude reaction mixtures were analyzed by thin layer chromatography in hexanes/ethyl acetate. Purification of final compounds was performed using a Waters semipreparative HPLC with a Vydac protein and peptide C18 reverse phase column using a linear gradient of 100% solvent A (water with 0.1% TFA) to 100% solvent B (acetonitrile with 0.1% TFA) at a rate of 1% per minute with UV absorbance monitored at 230 nm. Purity of final compounds was determined on a Waters Alliance 2690 analytical HPLC with a Vydac protein and peptide C18 reverse phase column using the same gradient with UV absorbance monitored at 230 nm. Purity of final compounds used for testing was $\geq 95\%$ as determined by HPLC. ^1H NMR data for intermediates and final compounds in CDCl_3 or CD_3OD was obtained on a 400 MHz or 500 MHz Varian spectrometer. LC-MS data was obtained using an Agilent 6130 LC-MS in positive ion mode. HRMS data was obtained using an Agilent QTOF HPLC-MS in positive ion mode.

6.1.1. General Procedures

General Procedure A for Boc Protection of Tetrahydroisoquinoline Bromides. The appropriate aryl bromide (1.0 eq) and di-tert-butyl dicarbonate (1.1 eq) were combined in a microwave vessel equipped with a teflon stirbar. The system was flushed with argon, and the reaction was heated in a microwave to 100 °C for 15 minutes. The reaction mixture was diluted with DCM and washed with saturated aqueous NaHCO₃ and brine. The organic layer was dried over MgSO₄, filtered, and concentrated under vacuum to obtain the pure product.

General Procedure B for Suzuki Coupling of Boc-protected Tetrahydroisoquinoline Bromide and Pendant Boronic Acid or Boronic Ester. The appropriate Boc-protected aryl bromide (1.0 eq), the appropriate boronic acid or boronic acid pinacol ester (2.0 eq), Pd(dppf)Cl₂ (0.1 eq), and K₂CO₃ (3.0 eq) were combined in a microwave vessel equipped with a teflon stirbar. The system was flushed with argon. A degassed mixture of 3:1 acetone:water (2-3 mL) was added, and the reaction was heated in a microwave to 100 °C for 30 minutes. The product was purified via silica gel chromatography in ethyl acetate/hexanes.

General Procedure C for HCl Boc Deprotection, Peptide Coupling, and TFA Boc Deprotection for Synthesis of Final Products. The appropriate Boc-protected amine intermediate was dissolved in 1,4-dioxane (2-5 mL) and excess concentrated HCl (100-500 μL) was added. The reaction mixture stirred at room temperature for 1-3.5 hours. Solvent was removed under vacuum to yield the deprotected amine. The amine intermediate (1.0 eq), diBoc-DMT (1.05 eq) or BocTyrOH (1.05), PyBOP (1.0 eq), and 6Cl-HOBt (1.0 eq) were combined, and the reaction flask was flushed with argon. Dry

DMF (3-12 mL) and DIEA (10 eq) were added. The reaction mixture stirred at room temperature for 6-24 hours. Solvent was removed under vacuum, and the coupled product was purified via silica gel chromatography in ethyl acetate/hexanes. The Boc-protected compound was dissolved in DCM (2-2.5 mL). An equal volume of TFA was added, and the reaction mixture stirred at room temperature for 1-1.5 hours. Solvent was removed under vacuum, and the product was purified by semi-preparative HPLC and lyophilized.

General Procedure D for Suzuki Coupling of Boronic Ester Tetrahydroisoquinoline and Pendant Benzyl Bromide. The appropriate benzyl bromide (1.0 eq), **5** (1.5 eq), Pd(dppf)Cl₂ (0.1 eq), and K₂CO₃ (3.0 eq) were combined in a microwave vessel equipped with a teflon stirbar. The system was flushed with argon. A degassed mixture of 3:1 acetone:water (2-3 mL) was added, and the reaction was heated in a microwave to 100 °C for 30 minutes. The product was purified via silica gel chromatography in ethyl acetate/hexanes. NMR spectroscopy indicated the presence of **5** as a remaining impurity in a 1:1 or lower ratio with the desired product. As a result, not all intermediates were isolated and characterized, and reported yields are adjusted accordingly.

General Procedure D2 for Suzuki Coupling of Boronic Ester Tetrahydroisoquinoline and Pendant Benzyl Bromide. The appropriate benzyl bromide (1.5-2.0 eq), **5** (1.0 eq), Pd(dppf)Cl₂ (0.1 eq), and K₂CO₃ (3.0 eq) were combined in a microwave vessel equipped with a teflon stirbar. The system was flushed with argon. A degassed mixture of 3:1 acetone:water (2-3 mL) was added, and the

reaction was heated in a microwave to 100 °C for 30 minutes. The product was purified via silica gel chromatography in ethyl acetate/hexanes.

General Procedure E for HCl Boc Deprotection, Peptide Coupling, Nitro Reduction, and TFA Boc Deprotection for Synthesis of Final Products. The appropriate Boc-protected amine was dissolved in 1,4-dioxane (3-5 mL), and excess (200-300 μ L) concentrated HCl was added. The reaction mixture stirred at room temperature for 2 hours. Solvent was removed under vacuum to yield the deprotected amine. The amine intermediate (1.0 eq), diBoc-DMT (1.05 eq), PyBOP (1.0 eq), and 6Cl-HOBt (1.0 eq) were combined, and the reaction flask was flushed with argon. Dry DMF (5-7 mL) and DIEA (10 eq) were added. The reaction mixture stirred at room temperature overnight. Solvent was removed under vacuum, and the coupled product was purified via silica gel chromatography in ethyl acetate/hexanes. The resulting nitro intermediate (1.0 eq) was dissolved in acetone (2 mL). NH_4Cl (40 eq), Zn dust (20 eq), and water (220 eq) were added. The mixture stirred at room temperature for 1 hour. Solvent was removed under vacuum, and the crude product was partitioned between ethyl acetate and water. The layers were separated, and the aqueous layer was extracted with ethyl acetate. The combined organic layers were washed with brine, dried over MgSO_4 , filtered, and concentrated under vacuum to obtain the corresponding aniline. The Boc-protected compound was then dissolved in DCM (1.5 mL). An equal volume of TFA was added, and the reaction mixture stirred at room temperature for 1 hour. Solvent was removed under vacuum, and the product was purified by semi-preparative HPLC.

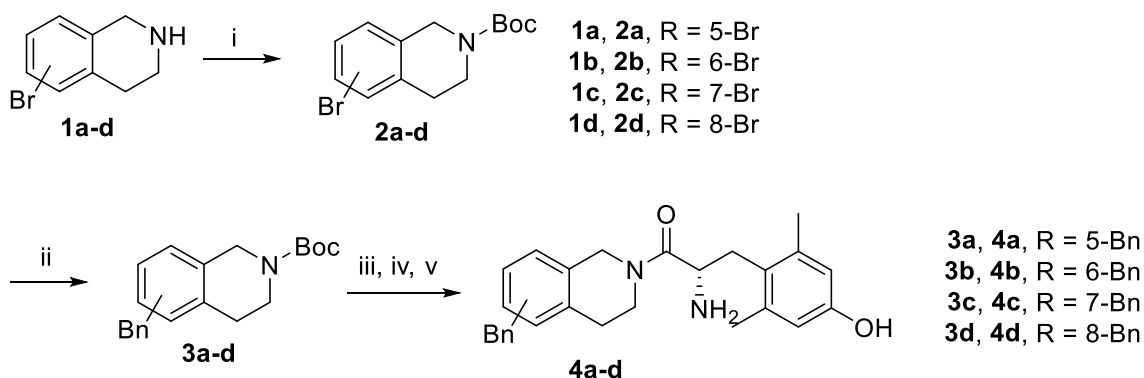
General Procedure F for Microwave Suzuki Coupling of Benzyl Bromide Tetrahydroisoquinoline and Pendant Boronic Acid. Benzyl bromide **10** (1.0 eq), the appropriate boronic acid (1.5 eq), Pd(dppf)Cl₂ (0.1 eq), and K₂CO₃ (3.0 eq) were combined in a microwave vessel equipped with a teflon stirbar. The system was flushed with argon. A degassed mixture of 3:1 acetone:water (3 mL) was added, and the reaction was heated in a microwave to 100 °C for 30 minutes. The product was purified via silica gel chromatography in ethyl acetate/hexanes.

General Procedure G for S_N2 reaction of Benzyl Bromide Tetrahydroisoquinoline and Pendant Nucleophile. Benzyl bromide **10** (1.0 eq), the appropriate nucleophile (1.2 eq), and K₂CO₃ (1.2 eq) were dissolved in dry DMF (3 mL) under an inert atmosphere. The reaction stirred at room temperature overnight. The reaction mixture was partitioned between 2 M NaOH and ethyl acetate. The aqueous layer was extracted with additional ethyl acetate. Combined organic layers were dried over MgSO₄, filtered, and concentrated under vacuum to obtain the product.

General Procedure H for Coupling of Boc-Protected Tetrahydroisoquinoline Bromide and Pendant Acetophenone. Intermediate **2c** (1.0 eq), the appropriately substituted acetophenone (2.0 eq), Pd₂(dba)₃ (0.1 eq), racemic BINAP (0.24 eq), and sodium tert-butoxide (1.3 eq) were combined in a microwave vessel equipped with a teflon stirbar. The system was flushed with argon. Degassed THF (2–3 mL) was added, and the reaction mixture was heated in a microwave to 100 °C for 1 hour. The crude reaction mixture was filtered through celite, and the product was purified via silica gel chromatography in ethyl acetate/hexanes.

6.1.2. Procedures and Characterization for Compounds Contained in Chapter 2

Scheme 12. Synthesis of 4a-4d



4a

Tert-butyl 5-bromo-3,4-dihydroisoquinoline-2(1H)-carboxylate (2a). **2a** was synthesized following General Procedure A from 5-bromo-1,2,3,4-tetrahydroisoquinoline (100 mg, 0.47 mmol, 1.0 eq) and di-tert-butyl dicarbonate (113 mg, 0.52 mmol, 1.1 eq) to yield the product as an off-white solid (136 mg, 93%). ^1H NMR (500 MHz, CDCl_3) δ 7.41 (m, 1H), 7.04 (m, 2H), 4.56 (s, 2H), 3.65 (t, $J = 6.0$ Hz, 2H), 2.84 (t, $J = 6.1$ Hz, 2H), 1.48 (s, 9H).

Tert-butyl 5-benzyl-3,4-dihydroisoquinoline-2(1H)-carboxylate (3a). **3a** was synthesized following General Procedure B from **2a** (136 mg, 0.40 mmol, 1.0 eq), benzylboronic acid pinacol ester (180 μL , 0.81 mmol, 2.0 eq), $\text{Pd}(\text{dppf})\text{Cl}_2$ (29 mg, 0.04 mmol, 0.1 eq), and K_2CO_3 (167 mg, 1.21 mmol, 3.0 eq) to yield the product as a colorless oil (101 mg, 77%). ^1H NMR (500 MHz, CDCl_3) δ 7.29 (t, $J = 7.5$ Hz, 2H), 7.23 (m, 1H), 7.18 (t, $J = 7.6$, 1H), 7.13 (d, $J = 7.6$, 2H), 7.04 (d, $J = 7.5$, 2H), 4.60 (s, 2H), 4.00 (s, 2H), 3.62 (br. s, 2H), 2.71 (t, $J = 6.0$ Hz, 2H), 1.50 (s, 9H).

(S)-2-amino-1-(5-benzyl-3,4-dihydroisoquinolin-2(1H)-yl)-3-(4-hydroxy-2,6-dimethylphenyl)propan-1-one (4a). Following General Procedure C, **3a** (50 mg, 0.15

mmol) was deprotected to yield the amine intermediate as a white solid. This intermediate was coupled to diBoc-DMT (67 mg, 0.16 mmol, 1.05 eq) in the presence of PyBOP (81 mg, 0.15 mmol, 1.0 eq), 6Cl-HOBt (26 mg, 0.15 mmol, 1.0 eq), and DIEA (217 μ L, 1.5 mmol, 10 eq). Silica gel chromatography yielded the coupled product as a colorless oil. TFA deprotection yielded the product as a white, fluffy solid (21 mg, 29%, 3 steps). Two rotamers were visible by NMR and present in about 1:1 ratio. ^1H NMR (500 MHz, CD_3OD , rotamers) δ 7.26 (t, J = 7.6 Hz, 2H), 7.23 (t, J = 7.6 Hz, 2H), 7.23 (d, J = 13.0 Hz, 1H) 7.14 (quin, J = 7.4 Hz, 3H), 7.11 (d, J = 8.2 Hz, 2H), 7.07 – 7.03 (m, 4H), 7.01 (d, J = 8.0 Hz, 1H), 6.99 (d, J = 10.2 Hz, 1H), 6.57 (dd, J = 6.5, 2.5 Hz, 1H), 6.42 (s, 2H), 6.26 (s, 2H), 4.66 (d, J = 16.7 Hz, 1H), 4.57 (d, J = 16.5 Hz, 1H), 4.56 (t, J = 4.4 Hz, 1H), 4.53 (t, J = 4.5 Hz, 1H), 4.21 (d, J = 15.8 Hz, 1H), 3.93 (s, 2H), 3.84 (d, J = 4.3 Hz, 2H), 3.78 (dt, J = 12.9, 5.4 Hz, 1H), 3.49 (m, 1H), 3.43 (d, J = 15.9 Hz, 1H), 3.26 – 3.14 (m, 3H), 3.07 (m, 2H), 2.73 (dt, J = 12.7, 5.9 Hz, 1H), 2.62 (dt, J = 16.5, 5.5 Hz, 1H), 2.55 – 2.47 (m, 1H), 2.32 (dt, J = 16.4, 5.8 Hz, 1H), 2.19 (s, 6H), 2.17 (s, 6H), 1.82 (dt, J = 16.5, 6.4 Hz, 1H). HPLC retention time: 37.4 min. HRMS calculated for $[\text{C}_{27}\text{H}_{30}\text{N}_2\text{O}_2 + \text{H}]^+$: 415.2380, found: 415.2386.

4b

Tert-butyl 6-bromo-3,4-dihydroisoquinoline-2(1H)-carboxylate (2b). **2b** was synthesized following General Procedure A from 6-bromo-1,2,3,4-tetrahydroisoquinoline (100 mg, 0.47 mmol, 1.0 eq) and di-tert-butyl dicarbonate (113 mg, 0.52 mmol, 1.1 eq) to yield the product as yellow oil (143 mg, 97%). ^1H NMR (500 MHz, CDCl_3) δ 7.29 (m, 2H), 6.98 (d, J = 8.0 Hz, 1H), 4.51 (s, 2H), 3.62 (t, J = 5.8 Hz, 2H), 2.80 (t, J = 5.9 Hz, 2H), 1.49 (s, 9H).

Tert-butyl 6-benzyl-3,4-dihydroisoquinoline-2(1H)-carboxylate (3b). **3b** was synthesized following General Procedure B from **2b** (73 mg, 0.23 mmol, 1.0 eq), benzylboronic acid pinacol ester (102 mg, 0.47 mmol, 2.0 eq), Pd(dppf)Cl₂ (17 mg, 0.023 mmol, 0.1 eq), and K₂CO₃ (97 mg, 0.70 mmol, 3.0 eq) to yield the product as a colorless oil (76 mg, 100%). ¹H NMR (500 MHz, CDCl₃) δ 7.29 (m, 2H), 7.19 (m, 3H), 7.02 (d, *J* = 1.5 Hz, 2H), 6.96 (s, 1H), 4.54 (s, 2H), 3.94 (s, 2H), 3.62 (br. s, 2H), 2.78 (t, *J* = 5.8 Hz, 2H), 1.49 (s, 9H).

(S)-2-amino-1-(6-benzyl-3,4-dihydroisoquinolin-2(1H)-yl)-3-(4-hydroxy-2,6-dimethylphenyl)propan-1-one (4b). Following General Procedure C, **3b** (98 mg, 0.30 mmol) was deprotected to yield the amine intermediate as a yellow solid. This intermediate was coupled to diBoc-DMT (130 mg, 0.32 mmol, 1.05 eq) in the presence of PyBOP (158 mg, 0.30 mmol, 1.0 eq), 6Cl-HOBt (51 mg, 0.30 mmol, 1.0 eq), and DIEA (425 μL, 3.0 mmol, 10 eq). Silica gel chromatography yielded the coupled product as a colorless oil. TFA deprotection yielded the product as a white solid (21 mg, 67%, 3 steps). ¹H NMR (500 MHz, CD₃OD, rotamers) δ 7.24 (t, *J* = 7.6 Hz, 3H), 7.17 – 7.13 (m, 5H), 7.04 – 6.98 (m, 2H), 6.92 (d, *J* = 7.9 Hz, 1H), 6.88 (s, 1H), 6.85 (s, 1H), 6.63 (d, *J* = 7.8 Hz, 1H), 6.43 (s, 2H), 6.34 (s, 2H), 4.66 (dd, *J* = 16.8, 3.2 Hz, 1H), 4.58 – 4.50 (m, 2H), 4.47 (d, *J* = 16.9 Hz, 1H), 4.19 (d, *J* = 15.7 Hz, 1H), 3.88 (s, 4H), 3.70 – 3.62 (m, 2H), 3.32 (d, *J* = 15.0 Hz, 6H), 3.28 – 3.16 (m, 3H), 3.13 – 3.05 (m, 2H), 2.74 – 2.61 (m, 2H), 2.55 – 2.47 (m, 1H), 2.26 (s, 6H), 2.22 (s, 6H), 2.05 – 1.96 (m, 1H). HPLC retention time: 38.8 min. HRMS calculated for [C₂₇H₃₀N₂O₂ + H]⁺: 415.2380, found: 415.2388.

4c

Tert-butyl 7-bromo-3,4-dihydroisoquinoline-2(1H)-carboxylate (2c). **2c** was synthesized following General Procedure A from 7-bromo-1,2,3,4-tetrahydroisoquinoline (75 μ L, 0.50 mmol, 1.0 eq) and di-tert-butyl dicarbonate (120 mg, 0.55 mmol, 1.1 eq) to yield the product as a pale orange oil (145 mg, 99%). ^1H NMR (500 MHz, CDCl_3) δ 7.25 (m, 2H), 6.98 (d, J = 8.0 Hz, 1H), 4.52 (s, 2H), 3.61 (t, J = 5.7 Hz, 2H), 2.75 (t, J = 6.0 Hz, 2H), 1.48 (s, 9H).

Tert-butyl 7-benzyl-3,4-dihydroisoquinoline-2(1H)-carboxylate (3c). **3c** was synthesized following General Procedure B from **2c** (145 mg, 0.46 mmol, 1.0 eq), benzylboronic acid pinacol ester (207 μ L, 0.93 mmol, 2.0 eq), $\text{Pd}(\text{dppf})\text{Cl}_2$ (34 mg, 0.05 mmol, 0.1 eq), and K_2CO_3 (192 mg, 1.39 mmol, 3.0 eq) to yield the product as a colorless oil (92 mg, 61%). ^1H NMR (500 MHz, CDCl_3) δ 7.30 (m, 2H), 7.21 (m, 3H), 7.05 (m, 2H), 6.95 (s, 1H), 4.55 (s, 2H), 3.96 (s, 2H), 3.65 (br. s, 2H), 2.81 (t, J = 6.1 Hz, 2H), 1.51 (s, 9H).

(S)-2-amino-1-(7-benzyl-3,4-dihydroisoquinolin-2(1H)-yl)-3-(4-hydroxy-2,6-dimethylphenyl)propan-1-one (4c). Following General Procedure C, **3c** (92 mg, 0.28 mmol) was deprotected to yield the amine intermediate as an off-white solid. This intermediate was coupled to diBoc-DMT (122 mg, 0.30 mmol, 1.05 eq) in the presence of PyBOP (148 mg, 0.28 mmol, 1.0 eq), 6Cl-HOBt (48 mg, 0.28 mmol, 1.0 eq), and DIEA (398 μ L, 2.8 mmol, 10 eq). Silica gel chromatography yielded the coupled product as a colorless oil. TFA deprotection yielded the product as a white solid (13 mg, 9%, 3 steps). ^1H NMR (500 MHz, CD_3OD , rotamers) δ 7.28 – 7.22 (m, 4H), 7.17 (s, 3H), 7.15 (s, 3H), 6.99 (d, J = 7.7 Hz, 1H), 6.95 (d, J = 3.6 Hz, 3H), 6.91 (d, J = 7.8 Hz, 1H), 6.49 (s, 1H), 6.40 (s, 2H), 6.32 (s, 2H), 4.61 (d, J = 16.9 Hz, 1H), 4.59 – 4.48 (m, 2H), 4.49

(d, $J = 17.3$ Hz, 2H), 4.17 (d, $J = 15.8$ Hz, 1H), 3.90 (s, 2H), 3.89 (s, 2H), 3.75 (dt, $J = 12.1, 5.6$ Hz, 1H), 3.65 – 3.55 (m, 1H), 3.36 (d, $J = 17.4$ Hz, 1H), 3.26 – 3.18 (m, 3H), 3.09 (d, $J = 4.1$ Hz, 1H), 3.06 (d, $J = 4.1$ Hz, 1H), 2.70 (q, $J = 6.7, 6.3$ Hz, 2H), 2.67 – 2.61 (m, 1H), 2.56 – 2.47 (m, 1H), 2.24 (s, 6H), 2.19 (s, 6H), 1.98 (dt, $J = 15.7, 5.5$ Hz, 1H). HPLC retention time: 38.4 min. HRMS calculated for $[C_{27}H_{30}N_2O_2 + H]^+$: 415.2380, found: 415.2384.

4d

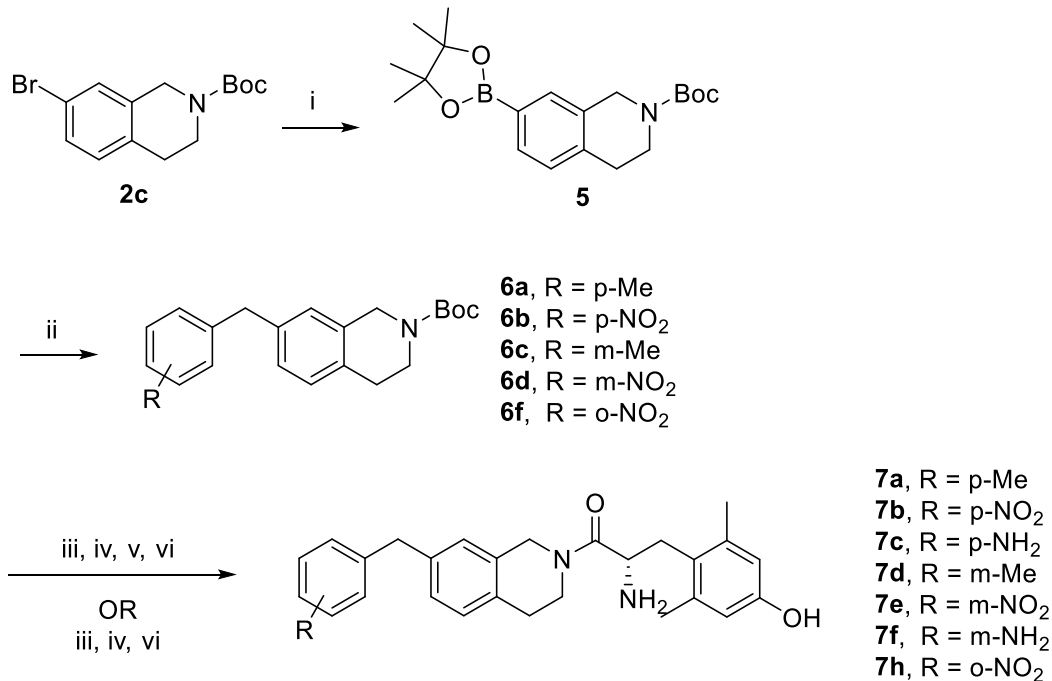
Tert-butyl 8-bromo-3,4-dihydroisoquinoline-2(1H)-carboxylate (2d). 8-bromo-1,2,3,4-tetrahydroisoquinoline hydrochloride (100 mg, 0.40 mmol, 1.0 eq), di-tert-butyl dicarbonate (175 mg, 0.80 mmol, 2.0 eq), and DMAP (5 mg, 0.04 mmol, 0.1 eq) were combined in DCM (10 mL). DIEA (140 μ L, 0.80 mmol, 2.0 eq) was added. The reaction mixture was heated to reflux overnight. The cooled reaction mixture was diluted with DCM and washed with saturated aqueous NH_4Cl . The aqueous layer was extracted with DCM. The combined organic layers were washed with brine, dried over $MgSO_4$, filtered, and concentrated under vacuum to yield the product as a pale orange oil (117 mg, 93%). 1H NMR (500 MHz, $CDCl_3$) δ 7.41 (d, $J = 7.7$ Hz, 1H), 7.08 (d, $J = 7.6$ Hz, 1H), 7.03 (t, $J = 7.7$ Hz, 1H), 4.53 (s, 2H), 3.63 (t, $J = 6.1$ Hz, 2H), 2.83 (t, $J = 5.9$ Hz, 2H), 1.50 (s, 9H).

Tert-butyl 8-benzyl-3,4-dihydroisoquinoline-2(1H)-carboxylate (3d). **3d** was synthesized following General Procedure B from **2d** (117 mg, 0.37 mmol, 1.0 eq), benzylboronic acid pinacol ester (164 mg, 0.75 mmol, 2.0 eq), $Pd(dppf)Cl_2$ (27 mg, 0.04 mmol, 0.1 eq), and K_2CO_3 (155 mg, 1.12 mmol, 3.0 eq) to yield the product as a colorless oil (83 mg, 69%). 1H NMR (500 MHz, $CDCl_3$) δ 7.33 – 7.24 (m, 2H), 7.22 (d, J

= 7.2 Hz, 1H), 7.16 (d, $J = 6.6$ Hz, 3H), 7.06 (s, 2H), 4.48 (d, $J = 29.0$ Hz, 2H), 3.96 (s, 2H), 3.62 (s, 2H), 2.86 (s, 2H), 1.46 (d, $J = 22.2$ Hz, 9H).

(S)-2-amino-1-(8-benzyl-3,4-dihydroisoquinolin-2(1H)-yl)-3-(4-hydroxy-2,6-dimethylphenyl)propan-1-one (4d). Following General Procedure C, **3d** (83 mg, 0.26 mmol) was deprotected to yield the amine intermediate as an off-white solid. This intermediate was coupled to diBoc-DMT (55 mg, 0.13 mmol, 1.05 eq) in the presence of PyBOP (66 mg, 0.13 mmol, 1.0 eq), 6Cl-HOBt (22 mg, 0.13 mmol, 1.0 eq), and DIEA (178 μ L, 1.3 mmol, 10 eq). Silica gel chromatography yielded the coupled product as a colorless oil. TFA deprotection yielded the product as a white solid (28 mg, 41%, 3 steps). ^1H NMR (500 MHz, CD_3OD , rotamers) δ 7.27 (dt, $J = 20.5, 7.5$ Hz, 4H), 7.20 (dd, $J = 15.7, 7.2$ Hz, 2H), 7.16 – 7.06 (m, 4H), 7.08 – 7.00 (m, 3H), 6.97 (t, $J = 6.0$ Hz, 1H), 6.91 (t, $J = 6.9$ Hz, 1H), 6.84 (t, $J = 5.6$ Hz, 1H), 6.38 (s, 4H), 4.55 (d, $J = 17.0$ Hz, 1H), 4.53 (m, 1H), 4.41 (d, $J = 17.4$ Hz, 1H), 4.36 – 4.30 (m, 1H), 4.03 (d, $J = 16.3$ Hz, 1H), 3.98 – 3.94 (m, 2H), 3.93 – 3.83 (m, 1H), 3.73 (d, $J = 15.9$ Hz, 1H), 3.60 (d, $J = 16.2$ Hz, 1H), 3.52 – 3.43 (m, 1H), 3.24 – 3.14 (m, 5H), 3.10 – 3.03 (m, 2H), 2.86 – 2.71 (m, 2H), 2.57 – 2.51 (m, 2H), 2.17 (s, 6H), 2.14 (s, 6H), 2.04 – 1.99 (m, 1H). HPLC retention time: 36.8 min. HRMS calculated for $[\text{C}_{27}\text{H}_{30}\text{N}_2\text{O}_2 + \text{H}]^+$: 415.2380, found: 415.2381.

Scheme 13. Synthesis of 7a-7f and 7h



Tert-butyl

7-(4,4,5,5-tetramethyl-1,3,2-dioxaborolan-2-yl)-3,4-

dihydroisoquinoline-2(1H)-carboxylate (5). Intermediate **2c** (945 mg, 3.03 mmol, 1.0 eq), bis(pinacolato)diboron (1.54 g, 6.06 mmol, 2.0 eq), Pd(dppf)Cl₂ (222 mg, 0.303 mmol, 0.1 eq), and potassium acetate (892 mg, 9.09 mmol, 3.0 eq) were combined in DMSO (20 mL), and the system was flushed with argon. The reaction was heated to 90 °C overnight. The reaction mixture was concentrated under vacuum to remove most DMSO. The remaining mixture was diluted with water and extracted with three portions of DCM. The combined organic layers were washed with water and brine, dried over MgSO₄, filtered, and concentrated under vacuum. The product was purified via silica gel chromatography in ethyl acetate/hexanes to yield a pale yellow oil (1.05 g, 96%). ¹H NMR (500 MHz, CDCl₃) δ 7.59 (d, *J* = 5.7 Hz, 1H), 7.14 (d, *J* = 5.5 Hz, 1H), 4.58 (s, 2H), 3.63 (br s, 2H), 2.84 (br s, 2H), 1.48 (s, 9H), 1.34 (s, 12H).

7a

Tert-butyl 7-(4-methylbenzyl)-3,4-dihydroisoquinoline-2(1H)-carboxylate

(6a). **6a** was synthesized following General Procedure D from 4-methylbenzyl bromide (51 mg, 0.27 mmol, 1.0 eq), **5** (148 mg, 0.41 mmol, 1.5 eq), Pd(dppf)Cl₂ (20 mg, 0.03 mmol, 0.1 eq), and K₂CO₃ (114 mg, 0.82 mmol, 3.0 eq) to yield the product (18 mg, 19%).

(S)-2-amino-3-(4-hydroxy-2,6-dimethylphenyl)-1-(7-(4-methylbenzyl)-3,4-dihydroisoquinolin-2(1H)-yl)propan-1-one (7a). Following General Procedure C, **6a** (33 mg, 0.098 mmol) was deprotected to yield the amine intermediate as a white solid. This intermediate was coupled to diBoc-DMT (20 mg, 0.049 mmol, 1.05 eq) in the presence of PyBOP (24 mg, 0.047 mmol, 1.0 eq), 6Cl-HOBt (8 mg, 0.047 mmol, 1.0 eq), and DIEA (66 μ L, 0.47 mmol, 10 eq). Silica gel chromatography yielded the coupled product as a colorless oil. TFA deprotection yielded the product as a white, fluffy solid (15 mg, 30%, 3 steps). ¹H NMR (500 MHz, CD₃OD, rotamers) δ 7.08 – 7.02 (m, 8H), 6.97 (d, *J* = 8.0 Hz, 1H), 6.92 (p, *J* = 7.9 Hz, 4H), 6.48 (s, 1H), 6.40 (s, 2H), 6.32 (s, 2H), 4.60 (d, *J* = 16.9 Hz, 1H), 4.58 – 4.51 (m, 2H), 4.48 (d, *J* = 16.8 Hz, 1H), 4.16 (d, *J* = 15.7 Hz, 1H), 3.85 (s, 2H), 3.84 (s, 2H), 3.74 (dt, *J* = 12.0, 5.7 Hz, 1H), 3.65 – 3.55 (m, 1H), 3.36 (d, *J* = 15.7 Hz, 1H), 3.26 – 3.18 (m, 3H), 3.09 (dd, *J* = 4.2, 1.5 Hz, 1H), 3.06 (dd, *J* = 4.3, 1.5 Hz, 1H), 2.70 (q, *J* = 7.2, 6.6 Hz, 2H), 2.66 – 2.60 (m, 1H), 2.55 – 2.47 (m, 1H), 2.28 (s, 3H), 2.27 (s, 3H), 2.24 (s, 6H), 2.19 (s, 6H), 1.98 (dt, *J* = 16.1, 6.0 Hz, 1H). HPLC retention time: 41.5 min. MS calculated for [C₂₈H₃₂N₂O₂ + H]⁺: 429.2, found: 429.3.

7b

Tert-butyl 7-(4-nitrobenzyl)-3,4-dihydroisoquinoline-2(1H)-carboxylate (6b).

6b was synthesized following General Procedure D from 4-nitrobenzyl bromide (59 mg, 0.27 mmol, 1.0 eq), **5** (146 mg, 0.41 mmol, 1.5 eq), Pd(dppf)Cl₂ (20 mg, 0.03 mmol, 0.1 eq), and K₂CO₃ (112 mg, 0.81 mmol, 3.0 eq). Additional purification was performed by silica gel chromatography in DCM to yield the product as a yellow oil (15 mg, 15%). ¹H NMR (400 MHz, CDCl₃) δ 8.15 (d, *J* = 8.7 Hz, 2H), 7.34 (d, *J* = 8.7 Hz, 2H), 7.10 (d, *J* = 7.8 Hz, 1H), 6.99 (d, *J* = 7.5 Hz, 1H), 6.93 (s, 1H), 4.54 (s, 2H), 4.03 (s, 2H), 3.64 (t, *J* = 5.9 Hz, 2H), 2.82 (t, *J* = 5.9 Hz, 2H), 1.50 (s, 9H).

(S)-2-amino-3-(4-hydroxy-2,6-dimethylphenyl)-1-(7-(4-nitrobenzyl)-3,4-dihydroisoquinolin-2(1H)-yl)propan-1-one (7b). Following General Procedure C, **6b** (20 mg, 0.054 mmol) was deprotected to yield the amine intermediate as a yellow solid. This intermediate was coupled to diBoc-DMT (24 mg, 0.059 mmol, 1.05 eq) in the presence of PyBOP (29 mg, 0.056 mmol, 1.0 eq), 6Cl-HOBt (10 mg, 0.056 mmol, 1.0 eq), and DIEA (79 μL, 0.56 mmol, 10 eq). Silica gel chromatography yielded the coupled product as a yellow oil. TFA deprotection yielded the product as a white, fluffy solid (15 mg, 65%, 3 steps). ¹H NMR (500 MHz, CD₃OD, rotamers) δ 8.17 (t, *J* = 2.0 Hz, 1H), 8.15 (d, *J* = 2.6 Hz, 2H), 8.14 (t, *J* = 2.0 Hz, 1H), 7.43 (d, *J* = 2.3 Hz, 2H), 7.42 (d, *J* = 2.3 Hz, 2H), 7.05 – 6.99 (m, 3H), 6.99 – 6.94 (m, 2H), 6.50 (s, 2H), 6.40 (s, 2H), 6.30 (s, 2H), 4.63 (d, *J* = 17.0 Hz, 1H), 4.54 (ddd, *J* = 11.3, 10.7, 4.1 Hz, 2H), 4.54 (d, *J* = 17.6 Hz, 1H), 4.18 (d, *J* = 15.7 Hz, 1H), 4.05 (s, 2H), 4.03 (s, 2H), 3.83 (dt, *J* = 12.9, 5.6 Hz, 1H), 3.58 – 3.52 (m, 1H), 3.41 (d, *J* = 15.7 Hz, 1H), 3.26 – 3.19 (m, 3H), 3.09 (t, *J* = 4.0 Hz, 1H), 3.06 (t, *J* = 4.1 Hz, 1H), 2.72 (t, *J* = 5.9 Hz, 2H), 2.68 – 2.62 (m, 1H), 2.53 (dt, *J*

= 16.1, 5.9 Hz, 1H), 2.24 (s, 6H), 2.20 (s, 6H), 1.99 (dt, $J = 16.1, 5.9$ Hz, 1H). HPLC retention time: 37.3 min. MS calculated for $[C_{27}H_{29}N_3O_4 + H]^+$: 460.2, found: 460.3.

7c

(S)-2-amino-1-(7-(4-aminobenzyl)-3,4-dihydroisoquinolin-2(1H)-yl)-3-(4-hydroxy-2,6-dimethylphenyl)propan-1-one (7c). Following General Procedure E, **6b** (20 mg, 0.054 mmol) was deprotected to yield the amine intermediate as a yellow solid. This intermediate was coupled to diBoc-DMT (24 mg, 0.059 mmol, 1.05 eq) in the presence of PyBOP (29 mg, 0.056 mmol, 1.0 eq), 6Cl-HOBt (10 mg, 0.056 mmol, 1.0 eq), and DIEA (79 μ L, 0.56 mmol, 10 eq). Silica gel chromatography yielded the coupled product as a yellow oil. Half of the nitro intermediate was reduced in the presence of NH_4Cl (39 mg, 0.73 mmol, 40 eq), Zn (24 mg, 0.36 mmol, 20 eq), and water (72 μ L, 4.0 mmol, 220 eq) to yield the aniline as a yellow oil. TFA deprotection yielded the product as a white, fluffy solid (10 mg, 65%, 4 steps). 1H NMR (500 MHz, CD_3OD , rotamers) δ 7.36 (d, $J = 2.8$ Hz, 2H), 7.34 (d, $J = 2.9$ Hz, 2H), 7.31 – 7.27 (m, 4H), 7.01 – 6.96 (m, 3H), 6.95 – 6.90 (m, 2H), 6.52 (s, 1H), 6.39 (s, 2H), 6.29 (s, 2H), 4.61 (d, $J = 17.0$ Hz, 1H), 4.58 – 4.52 (m, 2H), 4.50 (d, $J = 16.7$ Hz, 1H), 4.19 (d, $J = 15.7$ Hz, 1H), 3.97 (s, 2H), 3.95 (s, 2H), 3.87 – 3.80 (m, 1H), 3.58 – 3.50 (m, 1H), 3.42 (d, $J = 15.9$ Hz, 1H), 3.26 – 3.19 (m, 3H), 3.11 – 3.09 (m, 1H), 3.08 – 3.06 (m, 1H), 2.73 – 2.68 (m, 2H), 2.67 – 2.61 (m, 1H), 2.55 – 2.48 (m, 1H), 2.24 (s, 6H), 2.19 (s, 6H), 1.98 (dt, $J = 16.4, 6.4$ Hz, 1H). HPLC retention time: 21.4 min. MS calculated for $[C_{27}H_{31}N_3O_2 + H]^+$: 430.2, found: 430.3.

7d

Tert-butyl 7-(3-methylbenzyl)-3,4-dihydroisoquinoline-2(1H)-carboxylate (6c). **6c** was synthesized following General Procedure D from 3-methylbenzyl bromide (38 μ L, 0.28 mmol, 1.0 eq), **5** (152 mg, 0.42 mmol, 1.5 eq), Pd(dppf)Cl₂ (20 mg, 0.03 mmol, 0.1 eq), and K₂CO₃ (117 mg, 0.85 mmol, 3.0 eq) to yield the product as a colorless oil (20 mg, 21%).

(S)-2-amino-3-(4-hydroxy-2,6-dimethylphenyl)-1-(7-(3-methylbenzyl)-3,4-dihydroisoquinolin-2(1H)-yl)propan-1-one (7d). Following General Procedure C, **6c** (39 mg, 0.12 mmol) was deprotected to yield the amine intermediate as an oily, white solid. This intermediate was coupled to diBoc-DMT (50 mg, 0.12 mmol, 1.05 eq) in the presence of PyBOP (61 mg, 0.12 mmol, 1.0 eq), 6Cl-HOBt (20 mg, 0.12 mmol, 1.0 eq), and DIEA (164 μ L, 1.17 mmol, 10 eq). Silica gel chromatography yielded the coupled product as a colorless oil. TFA deprotection yielded the product as a white, fluffy solid (26 mg, 47%, 3 steps). ¹H NMR (500 MHz, CD₃OD, rotamers) δ 7.13 (td, J = 7.9, 2.8 Hz, 2H), 7.00 – 6.97 (m, 5H), 6.95 (d, J = 5.8 Hz, 5H), 6.91 (d, J = 7.8 Hz, 1H), 6.49 (s, 1H), 6.40 (s, 2H), 6.32 (s, 2H), 4.62 (d, J = 16.8 Hz, 1H), 4.55 (dd, J = 11.8, 4.3 Hz, 1H), 4.51 (dd, J = 11.5, 4.3 Hz, 1H), 4.50 (d, J = 17.3 Hz, 1H), 4.17 (d, J = 15.7 Hz, 1H), 3.86 (s, 2H), 3.85 (s, 2H), 3.75 (dt, J = 12.1, 5.7 Hz, 1H), 3.65 – 3.58 (m, 1H), 3.37 (d, J = 18.0 Hz, 1H), 3.25 – 3.18 (m, 3H), 3.08 (d, J = 4.2 Hz, 1H), 3.06 (d, J = 4.1 Hz, 1H), 2.71 (q, J = 7.0, 6.4 Hz, 2H), 2.67 – 2.61 (m, 1H), 2.55 – 2.49 (m, 1H), 2.29 (s, 3H), 2.28 (s, 3H), 2.24 (s, 6H), 2.19 (s, 6H), 2.02 – 1.96 (m, 1H). HPLC retention time: 41.4 min. MS calculated for [C₂₈H₃₂N₂O₂ + H]⁺: 429.2, found: 429.3.

7e

Tert-butyl 7-(3-nitrobenzyl)-3,4-dihydroisoquinoline-2(1H)-carboxylate (6d).

6d was synthesized following General Procedure D from 3-nitrobenzyl bromide (57 mg, 0.26 mmol, 1.0 eq), **5** (141 mg, 0.39 mmol, 1.5 eq), Pd(dppf)Cl₂ (19 mg, 0.03 mmol, 0.1 eq), and K₂CO₃ (109 mg, 0.79 mmol, 3.0 eq) to yield the product as a yellow oil (34 mg, 35%). ¹H NMR (400 MHz, CDCl₃) δ 8.05 (s, 2H), 7.52 (d, *J* = 7.7 Hz, 1H), 7.45 (t, *J* = 7.7 Hz, 1H), 7.08 (d, *J* = 7.8 Hz, 1H), 6.98 (d, *J* = 7.9 Hz, 1H), 6.92 (s, 1H), 4.53 (s, 2H), 4.03 (s, 2H), 3.63 (t, *J* = 5.2 Hz, 2H), 2.80 (t, *J* = 6.2 Hz, 2H), 1.48 (s, 9H).

(S)-2-amino-3-(4-hydroxy-2,6-dimethylphenyl)-1-(7-(3-methylbenzyl)-3,4-dihydroisoquinolin-2(1H)-yl)propan-1-one (7e). Following General Procedure C, **6d** (37 mg, 0.10 mmol) was deprotected to yield the amine intermediate as a yellow solid. This intermediate was coupled to diBoc-DMT (44 mg, 0.11 mmol, 1.05 eq) in the presence of PyBOP (53 mg, 0.10 mmol, 1.0 eq), 6Cl-HOBt (17 mg, 0.10 mmol, 1.0 eq), and DIEA (143 μL, 1.02 mmol, 10 eq). Silica gel chromatography yielded the coupled product as a yellow oil. TFA deprotection yielded the product as a white, fluffy solid (24 mg, 57%, 3 steps). ¹H NMR (500 MHz, CD₃OD, rotamers) δ 8.09 – 8.06 (m, 1H), 8.05 (d, *J* = 2.0 Hz, 1H), 8.03 (t, *J* = 2.0 Hz, 1H), 7.63 (d, *J* = 3.5 Hz, 1H), 7.61 (d, *J* = 3.8 Hz, 1H), 7.53 (dd, *J* = 15.8, 5.1 Hz, 1H), 7.53 (d, *J* = 5.1 Hz, 1H), 7.06 – 6.95 (m, 6H), 6.50 (s, 1H), 6.40 (s, 2H), 6.29 (s, 2H), 4.63 (d, *J* = 17.0 Hz, 1H), 4.59 – 4.49 (m, 2H), 4.53 (d, *J* = 17.1 Hz, 2H), 4.19 (d, *J* = 15.8 Hz, 1H), 4.06 (s, 2H), 4.05 – 4.04 (m, 2H), 3.83 (dt, *J* = 11.9, 5.7 Hz, 1H), 3.59 – 3.52 (m, 1H), 3.42 (d, *J* = 15.8 Hz, 1H), 3.26 – 3.18 (m, 3H), 3.09 (t, *J* = 4.5 Hz, 1H), 3.06 (t, *J* = 4.5 Hz, 1H), 2.76 – 2.71 (m, 2H), 2.71 – 2.65 (m, 2H), 2.53 (dt, *J* = 16.0, 6.3 Hz, 1H), 2.23 (s, 6H), 2.20 (s, 6H), 1.98 (dt, *J* = 16.2, 5.9

Hz, 1H). HPLC retention time: 37.3 min. MS calculated for $[C_{27}H_{29}N_3O_4 + H]^+$: 460.2, found: 460.3.

7f

(S)-2-amino-1-(7-(3-aminobenzyl)-3,4-dihydroisoquinolin-2(1H)-yl)-3-(4-hydroxy-2,6-dimethylphenyl)propan-1-one (7f). Following General Procedure E, **6d** (37 mg, 0.10 mmol) was deprotected to yield the amine intermediate as a yellow solid. This intermediate was coupled to diBoc-DMT (44 mg, 0.11 mmol, 1.05 eq) in the presence of PyBOP (53 mg, 0.10 mmol, 1.0 eq), 6Cl-HOBt (17 mg, 0.10 mmol, 1.0 eq), and DIEA (143 μ L, 1.02 mmol, 10 eq). Silica gel chromatography yielded the coupled product as a yellow oil. Half of the nitro intermediate was reduced in the presence of NH_4Cl (62 mg, 1.1 mmol, 40 eq), Zn (38 mg, 0.58 mmol, 20 eq), and water (114 μ L, 6.34 mmol, 220 eq) to yield the aniline as an orange oil. TFA deprotection yielded the product as a white, fluffy solid (17 mg, 57%, 4 steps). 1H NMR (500 MHz, CD_3OD , rotamers) δ 7.46 – 7.41 (m, 2H), 7.32 (s, 1H), 7.31 (s, 1H), 7.22 – 7.20 (m, 1H), 7.19 (s, 2H), 7.17 (t, $J = 1.8$ Hz, 1H), 7.03 – 6.97 (m, 3H), 6.95 (d, $J = 7.9$ Hz, 1H), 6.94 (dd, $J = 8.0, 1.5$ Hz, 1H), 6.52 (s, 1H), 6.40 (s, 2H), 6.29 (s, 2H), 4.62 (d, $J = 17.1$ Hz, 1H), 4.56 (td, $J = 11.4, 4.3$ Hz, 2H), 4.49 (d, $J = 17.1$ Hz, 1H), 4.19 (d, $J = 15.8$ Hz, 1H), 3.99 (s, 2H), 3.97 (s, 2H), 3.82 (dt, $J = 12.0, 5.6$ Hz, 1H), 3.57 – 3.50 (m, 1H), 3.41 (d, $J = 15.7$ Hz, 1H), 3.26 – 3.19 (m, 3H), 3.10 (t, $J = 3.9$ Hz, 1H), 3.07 (t, $J = 3.9$ Hz, 1H), 2.73 – 2.69 (m, 2H), 2.66 – 2.60 (m, 1H), 2.56 – 2.48 (m, 1H), 2.24 (s, 6H), 2.20 (s, 6H), 1.98 (dt, $J = 16.3, 5.8$ Hz, 1H). HPLC retention time: 21.8 min. MS calculated for $[C_{27}H_{31}N_3O_2 + H]^+$: 430.2, found: 430.3.

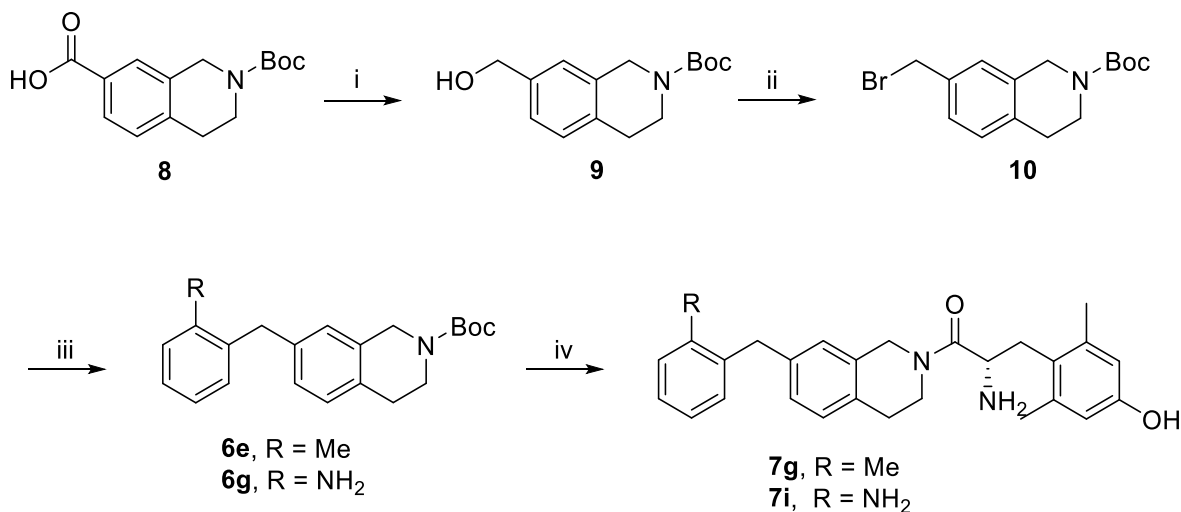
7h

Tert-butyl 7-(2-nitrobenzyl)-3,4-dihydroisoquinoline-2(1H)-carboxylate (6f). **6f** was synthesized following General Procedure D from 2-nitrobenzyl bromide (43 mg, 0.20 mmol, 1.0 eq), **5** (108 mg, 0.30 mmol, 1.5 eq), Pd(dppf)Cl₂ (15 mg, 0.02 mmol, 0.1 eq), and K₂CO₃ (83 mg, 0.60 mmol, 3.0 eq). Additional purification was performed by silica gel chromatography in DCM to yield the product (8 mg, 11%). ¹H NMR (500 MHz, CDCl₃) δ 7.94 (d, *J* = 8.1 Hz, 1H), 7.53 (t, *J* = 7.5 Hz, 1H), 7.39 (t, *J* = 7.9 Hz, 1H), 7.31 – 7.28 (m, 1H), 7.06 (d, *J* = 7.8 Hz, 1H), 6.95 (d, *J* = 7.8 Hz, 1H), 6.89 (s, 1H), 4.51 (s, 2H), 4.19 (d, *J* = 73.3 Hz, 4H), 3.63 (t, *J* = 5.7 Hz, 2H), 2.79 (t, *J* = 5.5 Hz, 2H), 1.48 (s, 9H).

(S)-2-amino-3-(4-hydroxy-2,6-dimethylphenyl)-1-(7-(2-nitrobenzyl)-3,4-dihydroisoquinolin-2(1H)-yl)propan-1-one (7h). Following General Procedure C, **6f** (10 mg, 0.03 mmol) was deprotected to yield the amine intermediate as an off-white solid. This intermediate was coupled to diBoc-DMT (11 mg, 0.027 mmol, 1.05 eq) in the presence of PyBOP (14 mg, 0.026 mmol, 1.0 eq), 6Cl-HOBt (4 mg, 0.026 mmol, 1.0 eq), and DIEA (36 μL, 0.26 mmol, 10 eq). Silica gel chromatography yielded the coupled product as a yellow oil. TFA deprotection yielded the product as a white, fluffy solid (11 mg, 53%, 3 steps). ¹H NMR (500 MHz, CD₃OD, rotamers) δ 7.90 (dd, *J* = 3.1, 1.3 Hz, 1H), 7.89 (dd, *J* = 3.2, 1.3 Hz, 1H), 7.64 – 7.58 (m, 2H), 7.45 (td, *J* = 7.9, 1.5 Hz, 2H), 7.42 (td, *J* = 7.9, 1.4 Hz, 2H), 6.96 (d, *J* = 7.9 Hz, 1H), 6.91 (s, 2H), 6.90 – 6.86 (m, 2H), 6.44 (s, 1H), 6.40 (s, 2H), 6.29 (s, 2H), 4.59 (d, *J* = 17.1 Hz, 1H), 4.58 – 4.48 (m, 2H), 4.49 (d, *J* = 16.8 Hz, 2H), 4.24 (s, 2H), 4.22 (d, *J* = 2.4 Hz, 2H), 4.16 (d, *J* = 15.8 Hz, 1H), 3.82 (dt, *J* = 11.9, 5.6 Hz, 1H), 3.59 – 3.51 (m, 1H), 3.40 (d, *J* = 15.8 Hz, 1H), 3.24

– 3.18 (m, 3H), 3.08 (t, $J = 3.9$ Hz, 1H), 3.06 (t, $J = 3.9$ Hz, 1H), 2.73 – 2.68 (m, 2H), 2.68 – 2.64 (m, 1H), 2.54 – 2.48 (m, 1H), 2.24 (s, 6H), 2.19 (s, 6H), 1.99 – 1.93 (m, 1H). HPLC retention time: 36.6 min. MS calculated for $[C_{27}H_{29}N_3O_4 + H]^+$: 460.2, found: 460.3.

Scheme 14. Synthesis of 7g and 7i



Tert-butyl 7-(hydroxymethyl)-3,4-dihydroisoquinoline-2(1H)-carboxylate (**9**).

To a solution of **8** in dry THF (15 mL), a 2.0 M solution of borane dimethyl sulfide in THF (2.7 mL, 5.41 mmol, 3.0 eq) was added dropwise over 15 minutes under inert atmosphere. The reaction mixture stirred at room temperature overnight. The reaction was quenched by the addition of methanol (20 mL). Solvent was removed under vacuum. The crude product was dissolved in ethyl acetate and washed with saturated aqueous NaHCO₃ and brine. The combined aqueous layers were extracted with ethyl acetate. The combined organic layers were dried over MgSO₄, filtered, and concentrated under vacuum to yield the product as a colorless oil (475 mg, 100%). ¹H NMR (500 MHz, CDCl₃) δ 7.16 (d, $J = 7.9$ Hz, 1H), 7.13 (d, $J = 5.8$ Hz, 1H), 7.12 (s, 1H), 4.65 (s, 2H), 4.57 (s, 2H), 3.63 (t, $J = 5.9$ Hz, 2H), 2.82 (t, $J = 5.8$ Hz, 2H), 1.49 (s, 9H).

Tert-butyl 7-(bromomethyl)-3,4-dihydroisoquinoline-2(1H)-carboxylate (10).

To a solution of **9** (950 mg, 3.61 mmol, 1.0 eq) in DCM (40 mL), CBr₄ (1.32 g, 3.97 mmol, 1.1 eq) and a solution of PPh₃ (1.14 g, 4.33 mmol, 1.2 eq) in DCM (5 mL) were added. The reaction stirred at room temperature for 2 hours. The product was purified via silica gel chromatography in ethyl acetate/hexanes to yield a white solid (1.08 g, 92%). ¹H NMR (500 MHz, CDCl₃) δ 7.19 (d, *J* = 8.3 Hz, 1H), 7.14 (s, 1H), 7.11 (d, *J* = 7.8 Hz, 1H), 4.56 (s, 2H), 4.47 (s, 2H), 3.64 (t, *J* = 6.0 Hz, 2H), 2.82 (t, *J* = 5.9 Hz, 2H), 1.49 (s, 9H).

7g

Tert-butyl 7-(2-methylbenzyl)-3,4-dihydroisoquinoline-2(1H)-carboxylate (6e). Intermediate **10** (34 mg, 0.10 mmol, 1.0 eq), 2-methylphenylboronic acid (21 mg, 0.16 mmol, 1.5 eq), Pd(dppf)Cl₂ (7 mg, 0.01 mmol, 0.1 eq), and K₂CO₃ (43 mg, 0.31 mmol, 3.0 eq) were combined. The system was flushed with argon. A degassed mixture of 3:1 acetone:water (15 mL) was added, and the reaction was heated to reflux overnight. The product was purified via silica gel chromatography in ethyl acetate/hexanes to yield a colorless oil (30 mg, 86%). ¹H NMR (500 MHz, CDCl₃) δ 7.19 – 7.14 (m, 3H), 7.12 – 7.08 (m, 1H), 7.04 (d, *J* = 7.8 Hz, 1H), 6.94 (d, *J* = 7.9 Hz, 1H), 6.87 (s, 1H), 4.51 (s, 2H), 3.95 (s, 2H), 3.64 (br, 2H), 2.80 (t, *J* = 6.0 Hz, 2H), 2.26 (s, 3H).

(S)-2-amino-3-(4-hydroxy-2,6-dimethylphenyl)-1-(7-(2-methylbenzyl)-3,4-dihydroisoquinolin-2(1H)-yl)propan-1-one (7g). Following General Procedure C, **6e** (30 mg, 0.089 mmol) was deprotected to yield the amine intermediate as an off-white solid. This intermediate was coupled to diBoc-DMT (38 mg, 0.092 mmol, 1.05 eq) in the

presence of PyBOP (46 mg, 0.088 mmol, 1.0 eq) and DIEA (123 μ L, 0.880 mmol, 10 eq) to yield the product as a red oil. No 6Cl-HOBt was used. TFA deprotection yielded the product as a white, fluffy solid (24 mg, 50%, 3 steps). ^1H NMR (500 MHz, CD_3OD , rotamers) δ 7.13 – 7.09 (m, 7H), 7.08 (d, J = 3.9 Hz, 1H), 6.94 (d, J = 7.8 Hz, 1H), 6.90 (s, 2H), 6.87 – 6.84 (m, 2H), 6.42 (s, 1H), 6.40 (s, 2H), 6.31 (s, 2H), 4.58 (d, J = 16.8 Hz, 1H), 4.56 – 4.50 (m, 2H), 4.47 (d, J = 16.9 Hz, 1H), 4.15 (d, J = 15.7 Hz, 1H), 3.93 (s, 2H), 3.91 (s, 2H), 3.78 (dt, J = 12.7, 5.6 Hz, 1H), 3.60 – 3.53 (m, 1H), 3.36 (d, J = 15.8 Hz, 1H), 3.24 – 3.18 (m, 3H), 3.09 (t, J = 4.4 Hz, 1H), 3.06 (t, J = 4.5 Hz, 1H), 2.70 (q, J = 7.3, 6.4 Hz, 2H), 2.67 – 2.62 (m, 1H), 2.51 (dt, J = 16.1, 6.1 Hz, 1H), 2.23 (s, 6H), 2.19 (s, 3H), 2.19 (s, 6H), 2.18 (s, 3H), 2.00 – 1.93 (m, 2H). HPLC retention time: 40.4 min. HRMS calculated for $[\text{C}_{28}\text{H}_{32}\text{N}_2\text{O}_2 + \text{H}]^+$: 429.2537, found: 429.2594.

7i

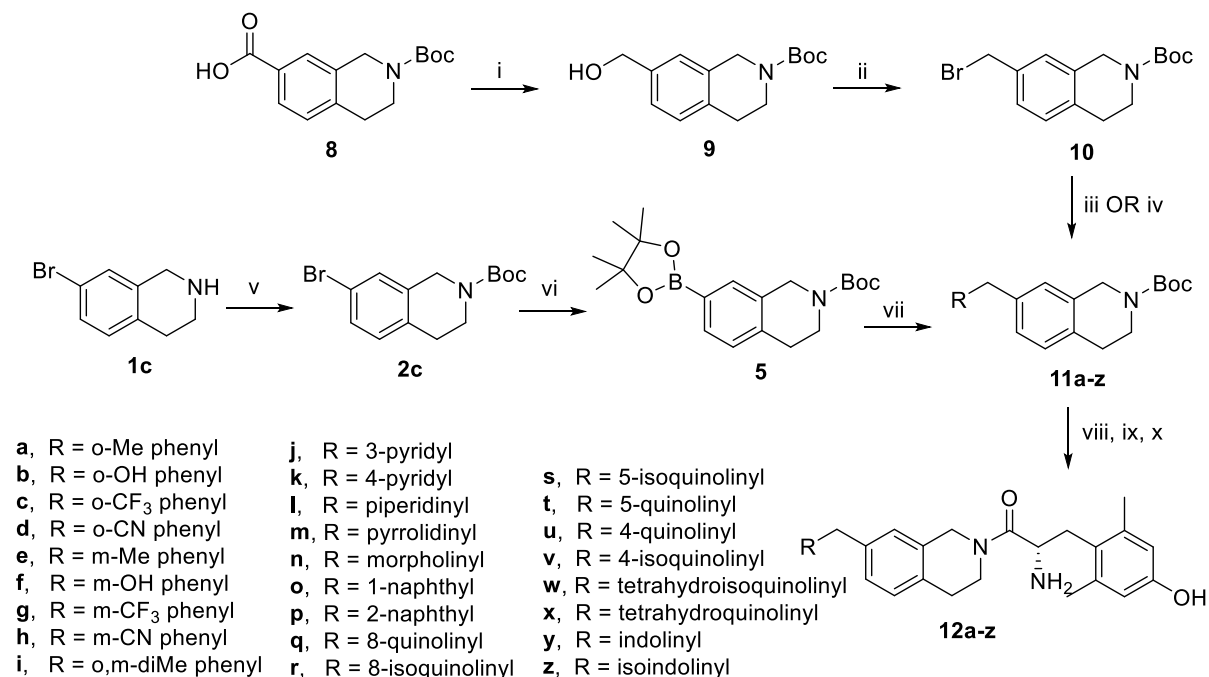
Tert-butyl 7-(2-aminobenzyl)-3,4-dihydroisoquinoline-2(1H)-carboxylate (6g). **6g** was synthesized following General Procedure F from **10** (79 mg, 0.24 mmol, 1.0 eq), 2-aminophenylboronic acid (50 mg, 0.36 mmol, 1.5 eq), $\text{Pd}(\text{dppf})\text{Cl}_2$ (18 mg, 0.02 mmol, 0.1 eq), and K_2CO_3 (100 mg, 0.73 mmol, 3.0 eq) to yield the product as an orange oil (21 mg, 26%). ^1H NMR (400 MHz, CDCl_3) δ 7.20 – 7.15 (m, 3H), 7.12 (s, 2H), 6.72 (t, J = 7.3 Hz, 1H), 6.65 – 6.63 (m, 1H), 6.63 – 6.61 (m, 1H), 4.56 (s, 2H), 4.28 (s, 2H), 3.64 (br, 2H), 2.82 (t, J = 4.8 Hz, 2H), 1.48 (s, 9H).

(S)-2-amino-1-(7-(2-aminobenzyl)-3,4-dihydroisoquinolin-2(1H)-yl)-3-(4-hydroxy-2,6-dimethylphenyl)propan-1-one (7i). Following General Procedure C, **6g** (21 mg, 0.062 mmol) was deprotected to yield the amine intermediate as a reddish solid. This intermediate was coupled to diBoc-DMT (27 mg, 0.065 mmol, 1.05 eq) in the

presence of PyBOP (32 mg, 0.062 mmol, 1.0 eq) and DIEA (87 μ L, 0.620 mmol, 10 eq) to yield the product as a reddish brown oil. No 6Cl-HOBt was used. TFA deprotection yielded the product as a white, fluffy solid (17 mg, 50%, 3 steps). ^1H NMR (500 MHz, CD_3OD , rotamers) δ 7.47 – 7.43 (m, 3H), 7.39 – 7.33 (m, 2H), 7.28 – 7.24 (m, 3H), 7.18 – 7.12 (m, 3H), 7.09 (d, J = 7.9 Hz, 1H), 7.04 (d, J = 7.8 Hz, 1H), 6.65 (s, 1H), 6.40 (s, 2H), 6.25 (s, 2H), 4.63 (d, J = 17.0 Hz, 1H), 4.61 – 4.53 (m, 2H), 4.55 (d, J = 17.0 Hz, 1H), 4.50 (s, 2H), 4.45 (s, 2H), 4.20 (d, J = 15.8 Hz, 1H), 3.93 (dt, J = 12.9, 5.5 Hz, 1H), 3.50 (dt, J = 13.1, 6.6 Hz, 1H), 3.45 (d, J = 15.9 Hz, 1H), 3.27 – 3.18 (m, 3H), 3.13 – 3.05 (m, 2H), 2.77 (t, J = 6.1 Hz, 2H), 2.73 – 2.68 (m, 1H), 2.55 (dt, J = 16.4, 5.3 Hz, 1H), 2.23 (s, 6H), 2.20 (s, 6H), 2.00 – 1.89 (m, 1H). HPLC retention time: 23.8 min. HRMS calculated for $[\text{C}_{27}\text{H}_{31}\text{N}_3\text{O}_2 + \text{H}]^+$: 430.2489, found: 430.2492.

6.1.3 Procedures and Characterization for Compounds Contained in Chapter 3

Scheme 15. Synthesis of 12a-12z



12a

Tert-butyl 7-(2-methoxybenzyl)-3,4-dihydroisoquinoline-2(1H)-carboxylate (11a). **11a** was synthesized following General Procedure F from **10** (60 mg, 0.18 mmol, 1.0 eq), (2-methoxyphenyl)boronic acid (42 mg, 0.28 mmol, 1.5 eq), Pd(dppf)Cl₂ (13 mg, 0.02 mmol, 0.1 eq), and K₂CO₃ (76 mg, 0.55 mmol, 3.0 eq) to yield the product as a colorless oil (37 mg, 57%). ¹H NMR (500 MHz, CDCl₃) δ 7.21 (t, *J* = 7.6 Hz, 1H), 7.07 (d, *J* = 7.2 Hz, 1H), 7.03 (s, 2H), 6.95 (s, 1H), 6.88 (t, *J* = 8.2 Hz, 2H), 4.52 (s, 2H), 3.93 (s, 2H), 3.83 (s, 3H), 3.63 (s, 2H), 2.79 (t, *J* = 5.8 Hz, 2H), 1.49 (s, 9H).

(S)-2-amino-3-(4-hydroxy-2,6-dimethylphenyl)-1-(7-(2-methoxybenzyl)-3,4-dihydroisoquinolin-2(1H)-yl)propan-1-one (12a). Following General Procedure C, **11a** (37 mg, 0.10 mmol) was deprotected to yield the amine intermediate as a colorless oil. This intermediate was coupled to diBoc-DMT (45 mg, 0.10 mmol, 1.05 eq) in the presence of PyBOP (54 mg, 0.10 mmol, 1.0 eq), and DIEA (142 μL, 1.04 mmol, 10 eq) to yield the product as a brown oil. No 6Cl-HOBt was used. TFA deprotection yielded the product as a white, fluffy solid. ¹H NMR (500 MHz, CD₃OD, rotamers) δ 7.17 (t, *J* = 7.9 Hz, 2H), 7.05 (t, *J* = 7.4 Hz, 2H), 6.97 (d, *J* = 7.7 Hz, 1H), 6.94 – 6.90 (m, 4H), 6.89 – 6.82 (m, 4H), 6.50 (d, *J* = 3.9 Hz, 1H), 6.39 (s, 2H), 6.33 (s, 2H), 4.59 – 4.45 (m, 4H), 4.15 (d, *J* = 15.7 Hz, 1H), 3.86 (d, *J* = 3.7 Hz, 2H), 3.85 (d, *J* = 2.8 Hz, 2H), 3.78 (d, *J* = 1.6 Hz, 3H), 3.78 (d, *J* = 1.2 Hz, 3H), 3.71 – 3.65 (m, 1H), 3.65 – 3.58 (m, 1H), 3.33 (d, *J* = 15.7 Hz, 1H), 3.25 – 3.17 (m, 2H), 3.09 (d, *J* = 11.4 Hz, 1H), 2.72 – 2.65 (m, 1H), 2.65 – 2.58 (m, 1H), 2.55 – 2.45 (m, 1H), 2.24 (s, 6H), 2.18 (s, 6H), 1.98 – 1.87 (m, 1H). HPLC retention time: 39.1 min. HRMS calculated for [C₂₈H₃₂N₂O₃ + H]⁺: 445.2486, found: 445.2494.

12b

Tert-butyl 7-(2-hydroxybenzyl)-3,4-dihydroisoquinoline-2(1H)-carboxylate (11b). **11b** was synthesized following General Procedure F from **10** (60 mg, 0.18 mmol, 1.0 eq), (2-hydroxyphenyl)boronic acid (38 mg, 0.28 mmol, 1.5 eq), Pd(dppf)Cl₂ (13 mg, 0.02 mmol, 0.1 eq), and K₂CO₃ (76 mg, 0.55 mmol, 3.0 eq) to yield the product as a yellow oil (33 mg, 53%). ¹H NMR (500 MHz, CDCl₃) δ 7.16 – 7.10 (m, 2H), 7.08 – 7.01 (m, 2H), 6.96 (s, 1H), 6.89 (t, *J* = 7.5 Hz, 1H), 6.79 (d, *J* = 7.9 Hz, 1H), 4.51 (s, 2H), 3.95 (s, 2H), 3.62 (s, 2H), 2.78 (t, *J* = 5.9 Hz, 2H), 1.48 (s, 9H).

(S)-2-amino-3-(4-hydroxy-2,6-dimethylphenyl)-1-(7-(2-hydroxybenzyl)-3,4-dihydroisoquinolin-2(1H)-yl)propan-1-one (12b). Following General Procedure C, **11b** (33 mg, 0.10 mmol) was deprotected to yield the amine intermediate as an off-white solid. This intermediate was coupled to diBoc-DMT (42 mg, 0.10 mmol, 1.05 eq) in the presence of PyBOP (50 mg, 0.10 mmol, 1.0 eq), and DIEA (132 μL, 0.97 mmol, 10 eq) to yield the product as a brown oil. No 6Cl-HOBt was used. TFA deprotection yielded the product as a white, fluffy solid. ¹H NMR (500 MHz, CD₃OD, rotamers) δ 7.01 (ddt, *J* = 10.9, 5.1, 1.8 Hz, 4H), 6.97 (d, *J* = 7.6 Hz, 3H), 6.92 (d, *J* = 7.9 Hz, 1H), 6.88 (d, *J* = 7.9 Hz, 1H), 6.78 – 6.70 (m, 4H), 6.55 (s, 1H), 6.40 (s, 2H), 6.33 (s, 2H), 4.61 (d, *J* = 16.9 Hz, 1H), 4.58 – 4.49 (m, 2H), 4.47 (d, *J* = 16.5 Hz, 1H), 4.16 (d, *J* = 15.6 Hz, 1H), 3.87 (s, 2H), 3.86 (s, 2H), 3.75 – 3.68 (m, 1H), 3.66 – 3.59 (m, 1H), 3.34 (d, *J* = 15.8 Hz, 1H), 3.26 – 3.17 (m, 3H), 3.10 – 3.05 (m, 2H), 2.72 – 2.65 (m, 2H), 2.65 – 2.59 (m, 2H), 2.55 – 2.45 (m, 1H), 2.24 (s, 6H), 2.19 (s, 6H), 2.03 – 1.95 (m, 2H). HPLC retention time: 32.8 min. HRMS calculated for [C₂₇H₃₀N₂O₃ + H]⁺: 431.2329, found: 431.2337.

12c

Tert-Butyl 7-(2-(trifluoromethyl)benzyl)-3,4-dihydroisoquinoline-2(1H)-carboxylate (11c). **11c** was synthesized following General Procedure D2 from **5** (100 mg, 0.278 mmol, 1.0 eq), 1-(bromomethyl)-2-(trifluoromethyl)benzene (133 mg, 0.556 mmol, 2.0 eq), Pd(dppf)Cl₂ (20 mg, 0.028 mmol, 0.1 eq), and K₂CO₃ (115 mg, 0.834 mmol, 3.0 eq) to yield a colorless oil (27 mg 25%). ¹H NMR (400 MHz, CDCl₃) δ 7.67 (d, *J* = 7.9 Hz, 1H), 7.43 (t, *J* = 7.5 Hz, 1H), 7.31 (t, *J* = 7.7 Hz, 1H), 7.18 (d, *J* = 7.9 Hz, 1H), 7.06 (d, *J* = 7.8 Hz, 1H), 6.95 (d, *J* = 7.0 Hz, 1H), 6.89 (s, 1H), 4.52 (s, 2H), 4.14 (s, 2H), 3.63 (t, *J* = 5.4 Hz, 2H), 2.80 (t, *J* = 5.9 Hz, 2H), 1.48 (s, 9H).

(S)-2-amino-3-(4-hydroxy-2,6-dimethylphenyl)-1-(7-(2-(trifluoromethyl)benzyl)-3,4-dihydroisoquinolin-2(1H)-yl)propan-1-one (12c). Following General Procedure B, **11c** (27 mg, 0.069 mmol, 1.0 eq) was deprotected to yield the amine intermediate as a white solid. This intermediate was coupled to diBoc-DMT (30 mg, 0.074 mmol, 1.05 eq) in the presence of PyBOP (36 mg, 0.070 mmol, 1.0 eq) and DIEA (98 μL, 0.700 mmol, 10 eq) to yield the product as a brown oil. No 6-Cl-HOBt was used. TFA deprotection yielded the product as an off-white solid (24 mg, 57%, 3 steps). ¹H NMR (500 MHz, CD₃OD, rotamers) δ 7.70 – 7.66 (m, 2H), 7.54 – 7.48 (m, 2H), 7.40 – 7.35 (m, 2H), 7.28 – 7.22 (m, 2H), 6.98 (d, *J* = 7.8 Hz, 1H), 6.95 – 6.91 (m, 2H), 6.89 (s, 1H), 6.86 (d, 1H), 6.47 (s, 1H), 6.41 (s, 2H), 6.31 (s, 2H), 4.61 (d, *J* = 17.0 Hz, 1H), 4.58 – 4.51 (m, 2H), 4.49 (d, *J* = 17.0 Hz, 1H), 4.18 (d, *J* = 15.8 Hz, 1H), 4.12 (s, 2H), 4.11 (s, 2H), 3.86 – 3.80 (m, 1H), 3.59 – 3.52 (m, 1H), 3.39 (d, *J* = 15.8 Hz, 1H), 3.26 – 3.18 (m, 3H), 3.11 – 3.06 (m, 2H), 2.76 – 2.69 (m, 2H), 2.68 – 2.63 (m, 1H), 2.56 – 2.49 (m, 1H), 2.24 (s, 6H), 2.20 (s, 6H), 2.01 – 1.92 (m, 1H). ¹⁹F NMR (470 MHz,

CD₃OD, rotamers) δ -60.76, -77.10. HPLC retention time: 42.2 min. HRMS calculated for [C₂₈H₂₉F₃N₂O₂ + H]⁺: 483.2254, found: 483.2262.

12d

Tert-Butyl 7-(2-cyanobenzyl)-3,4-dihydroisoquinoline-2(1H)-carboxylate (11d). **11d** was synthesized following General Procedure D2 from **5** (75 mg, 0.209 mmol, 1.0 eq), 3-(bromomethyl)phenol (78 mg, 0.418 mmol, 2.0 eq), Pd(dppf)Cl₂ (15 mg, 0.021 mmol, 0.1 eq), and K₂CO₃ (87 mg, 0.627 mmol, 3.0 eq) to yield the product as a colorless oil (26 mg, 37%). ¹H NMR (500 MHz, CDCl₃) δ 7.15 (t, *J* = 7.8 Hz, 1H), 7.04 (d, *J* = 7.8 Hz, 1H), 6.99 (d, *J* = 7.3 Hz, 1H), 6.92 (s, 1H), 6.79 – 6.74 (m, 1H), 6.69 (d, *J* = 8.1 Hz, 1H), 6.65 (s, 1H), 4.52 (s, 2H), 3.87 (s, 2H), 3.62 (t, *J* = 5.9 Hz, 2H), 2.78 (t, *J* = 5.9 Hz, 2H), 1.49 (s, 9H).

(S)-2-((2-(2-amino-3-(4-hydroxy-2,6-dimethylphenyl)propanoyl)-1,2,3,4-tetrahydroisoquinolin-7-yl)methyl)benzotrile (12d). Following General Procedure C, **11d** (20 mg, 0.057 mmol, 1.0 eq) was deprotected to yield the amine intermediate as a colorless oil. This intermediate was coupled to diBoc-DMT (24 mg, 0.059 mmol, 1.05 eq) in the presence of PyBOP (29 mg, 0.056 mmol, 1.0 eq) and DIEA (80 μ L, 0.560 mmol, 10 eq) to yield the product as a brown oil. No 6Cl-HOBt was used. TFA deprotection yielded the product as a white, fluffy solid (3 mg, 10%, 3 steps). ¹H NMR (500 MHz, CD₃OD, rotamers) δ 7.70 (s, 1H), 7.68 (s, 1H), 7.62 – 7.57 (m, 2H), 7.45 – 7.35 (m, 4H), 7.03 (d, *J* = 8.1 Hz, 1H), 7.00 (s, 1H), 6.99 – 6.97 (m, 2H), 6.95 (d, *J* = 7.8 Hz, 1H), 6.56 (s, 1H), 6.39 (s, 2H), 6.29 (s, 2H), 4.62 (d, *J* = 16.9 Hz, 1H), 4.57 – 4.49 (m, 3H), 4.18 (d, *J* = 15.9 Hz, 1H), 4.15 (s, 2H), 4.13 (d, *J* = 3.1 Hz, 2H), 3.58 – 3.51 (m, 1H), 3.43 (d, *J* = 16.2 Hz, 0H), 3.26 – 3.18 (m, 4H), 3.06 (dd, *J* = 13.8, 4.2 Hz, 2H), 2.74

– 2.69 (m, 2H), 2.69 – 2.62 (m, 1H), 2.56 – 2.49 (m, 1H), 2.24 (s, 6H), 2.19 (s, 6H), 2.01 – 1.95 (m, 1H). HPLC retention time: 34.4 min. HRMS calculated for $[C_{28}H_{29}N_3O_2 + H]^+$: 440.2333, found: 440.2336.

12e

Tert-butyl 7-(3-methoxybenzyl)-3,4-dihydroisoquinoline-2(1H)-carboxylate (11e). **11e** was synthesized following General Procedure D from 3-methoxybenzyl bromide (42 μ L, 0.30 mmol, 1.0 eq), **5** (161 mg, 0.45 mmol, 1.5 eq), Pd(dppf)Cl₂ (22 mg, 0.03 mmol, 0.1 eq), and K₂CO₃ (124 mg, 0.90 mmol, 3.0 eq) to yield the product as a colorless oil (42 mg, 40%). ¹H NMR (500 MHz, CDCl₃) δ 7.22 (t, *J* = 7.8 Hz, 1H), 7.06 (d, *J* = 7.8 Hz, 1H), 7.01 (d, *J* = 7.9 Hz, 1H), 6.94 (s, 1H), 6.79 (d, *J* = 7.5 Hz, 1H), 6.77 – 6.73 (m, 2H), 4.53 (s, 2H), 3.91 (s, 2H), 3.79 (s, 3H), 3.63 (br s, 2H), 2.80 (t, *J* = 5.9 Hz, 2H), 1.50 (s, 9H).

(S)-2-amino-3-(4-hydroxy-2,6-dimethylphenyl)-1-(7-(3-methoxybenzyl)-3,4-dihydroisoquinolin-2(1H)-yl)propan-1-one (12e). Following General Procedure C, **11e** (42 mg, 0.119 mmol, 1.0 eq) was deprotected to yield the amine intermediate as a white solid. This intermediate was coupled to diBoc-DMT (50 mg, 0.123 mmol, 1.05 eq) in the presence of PyBOP (61 mg, 0.117 mmol, 1.0 eq), 6Cl-HOBt (20 mg, 0.117 mmol, 1.0 eq), and DIEA (164 μ L, 1.17 mmol, 10 eq). Silica gel chromatography yielded the coupled product as a colorless oil (66 mg, 88%). TFA deprotection yielded the product as a white solid. ¹H NMR (500 MHz, CD₃OD, rotamers) δ 7.16 (td, *J* = 7.8, 3.5 Hz, 2H), 6.99 (dd, *J* = 7.7, 1.7 Hz, 1H), 6.97 – 6.93 (m, 3H), 6.91 (d, *J* = 7.8 Hz, 1H), 6.76 – 6.70 (m, 6H), 6.49 (s, 1H), 6.40 (s, 2H), 6.32 (s, 2H), 4.61 (d, *J* = 16.9 Hz, 1H), 4.58 – 4.53 (m, 2H), 4.50 (d, *J* = 16.9 Hz, 1H), 4.17 (d, *J* = 15.7 Hz, 1H), 3.87 (s, 2H), 3.86 (s, 2H),

3.78 – 3.76 (m, 1H), 3.75 (s, 3H), 3.74 (s, 3H), 3.66 – 3.53 (m, 1H), 3.37 (d, $J = 15.8$ Hz, 1H), 3.26 – 3.17 (m, 3H), 3.11 – 3.05 (m, 2H), 2.70 (q, $J = 7.3, 6.7$ Hz, 2H), 2.67 – 2.62 (m, 1H), 2.52 (dt, $J = 16.2, 6.2$ Hz, 1H), 2.24 (s, 6H), 2.19 (s, 6H), 2.01 – 1.94 (m, 1H). HPLC retention time: 37.9 min. MS calculated for $[C_{28}H_{32}N_2O_3 + H]^+$: 445.2, found: 445.3.

12f

Tert-Butyl 7-(3-hydroxybenzyl)-3,4-dihydroisoquinoline-2(1H)-carboxylate (11f). **11f** was synthesized following General Procedure D2 from **5** (75 mg, 0.209 mmol, 1.0 eq), 3-(bromomethyl)phenol (78 mg, 0.418 mmol, 2.0 eq), Pd(dppf)Cl₂ (15 mg, 0.021 mmol, 0.1 eq), and K₂CO₃ (87 mg, 0.627 mmol, 3.0 eq) to yield the product as a colorless oil (26 mg, 37%). ¹H NMR (500 MHz, CDCl₃) δ 7.15 (t, $J = 7.8$ Hz, 1H), 7.04 (d, $J = 7.8$ Hz, 1H), 6.99 (d, $J = 7.3$ Hz, 1H), 6.92 (s, 1H), 6.79 – 6.74 (m, 1H), 6.69 (d, $J = 8.1$ Hz, 1H), 6.65 (s, 1H), 4.52 (s, 2H), 3.87 (s, 2H), 3.62 (t, $J = 5.9$ Hz, 2H), 2.78 (t, $J = 5.9$ Hz, 2H), 1.49 (s, 9H).

(S)-2-amino-3-(4-hydroxy-2,6-dimethylphenyl)-1-(7-(3-hydroxybenzyl)-3,4-dihydroisoquinolin-2(1H)-yl)propan-1-one (12f). Following General Procedure C, **11f** (26 mg, 0.077 mmol, 1.0 eq) was deprotected to yield the amine intermediate as a colorless oil. This intermediate was coupled to diBoc-DMT (33 mg, 0.080 mmol, 1.05 eq) in the presence of PyBOP (40 mg, 0.076 mmol, 1.0 eq) and DIEA (110 μL, 0.760 mmol, 10 eq) to yield the crude product as a brown oil. No 6Cl-HOBt was used. The crude product was purified via silica gel chromatography in ethyl acetate/hexanes. Subsequent TFA deprotection yielded the product as a white solid (8 mg, 40%, 3 steps). ¹H NMR (500 MHz, CD₃OD, rotamers) δ 7.09 – 7.03 (m, 2H), 6.99 (d, $J = 8.5$ Hz, 1H),

6.96 – 6.93 (m, 3H), 6.91 (d, $J = 7.8$ Hz, 1H), 6.65 (s, 1H), 6.64 (s, 1H), 6.61 – 6.57 (m, 3H), 6.49 (s, 1H), 6.40 (s, 2H), 6.32 (s, 2H), 4.62 (d, $J = 16.9$ Hz, 1H), 4.58 – 4.52 (m, 2H), 4.49 (d, $J = 16.7$ Hz, 1H), 4.17 (d, $J = 15.7$ Hz, 1H), 3.82 (s, 2H), 3.81 (s, 2H), 3.79 – 3.72 (m, 1H), 3.62 – 3.56 (m, 1H), 3.37 (d, $J = 15.8$ Hz, 1H), 3.26 – 3.17 (m, 3H), 3.07 (dd, $J = 13.7, 4.2$ Hz, 2H), 2.75 – 2.67 (m, 2H), 2.67 – 2.60 (m, 1H), 2.55 – 2.48 (m, 1H), 2.24 (s, 6H), 2.20 (s, 6H), 2.02 – 1.95 (m, 1H). HPLC retention time: 30.9 min. HRMS calculated for $[C_{27}H_{30}N_2O_3 + H]^+$: 431.2329, found: 431.2331.

12g

Tert-butyl 7-(3-(trifluoromethyl)benzyl)-3,4-dihydroisoquinoline-2(1H)-carboxylate (11g). **11g** was synthesized following General Procedure D from 3-(trifluoromethyl)benzyl bromide (33 μ L, 0.21 mmol, 1.0 eq), **5** (114 mg, 0.32 mmol, 1.5 eq), Pd(dppf)Cl₂ (15 mg, 0.02 mmol, 0.1 eq), and K₂CO₃ (88 mg, 0.64 mmol, 3.0 eq) to yield the product as a colorless oil (28 mg, 34%). MS calculated for $[C_{22}H_{24}F_3NO_2 + Na]^+$: 414.2, found: 414.2.

(S)-2-amino-3-(4-hydroxy-2,6-dimethylphenyl)-1-(7-(3-(trifluoromethyl)benzyl)-3,4-dihydroisoquinolin-2(1H)-yl)propan-1-one (12g). Following General Procedure C, **11g** (28 mg, 0.072 mmol, 1.0 eq) was deprotected to yield the amine intermediate as a yellow oil. The crude product was rinsed with two 2 mL portions of diethyl ether to yield a white solid. This intermediate was coupled to diBoc-DMT (56 mg, 0.138 mmol, 1.92 eq) in the presence of PyBOP (68 mg, 0.131 mmol, 1.82 eq), 6Cl-HOBt (22 mg, 0.131 mmol, 1.82 eq), and DIEA (184 μ L, 1.31 mmol, 18 eq). Silica gel chromatography yielded the coupled product as a colorless oil (64 mg, 72%). TFA deprotection yielded the product as a white solid. ¹H NMR (500 MHz,

CD₃OD, rotamers) δ 7.50 – 7.43 (m, 8H), 7.02 – 6.97 (m, 3H), 6.96 – 6.93 (m, 2H), 6.48 (s, 1H), 6.39 (s, 2H), 6.30 (s, 2H), 4.62 (d, J = 16.9 Hz, 1H), 4.59 – 4.51 (m, 2H), 4.52 (d, J = 17.3 Hz, 1H), 4.18 (d, J = 15.8 Hz, 1H), 4.00 (s, 2H), 3.99 (s, 2H), 3.81 (dt, J = 12.9, 5.7 Hz, 1H), 3.59 – 3.52 (m, 1H), 3.40 (d, J = 15.8 Hz, 1H), 3.26 – 3.17 (m, 3H), 3.08 (dt, J = 13.8, 4.1 Hz, 2H), 2.71 (q, J = 5.4 Hz, 2H), 2.68 – 2.64 (m, 1H), 2.56 – 2.49 (m, 1H), 2.23 (s, 6H), 2.19 (s, 6H), 2.00 – 1.93 (m, 1H). ¹⁹F NMR (470 MHz, CD₃OD, rotamers) δ -64.03 (d, J = 28.1 Hz), -77.17. HPLC retention time: 43.3 min. MS calculated for [C₂₈H₂₉F₃N₂O₂ + H]⁺: 483.2, found: 483.3.

12h

Tert-butyl 7-(3-cyanobenzyl)-3,4-dihydroisoquinoline-2(1H)-carboxylate (11h). **11h** was synthesized following General Procedure D from 3-(bromomethyl)benzotrile (40 mg, 0.20 mmol, 1.0 eq), **5** (109 mg, 0.30 mmol, 1.5 eq), Pd(dppf)Cl₂ (15 mg, 0.02 mmol, 0.1 eq), and K₂CO₃ (84 mg, 0.61 mmol, 3.0 eq) to yield the product as a colorless oil (30 mg, 43%). ¹H NMR (500 MHz, CDCl₃) δ 7.50 (dt, J = 7.4, 1.5 Hz, 1H), 7.45 (s, 1H), 7.43 (t, J = 8.0 Hz, 1H), 7.39 (t, J = 7.6 Hz, 2H), 7.08 (d, J = 7.8 Hz, 1H), 6.96 (d, J = 7.7 Hz, 1H), 6.90 (s, 1H), 4.54 (s, 2H), 3.96 (s, 2H), 3.64 (t, J = 5.9 Hz, 2H), 2.81 (t, J = 5.9 Hz, 2H), 1.49 (s, 9H).

(S)-2-amino-3-(4-hydroxy-2,6-dimethylphenyl)-1-(7-(3-isocyanobenzyl)-3,4-dihydroisoquinolin-2(1H)-yl)propan-1-one (12h). Following General Procedure C, **11h** (30 mg, 0.086 mmol, 1.0 eq) was deprotected to yield the amine intermediate as a off-white solid (21 mg, 84%). The crude product was rinsed with three small portions of diethyl ether. This intermediate was coupled to diBoc-DMT (32 mg, 0.077 mmol, 1.05 eq) in the presence of PyBOP (39 mg, 0.074 mmol, 1.0 eq), 6Cl-HOBt (13 mg, 0.074

mmol, 1.0 eq), and DIEA (104 μ L, 0.74 mmol, 10 eq). Silica gel chromatography yielded the coupled product as a white solid (27 mg, 57%). TFA deprotection yielded the product as a white solid. ^1H NMR (500 MHz, CD_3OD , rotamers) δ 7.57 – 7.51 (m, 6H), 7.48 – 7.43 (m, 2H), 7.03 – 6.99 (m, 3H), 6.97 – 6.94 (m, 2H), 6.48 (s, 1H), 6.39 (s, 2H), 6.29 (s, 2H), 4.63 (d, J = 17.0 Hz, 1H), 4.59 – 4.49 (m, 2H), 4.53 (d, J = 17.6 Hz, 2H), 4.18 (d, J = 15.8 Hz, 1H), 3.98 (s, 2H), 3.97 (s, 2H), 3.83 (dt, J = 12.3, 5.6 Hz, 1H), 3.59 – 3.51 (m, 1H), 3.41 (d, J = 15.7 Hz, 1H), 3.27 – 3.18 (m, 3H), 3.07 (dt, J = 13.8, 4.0 Hz, 2H), 2.74 – 2.70 (m, 2H), 2.69 – 2.63 (m, 1H), 2.53 (dt, J = 16.2, 5.9 Hz, 1H), 2.24 (s, 6H), 2.20 (s, 6H), 1.98 (dt, J = 16.0, 5.8 Hz, 1H). HPLC retention time: 35.2 min. MS calculated for $[\text{C}_{28}\text{H}_{29}\text{N}_3\text{O}_2 + \text{H}]^+$: 440.2, found: 440.2.

12i

Tert-butyl 7-(2,3-dimethylbenzyl)-3,4-dihydroisoquinoline-2(1H)-carboxylate (11i). **11i** was synthesized following General Procedure D2 from **5** (100 mg, 0.278 mmol, 1.0 eq), 1-(bromomethyl)-2,3-dimethylbenzene (83 mg, 0.417 mmol, 1.5 eq), $\text{Pd}(\text{dppf})\text{Cl}_2$ (20 mg, 0.028 mmol, 0.1 eq), and K_2CO_3 (115 mg, 0.834 mmol, 3.0 eq) to yield the product as a colorless oil (51 mg, 52%). ^1H NMR (500 MHz, CDCl_3) δ 7.09 – 7.06 (m, 2H), 7.04 (d, J = 7.6 Hz, 1H), 6.99 (d, J = 6.1 Hz, 1H), 6.93 (d, J = 7.9 Hz, 1H), 6.86 (s, 1H), 4.51 (s, 2H), 3.98 (s, 2H), 3.63 (t, J = 6.8 Hz, 2H), 2.79 (t, J = 6.0 Hz, 2H), 2.30 (s, 3H), 2.15 (s, 3H), 1.50 (s, 9H).

(S)-2-amino-1-(7-(2,3-dimethylbenzyl)-3,4-dihydroisoquinolin-2(1H)-yl)-3-(4-hydroxy-2,6-dimethylphenyl)propan-1-one (12i). Following General Procedure C, **11i** (51 mg, 0.145 mmol) was deprotected to yield the amine intermediate. This intermediate was coupled to diBoc-DMT (63 mg, 0.153 mmol, 1.05 eq) in the presence of PyBOP (76

mg, 0.146 mmol, 1.0 eq), and DIEA (199 μ L, 1.46 mmol, 10 eq) to yield the product as a brown oil. No 6Cl-HOBt was used. TFA deprotection yielded the product as a white, fluffy solid. ^1H NMR (500 MHz, CD_3OD , rotamers) δ 7.04 – 6.97 (m, 5H), 6.97 – 6.92 (m, 2H), 6.90 – 6.88 (m, 2H), 6.86 – 6.82 (m, 2H), 6.41 (s, 1H), 6.40 (s, 2H), 6.30 (s, 2H), 4.58 (d, J = 17.0 Hz, 1H), 4.62 – 4.48 (m, 2H), 4.46 (d, J = 16.9 Hz, 1H), 4.14 (d, J = 15.7 Hz, 1H), 3.95 (d, J = 2.8 Hz, 2H), 3.93 (s, 2H), 3.83 – 3.74 (m, 1H), 3.62 – 3.49 (m, 1H), 3.36 (d, J = 14.8 Hz, 1H), 3.26 – 3.17 (m, 3H), 3.08 (t, J = 4.9 Hz, 1H), 3.05 (t, J = 4.9 Hz, 1H), 2.72 – 2.61 (m, 3H), 2.54 – 2.47 (m, 1H), 2.25 (s, 3H), 2.25 (s, 3H), 2.23 (s, 6H), 2.19 (s, 6H), 2.09 (d, J = 2.2 Hz, 3H), 2.07 (d, J = 1.6 Hz, 3H), 2.00 – 1.93 (m, 1H). HPLC retention time: 43.2 min. HRMS calculated for $[\text{C}_{29}\text{H}_{34}\text{N}_2\text{O}_2 + \text{H}]^+$: 443.2693, found: 443.2699.

12j

Tert-butyl 7-(pyridin-3-ylmethyl)-3,4-dihydroisoquinoline-2(1H)-carboxylate (11j). **11j** was synthesized following General Procedure D2 from **5** (104 mg, 0.289 mmol, 1.0 eq), 3-(bromomethyl)pyridine hydrobromide (110 mg, 0.433 mmol, 1.5 eq), $\text{Pd}(\text{dppf})\text{Cl}_2$ (21 mg, 0.029 mmol, 0.1 eq), and K_2CO_3 (120 mg, 0.867 mmol, 3.0 eq) to yield the product as a colorless oil (20 mg, 21%). ^1H NMR (500 MHz, CDCl_3) δ 8.49 (s, 1H), 8.46 (d, J = 4.1 Hz, 1H), 7.46 (d, J = 7.7 Hz, 1H), 7.20 (dd, J = 7.8, 4.8 Hz, 1H), 7.07 (d, J = 7.9 Hz, 1H), 6.97 (d, J = 7.9 Hz, 1H), 6.91 (s, 1H), 4.52 (s, 2H), 3.93 (s, 2H), 3.62 (br s, 2H), 2.79 (t, J = 6.0 Hz, 2H), 1.48 (s, 9H).

(S)-2-amino-3-(4-hydroxy-2,6-dimethylphenyl)-1-(7-(pyridin-3-ylmethyl)-3,4-dihydroisoquinolin-2(1H)-yl)propan-1-one (12j). Following General Procedure C, **11j** (20 mg, 0.062 mmol, 1.0 eq) was deprotected to yield the amine intermediate as a

colorless oil. The crude product was rinsed with several small portions of diethyl ether. This intermediate was coupled to diBoc-DMT (26 mg, 0.064 mmol, 1.05 eq) in the presence of PyBOP (32 mg, 0.061 mmol, 1.0 eq), 6Cl-HOBt (10 mg, 0.061 mmol, 1.0 eq), and DIEA (86 μ L, 0.61 mmol, 10 eq). Silica gel chromatography yielded the coupled product (8 mg, 21%, 2 steps). TFA deprotection yielded the product as a white solid. ^1H NMR (500 MHz, CD_3OD , rotamers) δ 8.67 – 8.61 (m, 4H), 8.29 (d, J = 8.1 Hz, 1H), 8.26 (d, J = 8.0 Hz, 1H), 7.87 (dd, J = 8.1, 5.5 Hz, 1H), 7.83 (dd, J = 8.0, 5.5 Hz, 1H), 7.09 – 6.98 (m, 5H), 6.56 (s, 1H), 6.39 (s, 2H), 6.23 (s, 2H), 4.64 (d, J = 17.1 Hz, 1H), 4.59 – 4.52 (m, 2H), 4.53 (d, J = 16.6 Hz, 1H), 4.21 (d, J = 15.8 Hz, 1H), 4.14 (s, 2H), 4.12 (d, J = 3.2 Hz, 2H), 3.97 (dt, J = 13.2, 5.3 Hz, 1H), 3.48 (d, J = 16.1 Hz, 1H), 3.43 (dd, J = 13.0, 6.5 Hz, 1H), 3.26 – 3.19 (m, 3H), 3.08 (ddd, J = 13.7, 6.4, 4.1 Hz, 2H), 2.72 (t, J = 6.0 Hz, 2H), 2.69 – 2.62 (m, 1H), 2.57 – 2.49 (m, 1H), 2.23 (s, 6H), 2.20 (s, 6H), 1.99 (dt, J = 16.1, 6.1 Hz, 1H). HPLC retention time: 16.9 min. MS calculated for $[\text{C}_{26}\text{H}_{29}\text{N}_3\text{O}_2 + \text{H}]^+$: 416.2, found: 416.2.

12k

Tert-butyl 7-(pyridin-4-ylmethyl)-3,4-dihydroisoquinoline-2(1H)-carboxylate (11k). **11k** was synthesized following General Procedure D2 from **5** (112 mg, 0.312 mmol, 1.0 eq), 4-(bromomethyl)pyridine hydrobromide (118 mg, 0.468 mmol, 1.5 eq), $\text{Pd}(\text{dppf})\text{Cl}_2$ (23 mg, 0.031 mmol, 0.1 eq), and K_2CO_3 (129 mg, 0.936 mmol, 3.0 eq) to yield the product as a colorless oil (20 mg, 20%). ^1H NMR (500 MHz, CDCl_3) δ 8.49 (d, J = 5.4 Hz, 2H), 7.13 – 7.05 (m, 3H), 6.97 (d, J = 7.8 Hz, 1H), 6.91 (s, 1H), 4.53 (s, 2H), 3.91 (s, 2H), 3.63 (s, 2H), 2.80 (t, J = 5.0 Hz, 2H), 1.48 (s, 9H).

(S)-2-amino-3-(4-hydroxy-2,6-dimethylphenyl)-1-(7-(pyridin-4-ylmethyl)-3,4-dihydroisoquinolin-2(1H)-yl)propan-1-one (12k). Following General Procedure C, **11k** (20 mg, 0.062 mmol, 1.0 eq) was deprotected to yield the amine intermediate as a cloudy, yellow oil. The crude product was rinsed with several small portions of diethyl ether. This intermediate was coupled to diBoc-DMT (26 mg, 0.064 mmol, 1.05 eq) in the presence of PyBOP (32 mg, 0.061 mmol, 1.0 eq), 6Cl-HOBt (10 mg, 0.061 mmol, 1.0 eq), and DIEA (86 μ L, 0.61 mmol, 10 eq). Silica gel chromatography yielded the coupled product (24 mg, 63%, 2 steps). TFA deprotection yielded the product as a white solid. ^1H NMR (500 MHz, CD_3OD , rotamers) δ 8.69 – 8.65 (m, 4H), 7.81 – 7.77 (m, 4H), 7.10 – 7.07 (m, 2H), 7.06 (d, J = 7.8 Hz, 1H), 7.01 (d, 2H), 6.58 (s, 1H), 6.40 (s, 2H), 6.25 (s, 2H), 4.65 (d, J = 17.1 Hz, 1H), 4.58 – 4.55 (m, 2H), 4.53 (d, J = 16.8 Hz, 1H), 4.25 – 4.22 (m, 3H), 4.20 (d, J = 3.0 Hz, 2H), 3.96 (dt, J = 12.9, 5.3 Hz, 1H), 3.48 (d, J = 15.0 Hz, 1H), 3.46 – 3.42 (m, 1H), 3.27 – 3.19 (m, 3H), 3.08 (ddd, J = 13.7, 6.2, 4.2 Hz, 2H), 2.74 (t, J = 6.1 Hz, 2H), 2.70 – 2.62 (m, 1H), 2.58 – 2.51 (m, 1H), 2.24 (s, 6H), 2.21 (s, 6H), 2.00 (dt, J = 16.2, 5.8 Hz, 1H). HPLC retention time: 17.0 min. MS calculated for $[\text{C}_{26}\text{H}_{29}\text{N}_3\text{O}_2 + \text{H}]^+$: 416.2, found: 416.3.

12l

Tert-butyl 7-(piperidin-1-ylmethyl)-3,4-dihydroisoquinoline-2(1H)-carboxylate (11l). **11l** was synthesized following General Procedure G from **10** (35 mg, 0.107 mmol, 1.0 eq), piperidine (13 μ L, 0.129 mmol, 1.2 eq), and K_2CO_3 (18 mg, 0.129 mmol, 1.2 eq) to yield the product as an orange oil (27 mg, 77%). ^1H NMR (500 MHz, CDCl_3) δ 7.10 (d, J = 8.0 Hz, 1H), 7.09 – 7.03 (m, 2H), 4.56 (s, 2H), 3.63 (s, 2H), 3.42

(s, 2H), 2.80 (t, $J = 5.7$ Hz, 2H), 2.36 (s, 4H), 1.57 (p, $J = 5.5$ Hz, 4H), 1.48 (s, 9H), 1.47 – 1.39 (m, 2H).

(S)-2-amino-3-(4-hydroxy-2,6-dimethylphenyl)-1-(7-(piperidin-1-ylmethyl)-3,4-dihydroisoquinolin-2(1H)-yl)propan-1-one (12l). Following General Procedure C, **11l** (27 mg, 0.082 mmol, 1.0 eq) was deprotected to yield the amine intermediate as an orange oil. The crude product was rinsed with several small portions of diethyl ether. This intermediate was coupled to diBoc-DMT (35 mg, 0.087 mmol, 1.05 eq) in the presence of PyBOP (43 mg, 0.082 mmol, 1.0 eq), 6Cl-HOBt (14 mg, 0.082 mmol, 1.0 eq), and DIEA (115 μ L, 0.82 mmol, 10 eq). TFA deprotection yielded the product as a white solid. ^1H NMR (500 MHz, CD_3OD , rotamers) δ 6.48 – 6.45 (m, 2H), 6.41 (d, $J = 7.8$ Hz, 1H), 6.35 (d, $J = 7.8$ Hz, 1H), 6.32 (d, $J = 8.3$ Hz, 1H), 5.97 (s, 1H), 5.59 (s, 2H), 5.41 (s, 2H), 3.89 (d, $J = 17.3$ Hz, 1H), 3.82 – 3.76 (m, 3H), 3.46 (d, $J = 16.0$ Hz, 1H), 3.43 – 3.32 (m, 4H), 3.24 (dt, $J = 13.0, 5.2$ Hz, 1H), 2.73 (d, $J = 16.1$ Hz, 2H), 2.67 – 2.56 (m, 5H), 2.46 – 2.37 (m, 3H), 2.32 – 2.25 (m, 2H), 2.10 (q, $J = 10.9$ Hz, 4H), 1.97 (t, $J = 5.7$ Hz, 2H), 1.93 – 1.85 (m, 1H), 1.79 (dt, $J = 16.4, 6.5$ Hz, 1H), 1.43 (s, 6H), 1.40 (s, 6H), 1.21 (dt, $J = 16.4, 5.4$ Hz, 1H), 1.13 (s, 2H), 1.10 (s, 3H), 1.01 (d, $J = 14.4$ Hz, 2H), 0.92 (q, $J = 13.2$ Hz, 4H), 0.74 – 0.66 (m, 2H). HPLC retention time: 16.7 min. MS calculated for $[\text{C}_{26}\text{H}_{35}\text{N}_3\text{O}_2 + \text{H}]^+$: 422.3, found: 422.3.

12m

Tert-butyl 7-(pyrrolidin-1-ylmethyl)-3,4-dihydroisoquinoline-2(1H)-carboxylate (11m). **11m** was synthesized following General Procedure G from **10** (29 mg, 0.089 mmol, 1.0 eq), pyrrolidine (9 μ L, 0.107 mmol, 1.2 eq), and K_2CO_3 (15 mg, 0.107 mmol, 1.2 eq) to yield the product as a dark yellow-orange oil (28 mg, 100%). ^1H

NMR (500 MHz, CDCl₃) δ 7.13 – 7.10 (m, 1H), 7.10 – 7.06 (m, 2H), 4.56 (s, 2H), 3.67 – 3.61 (m, 2H), 3.58 (s, 2H), 2.80 (d, *J* = 6.1 Hz, 2H), 2.55 – 2.47 (m, 4H), 1.79 (p, *J* = 3.0 Hz, 4H), 1.49 (s, 9H).

(S)-2-amino-3-(4-hydroxy-2,6-dimethylphenyl)-1-(7-(pyrrolidin-1-ylmethyl)-3,4-dihydroisoquinolin-2(1H)-yl)propan-1-one (12m). Following General Procedure C, **11m** (28 mg, 0.088 mmol, 1.0 eq) was deprotected to yield the amine intermediate. The crude product was rinsed with several small portions of diethyl ether. This intermediate was coupled to diBoc-DMT (37 mg, 0.091 mmol, 1.05 eq) in the presence of PyBOP (45 mg, 0.087 mmol, 1.0 eq), 6Cl-HOBt (15 mg, 0.087 mmol, 1.0 eq), and DIEA (122 μL, 0.87 mmol, 10 eq). TFA deprotection yielded the product as a white solid. ¹H NMR (500 MHz, CD₃OD, rotamers) δ 7.31 – 7.26 (m, 2H), 7.24 (d, *J* = 7.6 Hz, 2H), 7.17 (d, *J* = 7.9 Hz, 1H), 7.13 (d, *J* = 7.8 Hz, 1H), 6.79 (s, 1H), 6.41 (s, 2H), 6.23 (s, 2H), 4.70 (d, *J* = 17.2 Hz, 1H), 4.61 (d, *J* = 17.0 Hz, 1H), 4.62 – 4.51 (m, 2H), 4.31 (s, 2H), 4.31 – 4.22 (m, 3H), 4.03 (dt, *J* = 11.7, 5.2 Hz, 1H), 3.53 (d, *J* = 16.0 Hz, 1H), 3.51 – 3.41 (m, 5H), 3.29 – 3.25 (m, 1H), 3.26 – 3.21 (m, 2H), 3.20 – 3.13 (m, 4H), 3.12 – 3.06 (m, 2H), 2.79 (t, *J* = 6.0 Hz, 2H), 2.76 – 2.67 (m, 1H), 2.59 (dt, *J* = 16.4, 6.0 Hz, 1H), 2.24 (s, 6H), 2.22 (s, 6H), 2.19 – 2.16 (m, 4H), 2.05 – 1.97 (m, 5H). HPLC retention time: 15.3 min. HRMS calculated for [C₂₅H₃₃N₃O₂ + H]⁺: 408.2646, found: 408.2649.

12n

Tert-butyl 7-(morpholinomethyl)-3,4-dihydroisoquinoline-2(1H)-carboxylate (11n). **11n** was synthesized following General Procedure G from **10** (31 mg, 0.095 mmol, 1.0 eq), morpholine (10 μL, 0.114 mmol, 1.2 eq), and K₂CO₃ (16 mg, 0.114 mmol, 1.2 eq) to yield the product as a pale yellow oil (32 mg, 100%). ¹H NMR (500

MHz, CDCl₃) δ 7.11 (d, *J* = 7.8 Hz, 1H), 7.08 (s, 2H), 4.56 (s, 2H), 3.70 (t, *J* = 4.7 Hz, 4H), 3.64 (t, *J* = 6.5 Hz, 2H), 3.45 (s, 2H), 2.81 (t, *J* = 5.9 Hz, 2H), 2.43 (t, *J* = 4.6 Hz, 4H), 1.49 (s, 9H).

(S)-2-amino-3-(4-hydroxy-2,6-dimethylphenyl)-1-(7-(morpholinomethyl)-3,4-dihydroisoquinolin-2(1H)-yl)propan-1-one (12n). Following General Procedure C, **11n** (28 mg, 0.088 mmol, 1.0 eq) was deprotected to yield the amine intermediate. The crude product was rinsed with several small portions of diethyl ether. This intermediate was coupled to diBoc-DMT (37 mg, 0.091 mmol, 1.05 eq) in the presence of PyBOP (45 mg, 0.087 mmol, 1.0 eq), 6Cl-HOBt (15 mg, 0.087 mmol, 1.0 eq), and DIEA (122 μL, 0.87 mmol, 10 eq). TFA deprotection yielded the product as a white solid. ¹H NMR (500 MHz, CD₃OD, rotamers) δ 7.30 – 7.28 (m, 2H), 7.24 (d, *J* = 7.8 Hz, 1H), 7.17 (d, *J* = 7.6 Hz, 1H), 7.14 (d, *J* = 7.8 Hz, 1H), 6.81 (s, 1H), 6.40 (s, 2H), 6.22 (s, 2H), 4.70 (d, *J* = 17.3 Hz, 1H), 4.63 – 4.55 (m, 3H), 4.31 (s, 2H), 4.29 – 4.21 (m, 3H), 4.13 – 4.05 (m, 1H), 4.08 – 3.99 (m, 4H), 3.74 (q, *J* = 12.7 Hz, 4H), 3.55 (d, *J* = 16.0 Hz, 1H), 3.42 – 3.32 (m, 5H), 3.28 – 3.25 (m, 1H), 3.25 – 3.20 (m, 2H), 3.21 – 3.12 (m, 4H), 3.13 – 3.06 (m, 2H), 2.79 (t, *J* = 6.1 Hz, 2H), 2.75 – 2.66 (m, 1H), 2.60 (dt, *J* = 16.5, 5.9 Hz, 1H), 2.24 (s, 6H), 2.22 (s, 6H), 2.03 (dt, *J* = 11.1, 5.7 Hz, 1H). HPLC retention time: 14.0 min. HRMS calculated for [C₂₅H₃₃N₃O₃ + H]⁺: 424.2595, found: 424.2597.

12o

Tert-butyl 7-(naphthalen-1-ylmethyl)-3,4-dihydroisoquinoline-2(1H)-carboxylate (11o). **11o** was synthesized following General Procedure D2 from **5** (100 mg, 0.278 mmol, 1.0 eq), 1-(bromomethyl)naphthalene (123 mg, 0.556 mmol, 2.0 eq), Pd(dppf)Cl₂ (20 mg, 0.028 mmol, 0.1 eq), and K₂CO₃ (115 mg, 0.834 mmol, 3.0 eq) to

yield the product as a yellow oil (41 mg, 39%). ¹H NMR (500 MHz, CDCl₃) δ 8.03 – 7.98 (m, 1H), 7.89 – 7.86 (m, 1H), 7.78 (d, *J* = 8.2 Hz, 1H), 7.49 – 7.45 (m, 2H), 7.43 (d, *J* = 7.7 Hz, 1H), 7.31 (d, *J* = 7.1 Hz, 1H), 7.03 (s, 2H), 6.95 (s, 1H), 4.50 (s, 2H), 4.41 (s, 2H), 3.63 (s, 2H), 2.80 (t, *J* = 5.9 Hz, 2H), 1.49 (s, 9H).

(S)-2-amino-3-(4-hydroxy-2,6-dimethylphenyl)-1-(7-(naphthalen-1-ylmethyl)-3,4-dihydroisoquinolin-2(1H)-yl)propan-1-one (12o). Following General Procedure C, **11o** (41 mg, 0.110 mmol, 1.0 eq) was deprotected to yield the amine intermediate. This intermediate was coupled to diBoc-DMT (47 mg, 0.115 mmol, 1.05 eq) in the presence of PyBOP (57 mg, 0.110 mmol, 1.0 eq), 6Cl-HOBt (57 mg, 0.330 mmol, 3.0 eq), and DIEA (154 μL, 1.1 mmol, 10 eq). Silica gel chromatography yielded the coupled product (57 mg, 78%, 2 steps). TFA deprotection yielded the product as a white solid. ¹H NMR (500 MHz, CD₃OD, rotamers) δ 7.98 – 7.94 (m, 2H), 7.86 – 7.83 (m, 2H), 7.76 (d, *J* = 8.2 Hz, 2H), 7.46 – 7.39 (m, 6H), 7.35 (d, *J* = 7.0 Hz, 1H), 7.32 (d, *J* = 6.9 Hz, 1H), 7.00 (d, *J* = 7.8 Hz, 1H), 6.97 – 6.94 (m, 2H), 6.92 (s, 1H), 6.88 (d, *J* = 7.8 Hz, 1H), 6.47 (s, 1H), 6.38 (s, 2H), 6.32 (s, 2H), 4.55 (d, *J* = 17.1 Hz, 1H), 4.52 – 4.47 (m, 2H), 4.44 (d, *J* = 16.9 Hz, 1H), 4.38 (s, 4H), 4.10 (d, *J* = 15.8 Hz, 1H), 3.79 (dt, *J* = 11.9, 5.6 Hz, 1H), 3.56 – 3.49 (m, 1H), 3.36 (d, *J* = 15.8 Hz, 1H), 3.24 – 3.15 (m, 3H), 3.05 (dt, *J* = 13.7, 5.1 Hz, 2H), 2.68 (t, *J* = 6.2 Hz, 2H), 2.66 – 2.60 (m, 1H), 2.49 (dt, *J* = 16.0, 6.2 Hz, 1H), 2.21 (s, 6H), 2.16 (s, 6H), 1.94 (dt, *J* = 16.1, 6.0 Hz, 1H). HPLC retention time: 43.3 min. MS calculated for [C₃₁H₃₂N₂O₂ + H]⁺: 465.2, found: 465.2.

12p

Tert-butyl 7-(naphthalen-2-ylmethyl)-3,4-dihydroisoquinoline-2(1H)-carboxylate (11p). **11p** was synthesized following General Procedure D2 from **5** (100

mg, 0.278 mmol, 1.0 eq), 2-(bromomethyl)naphthalene (123 mg, 0.556 mmol, 2.0 eq), Pd(dppf)Cl₂ (20 mg, 0.028 mmol, 0.1 eq), and K₂CO₃ (115 mg, 0.834 mmol, 3.0 eq) to yield the product (42 mg, 40%). ¹H NMR (500 MHz, CDCl₃) δ 7.79 (q, *J* = 8.1, 7.7 Hz, 3H), 7.65 (s, 1H), 7.45 (p, *J* = 7.1, 6.5 Hz, 2H), 7.32 (d, *J* = 8.5 Hz, 1H), 7.06 (s, 2H), 6.97 (s, 1H), 4.53 (s, 2H), 4.11 (s, 2H), 3.64 (s, 2H), 2.81 (t, *J* = 6.0 Hz, 2H), 1.49 (s, 9H).

(S)-2-amino-3-(4-hydroxy-2,6-dimethylphenyl)-1-(7-(naphthalen-2-ylmethyl)-3,4-dihydroisoquinolin-2(1H)-yl)propan-1-one (12p). Following General Procedure C, **11p** (42 mg, 0.112 mmol, 1.0 eq) was deprotected to yield the amine intermediate. Half of this intermediate (18 mg, 0.058 mmol, 1.0 eq) was coupled to diBoc-DMT (25 mg, 0.061 mmol, 1.05 eq) in the presence of PyBOP (30 mg, 0.058 mmol, 1.0 eq), 6Cl-HOBt (10 mg, 0.058 mmol, 1.0 eq), and DIEA (81 μL, 0.58 mmol, 10 eq). TFA deprotection yielded the product as a brown solid. ¹H NMR (500 MHz, CD₃OD, rotamers) δ 7.81 – 7.72 (m, 6H), 7.63 (d, *J* = 6.7 Hz, 2H), 7.46 – 7.38 (m, 4H), 7.29 (d, *J* = 8.3 Hz, 2H), 7.05 (d, *J* = 8.5 Hz, 1H), 7.02 – 6.96 (m, 3H), 6.93 (d, *J* = 7.8 Hz, 1H), 6.53 (s, 1H), 6.40 (s, 2H), 6.32 (s, 2H), 4.61 (d, *J* = 16.9 Hz, 1H), 4.57 – 4.48 (m, 2H), 4.50 (d, *J* = 16.8 Hz, 1H), 4.16 (d, *J* = 15.8 Hz, 1H), 4.07 (s, 2H), 4.06 (s, 2H), 3.77 (dt, *J* = 12.1, 5.7 Hz, 1H), 3.61 – 3.53 (m, 1H), 3.38 (d, *J* = 15.8 Hz, 1H), 3.24 – 3.17 (m, 3H), 3.06 (dt, *J* = 13.8, 5.2 Hz, 2H), 2.71 (q, *J* = 5.8 Hz, 2H), 2.67 – 2.61 (m, 1H), 2.52 (dt, *J* = 15.7, 6.3 Hz, 1H), 2.22 (s, 6H), 2.18 (s, 6H), 1.98 (dt, *J* = 16.2, 5.9 Hz, 1H). HPLC retention time: 43.5 min. MS calculated for [C₃₁H₃₂N₂O₂ + H]⁺: 465.2, found: 465.3.

12q

Tert-butyl 7-(quinolin-8-ylmethyl)-3,4-dihydroisoquinoline-2(1H)-carboxylate (11q). **11q** was synthesized following General Procedure F from **10** (75 mg, 0.23 mmol, 1.0 eq), quinolin-8-ylboronic acid (60 mg, 0.345 mmol, 1.5 eq), Pd(dppf)Cl₂ (17 mg, 0.023 mmol, 0.1 eq), and K₂CO₃ (95 mg, 0.69 mmol, 3.0 eq) to yield the product as a colorless oil (18 mg, 21%). ¹H NMR (500 MHz, CDCl₃) δ 8.97 (dd, *J* = 4.2, 1.8 Hz, 1H), 8.15 (dd, *J* = 8.3, 1.8 Hz, 1H), 7.74 – 7.65 (m, 1H), 7.46 (s, 1H), 7.44 (s, 1H), 7.41 (dd, *J* = 8.3, 4.2 Hz, 1H), 7.13 (dd, *J* = 7.6, 1.8 Hz, 1H), 7.07 (s, 1H), 7.04 (d, *J* = 7.9 Hz, 1H), 4.64 (s, 2H), 4.52 (s, 2H), 3.62 (s, 2H), 2.79 (t, *J* = 5.3 Hz, 2H), 1.48 (s, 9H).

(S)-2-amino-3-(4-hydroxy-2,6-dimethylphenyl)-1-(7-(quinolin-8-ylmethyl)-3,4-dihydroisoquinolin-2(1H)-yl)propan-1-one (12q). Following General Procedure C, **11q** (18 mg, 0.048 mmol) was deprotected to yield the amine intermediate. This intermediate was coupled to diBoc-DMT (21 mg, 0.05 mmol, 1.05 eq) in the presence of PyBOP (25 mg, 0.048 mmol, 1.0 eq), and DIEA (84 μL, 0.48 mmol, 10 eq) to yield the product. No 6Cl-HOBt was used. TFA deprotection yielded the product as a white, fluffy solid. ¹H NMR (500 MHz, CD₃OD, rotamers) δ 9.03 (td, *J* = 4.9, 1.7 Hz, 2H), 8.79 (dd, *J* = 8.3, 1.7 Hz, 1H), 8.75 (dd, *J* = 8.3, 1.7 Hz, 1H), 8.04 (dd, *J* = 8.1, 1.6 Hz, 1H), 8.00 (dd, *J* = 8.1, 1.4 Hz, 1H), 7.81 (ddd, *J* = 13.0, 8.3, 4.9 Hz, 2H), 7.75 – 7.66 (m, 3H), 7.63 (dd, *J* = 7.3, 1.4 Hz, 1H), 7.04 (dd, *J* = 7.8, 1.8 Hz, 1H), 7.01 (d, *J* = 1.7 Hz, 1H), 6.96 (s, 2H), 6.94 (d, *J* = 7.9 Hz, 1H), 6.58 (s, 1H), 6.38 (s, 2H), 6.24 (s, 2H), 4.61 (d, *J* = 15.8 Hz, 1H), 4.58 (s, 2H), 4.56 (s, 2H), 4.56 – 4.52 (m, 2H), 4.47 (d, *J* = 17.0 Hz, 1H), 4.17 (d, *J* = 15.9 Hz, 1H), 3.84 (dt, *J* = 12.9, 5.5 Hz, 1H), 3.54 – 3.47 (m, 1H), 3.38 (d, *J* = 15.9 Hz, 1H), 3.25 – 3.16 (m, 3H), 3.11 – 3.05 (m, 2H), 2.69 (q, *J* = 5.5 Hz, 2H), 2.66 –

2.59 (m, 1H), 2.52 (dt, $J = 16.2, 7.4, 4.8$ Hz, 1H), 2.21 (s, 6H), 2.18 (s, 6H), 1.98 (ddd, $J = 16.2, 6.4, 4.4$ Hz, 1H). HPLC retention time: 25.0 min. MS calculated for $[C_{30}H_{31}N_3O_2 + H]^+$: 466.2, found: 466.3.

12r

Tert-butyl 7-(isoquinolin-8-ylmethyl)-3,4-dihydroisoquinoline-2(1H)-carboxylate (11r). **11r** was synthesized following General Procedure F from **10** (77 mg, 0.24 mmol, 1.0 eq), isoquinolin-8-ylboronic acid (49 mg, 0.283 mmol, 1.2 eq), Pd(dppf)Cl₂ (18 mg, 0.024 mmol, 0.1 eq), and K₂CO₃ (98 mg, 0.71 mmol, 3.0 eq) to yield the product as a pale pink oil (55 mg, 62%). ¹H NMR (500 MHz, CDCl₃) δ 9.47 (s, 1H), 8.52 (d, $J = 5.6$ Hz, 1H), 7.73 (d, $J = 8.3$ Hz, 1H), 7.68 – 7.60 (m, 2H), 7.40 (d, $J = 7.0$ Hz, 1H), 7.02 (q, $J = 8.0$ Hz, 2H), 6.94 (s, 1H), 4.48 (s, 4H), 3.61 (s, 2H), 2.77 (t, $J = 6.1$ Hz, 2H), 1.47 (s, 9H).

(S)-2-amino-3-(4-hydroxy-2,6-dimethylphenyl)-1-(7-(isoquinolin-8-ylmethyl)-3,4-dihydroisoquinolin-2(1H)-yl)propan-1-one (12r). Following General Procedure C, **11r** (27 mg, 0.072 mmol) was deprotected to yield the amine intermediate. This intermediate was coupled to diBoc-DMT (31 mg, 0.076 mmol, 1.05 eq) in the presence of PyBOP (37 mg, 0.072 mmol, 1.0 eq), and DIEA (125 μ L, 0.72 mmol, 10 eq) to yield the product. No 6Cl-HOBt was used. TFA deprotection yielded the product as a white, fluffy solid. ¹H NMR (500 MHz, CD₃OD, rotamers) δ 9.73 (s, 1H), 9.72 (s, 1H), 8.54 (t, $J = 5.0$ Hz, 2H), 8.38 (d, $J = 6.3$ Hz, 1H), 8.35 (d, $J = 6.2$ Hz, 1H), 8.17 – 8.10 (m, 3H), 8.08 (q, $J = 7.6$ Hz, 1H), 7.82 (d, $J = 6.6$ Hz, 1H), 7.76 (d, $J = 6.9$ Hz, 1H), 7.07 – 7.02 (m, 2H), 7.00 – 6.94 (m, 3H), 6.53 (s, 1H), 6.36 (s, 2H), 6.17 (s, 2H), 4.61 (s, 2H), 4.60 (s, 2H), 4.57 (d, $J = 14.3$ Hz, 1H), 4.54 (dd, $J = 11.9, 4.1$ Hz, 2H), 4.48 (d, $J = 17.0$ Hz,

1H), 4.16 (d, $J = 15.8$ Hz, 1H), 3.97 (dt, $J = 12.9, 5.3$ Hz, 1H), 3.45 (d, $J = 15.8$ Hz, 1H), 3.38 (dt, $J = 13.2, 6.7$ Hz, 1H), 3.24 – 3.15 (m, 3H), 3.07 (ddd, $J = 13.6, 11.5, 4.1$ Hz, 2H), 2.69 (t, $J = 6.0$ Hz, 2H), 2.62 (ddd, $J = 12.5, 7.5, 4.7$ Hz, 1H), 2.52 (ddd, $J = 16.2, 7.5, 4.8$ Hz, 1H), 2.19 (s, 6H), 2.17 (s, 6H), 1.96 (ddd, $J = 16.3, 6.9, 4.7$ Hz, 1H). HPLC retention time: 21.4 min. MS calculated for $[C_{30}H_{31}N_3O_2 + H]^+$: 466.2, found: 466.3.

12s

Tert-butyl 7-(isoquinolin-5-ylmethyl)-3,4-dihydroisoquinoline-2(1H)-carboxylate (11s). **11s** was synthesized following General Procedure F from **10** (73 mg, 0.224 mmol, 1.0 eq), isoquinolin-5-ylboronic acid (46 mg, 0.269 mmol, 1.2 eq), Pd(dppf)Cl₂ (16 mg, 0.022 mmol, 0.1 eq), and K₂CO₃ (93 mg, 0.672 mmol, 3.0 eq) to yield the product as a yellow oil (48 mg, 57%). ¹H NMR (500 MHz, CDCl₃) δ 9.26 (s, 1H), 8.50 (d, $J = 6.0$ Hz, 1H), 7.88 (d, $J = 8.1$ Hz, 1H), 7.76 (d, $J = 6.0$ Hz, 1H), 7.55 (t, $J = 7.6$ Hz, 1H), 7.50 (d, $J = 7.1$ Hz, 1H), 7.04 (d, $J = 7.8$ Hz, 1H), 6.97 (s, 1H), 6.91 (s, 1H), 4.49 (s, 2H), 4.36 (s, 2H), 3.62 (t, $J = 5.9$ Hz, 2H), 2.78 (t, $J = 5.9$ Hz, 2H), 1.47 (s, 9H).

(S)-2-amino-3-(4-hydroxy-2,6-dimethylphenyl)-1-(7-(isoquinolin-5-ylmethyl)-3,4-dihydroisoquinolin-2(1H)-yl)propan-1-one (12s). Following General Procedure C, **11s** (24 mg, 0.064 mmol) was deprotected to yield the amine intermediate. This intermediate was coupled to diBoc-DMT (28 mg, 0.067 mmol, 1.05 eq) in the presence of PyBOP (33 mg, 0.064 mmol, 1.0 eq), and DIEA (111 μL, 0.64 mmol, 10 eq) to yield the product. No 6Cl-HOBt was used. TFA deprotection yielded the product as a white, fluffy solid. ¹H NMR (500 MHz, CD₃OD, rotamers) δ 9.67 (d, $J = 7.1$ Hz, 2H), 8.52 (d, $J = 7.0$ Hz, 2H), 8.44 (t, $J = 7.6$ Hz, 2H), 8.35 (t, $J = 8.9$ Hz, 2H), 8.04 – 7.91 (m, 4H), 7.04

– 6.92 (m, 5H), 6.51 (s, 1H), 6.37 (s, 2H), 6.23 (s, 2H), 4.58 (d, $J = 17.4$ Hz, 2H), 4.56 – 4.50 (m, 2H), 4.53 (s, 2H), 4.52 (s, 2H), 4.47 (d, $J = 17.1$ Hz, 1H), 4.15 (d, $J = 15.8$ Hz, 1H), 3.90 (dt, $J = 12.9, 5.4$ Hz, 1H), 3.48 – 3.39 (m, 1H), 3.41 (d, $J = 15.8$ Hz, 1H), 3.24 – 3.16 (m, 3H), 3.07 (ddd, $J = 13.3, 8.5, 4.1$ Hz, 2H), 2.69 (t, 2H), 2.62 (ddd, $J = 12.6, 7.5, 4.7$ Hz, 1H), 2.51 (ddd, $J = 16.2, 7.3, 4.8$ Hz, 1H), 2.21 (s, 6H), 2.17 (s, 6H), 1.96 (ddd, $J = 16.2, 6.9, 4.9$ Hz, 1H). HPLC retention time: 21.5 min. MS calculated for $[\text{C}_{30}\text{H}_{31}\text{N}_3\text{O}_2 + \text{H}]^+$: 466.2, found: 466.3.

12t

Tert-butyl 7-(quinolin-5-ylmethyl)-3,4-dihydroisoquinoline-2(1H)-carboxylate (11t). **11t** was synthesized following General Procedure F from **10** (50 mg, 0.153 mmol, 1.0 eq), quinolin-5-ylboronic acid (32 mg, 0.184 mmol, 1.2 eq), Pd(dppf)Cl₂ (11 mg, 0.015 mmol, 0.1 eq), and K₂CO₃ (63 mg, 0.459 mmol, 3.0 eq) to yield the product as a yellow oil (36 mg, 63%). ¹H NMR (500 MHz, CDCl₃) δ 8.90 (dd, $J = 4.2, 1.7$ Hz, 1H), 8.30 (ddd, $J = 8.6, 1.7, 0.9$ Hz, 1H), 8.04 (d, $J = 8.5$ Hz, 1H), 7.66 (t, $J = 7.8$ Hz, 1H), 7.39 – 7.33 (m, 2H), 7.03 (d, $J = 7.6$ Hz, 1H), 6.99 – 6.85 (m, 2H), 4.48 (s, 2H), 4.39 (s, 2H), 3.60 (t, $J = 6.1$ Hz, 2H), 2.77 (t, $J = 6.0$ Hz, 2H), 1.47 (s, 9H).

(S)-2-amino-3-(4-hydroxy-2,6-dimethylphenyl)-1-(7-(quinolin-5-ylmethyl)-3,4-dihydroisoquinolin-2(1H)-yl)propan-1-one (12t). Following General Procedure C, **11t** (36 mg, 0.096 mmol) was deprotected to yield the amine intermediate. This intermediate was coupled to diBoc-DMT (41 mg, 0.100 mmol, 1.05 eq) in the presence of PyBOP (49 mg, 0.095 mmol, 1.0 eq), and DIEA (123 μL, 0.95 mmol, 10 eq) to yield the product. No 6Cl-HOBt was used. TFA deprotection yielded the product as a white, fluffy solid. ¹H NMR (500 MHz, CD₃OD, rotamers) δ 9.15 (dd, $J = 8.5, 5.5$ Hz, 2H), 9.10 (td, $J = 5.1,$

1.5 Hz, 2H), 8.13 (t, $J = 9.1$ Hz, 2H), 8.05 (ddd, $J = 18.3, 8.7, 7.1$ Hz, 2H), 7.93 (ddd, $J = 8.7, 7.4, 5.2$ Hz, 2H), 7.78 (d, $J = 7.1$ Hz, 1H), 7.74 (d, $J = 7.1$ Hz, 1H), 7.04 – 6.92 (m, 5H), 6.50 (s, 1H), 6.36 (s, 2H), 6.23 (s, 2H), 4.59 (d, $J = 16.4$ Hz, 1H), 4.55 (s, 2H), 4.54 (s, 2H), 4.54 – 4.52 (m, 2H), 4.47 (d, $J = 17.1$ Hz, 1H), 4.15 (d, $J = 15.8$ Hz, 1H), 3.90 (dt, $J = 12.9, 5.4$ Hz, 1H), 3.43 (dt, $J = 13.1, 6.6$ Hz, 1H), 3.41 (d, $J = 15.9$ Hz, 1H), 3.24 – 3.16 (m, 3H), 3.07 (ddd, $J = 13.3, 8.5, 4.1$ Hz, 2H), 2.69 (t, $J = 6.0$ Hz, 2H), 2.63 (ddd, $J = 12.5, 7.4, 4.7$ Hz, 1H), 2.50 (ddd, $J = 16.2, 7.4, 4.8$ Hz, 1H), 2.20 (s, 6H), 2.17 (s, 6H), 1.94 (ddd, $J = 16.1, 6.8, 4.6$ Hz, 1H). HPLC retention time: 21.6 min. MS calculated for $[C_{30}H_{31}N_3O_2 + H]^+$: 466.2, found: 466.3.

12u

Tert-butyl 7-(quinolin-4-ylmethyl)-3,4-dihydroisoquinoline-2(1H)-carboxylate (11u). **11u** was synthesized following General Procedure F from **10** (50 mg, 0.153 mmol, 1.0 eq), quinolin-4-ylboronic acid (32 mg, 0.184 mmol, 1.2 eq), Pd(dppf)Cl₂ (11 mg, 0.015 mmol, 0.1 eq), and K₂CO₃ (63 mg, 0.459 mmol, 3.0 eq) to yield the product as a colorless oil (32 mg, 56%). ¹H NMR (500 MHz, CDCl₃) δ 8.83 (d, $J = 4.4$ Hz, 1H), 8.13 (d, $J = 8.4$ Hz, 1H), 8.03 (dd, $J = 8.5, 1.3$ Hz, 1H), 7.70 (t, $J = 7.7$ Hz, 1H), 7.54 (t, $J = 7.7$ Hz, 1H), 7.15 (d, $J = 4.2$ Hz, 1H), 7.07 (d, $J = 7.6$ Hz, 1H), 7.03 – 6.88 (m, 2H), 4.50 (s, 2H), 4.40 (s, 2H), 3.63 (t, $J = 5.4$ Hz, 2H), 2.80 (t, $J = 5.8$ Hz, 2H), 1.47 (s, 9H).

(S)-2-amino-3-(4-hydroxy-2,6-dimethylphenyl)-1-(7-(quinolin-4-ylmethyl)-3,4-dihydroisoquinolin-2(1H)-yl)propan-1-one (12u). Following General Procedure C, **11u** (32 mg, 0.085 mmol) was deprotected to yield the amine intermediate. This intermediate was coupled to diBoc-DMT (37 mg, 0.089 mmol, 1.05 eq) in the presence of PyBOP (44 mg, 0.085 mmol, 1.0 eq), and DIEA (148 μL, 0.85 mmol, 10 eq) to yield

the product. No 6Cl-HOBt was used. TFA deprotection yielded the product as a white, fluffy solid. ^1H NMR (500 MHz, CD_3OD , rotamers) δ 9.07 (dd, $J = 9.2, 5.6$ Hz, 2H), 8.55 (t, $J = 9.6$ Hz, 2H), 8.26 (t, $J = 8.8$ Hz, 2H), 8.18 – 8.11 (m, 2H), 8.00 – 7.93 (m, 2H), 7.78 (d, $J = 5.6$ Hz, 2H), 7.12 (dd, $J = 7.7, 1.8$ Hz, 1H), 7.10 (s, 1H), 7.05 (s, 2H), 7.01 (d, $J = 7.8$ Hz, 1H), 6.60 (s, 1H), 6.37 (s, 2H), 6.20 (s, 2H), 4.74 (s, 2H), 4.71 (s, 2H), 4.61 (d, $J = 17.2$ Hz, 1H), 4.55 (dd, $J = 12.0, 4.1$ Hz, 2H), 4.51 (d, $J = 17.1$ Hz, 1H), 4.20 (d, $J = 15.8$ Hz, 1H), 3.99 (dt, $J = 12.9, 5.3$ Hz, 1H), 3.48 (d, $J = 15.8$ Hz, 1H), 3.40 (dt, $J = 13.2, 6.7$ Hz, 1H), 3.25 – 3.17 (m, 3H), 3.08 (ddd, $J = 13.9, 9.9, 4.1$ Hz, 2H), 2.73 (t, $J = 6.1$ Hz, 2H), 2.65 (ddd, $J = 12.5, 7.4, 4.8$ Hz, 1H), 2.54 (ddd, $J = 16.4, 7.4, 4.9$ Hz, 1H), 2.21 (s, 6H), 2.18 (s, 6H), 1.98 (ddd, $J = 16.3, 7.0, 4.7$ Hz, 1H). HPLC retention time: 21.2 min. MS calculated for $[\text{C}_{30}\text{H}_{31}\text{N}_3\text{O}_2 + \text{H}]^+$: 466.2, found: 466.3.

12v

Tert-butyl 7-(isoquinolin-4-ylmethyl)-3,4-dihydroisoquinoline-2(1H)-carboxylate (11v). **11v** was synthesized following General Procedure F from **10** (50 mg, 0.153 mmol, 1.0 eq), isoquinolin-4-ylboronic acid (32 mg, 0.184 mmol, 1.2 eq), $\text{Pd}(\text{dppf})\text{Cl}_2$ (11 mg, 0.015 mmol, 0.1 eq), and K_2CO_3 (63 mg, 0.459 mmol, 3.0 eq) to yield the crude product. Silica gel chromatography yielded a mixture of products. This mixture was used directly in the next step.

(S)-2-amino-3-(4-hydroxy-2,6-dimethylphenyl)-1-(7-(isoquinolin-4-ylmethyl)-3,4-dihydroisoquinolin-2(1H)-yl)propan-1-one (12v). Following General Procedure C, **11v** (19 mg, 0.051 mmol) was deprotected. The crude product was purified by semi-preparative HPLC to yield the product as a white solid (21 mg, 100%). MS calculated for $[\text{C}_{19}\text{H}_{18}\text{N}_2 + \text{H}]^+$: 275.15, found: 275.2. The amine was coupled to diBoc-DMT (23 mg,

0.057 mmol, 1.05 eq) in the presence of PyBOP (28 mg, 0.054 mmol, 1.0 eq), and DIEA (94 μ L, 0.54 mmol, 10 eq) to yield the product. No 6Cl-HOBt was used. TFA deprotection yielded the product as a white, fluffy solid. ^1H NMR (500 MHz, CD_3OD , rotamers) δ 9.65 (d, $J = 6.0$ Hz, 2H), 8.50 (t, $J = 8.3$ Hz, 2H), 8.42 – 8.35 (m, 4H), 8.22 – 8.14 (m, 2H), 8.04 – 7.97 (m, 2H), 7.10 (dd, $J = 7.8, 1.8$ Hz, 1H), 7.07 (s, 1H), 7.02 (s, 2H), 6.97 (d, $J = 7.9$ Hz, 1H), 6.56 (s, 1H), 6.37 (s, 2H), 6.21 (s, 2H), 4.61 (d, $J = 16.1$ Hz, 1H), 4.57 (s, 2H), 4.56 (s, 2H), 4.55 – 4.52 (m, 2H), 4.49 (d, $J = 17.2$ Hz, 1H), 4.17 (d, $J = 15.8$ Hz, 1H), 3.95 (dt, $J = 12.9, 5.3$ Hz, 1H), 3.45 (d, $J = 15.5$ Hz, 1H), 3.43 – 3.38 (m, 1H), 3.25 – 3.17 (m, 3H), 3.07 (ddd, $J = 13.7, 8.1, 4.1$ Hz, 2H), 2.72 (t, $J = 6.0$ Hz, 2H), 2.65 (ddd, $J = 12.7, 7.3, 4.8$ Hz, 1H), 2.52 (ddd, $J = 16.4, 7.1, 4.8$ Hz, 1H), 2.21 (s, 6H), 2.17 (s, 6H), 1.95 (dt, $J = 16.4, 6.2$ Hz, 1H). HPLC retention time: 21.5 min. MS calculated for $[\text{C}_{30}\text{H}_{31}\text{N}_3\text{O}_2 + \text{H}]^+$: 466.2, found: 466.3.

12w

Tert-butyl 7-((3,4-dihydroisoquinolin-2(1H)-yl)methyl)-3,4-dihydroisoquinoline-2(1H)-carboxylate (11w). **11w** was synthesized following General Procedure G from **10** (50 mg, 0.153 mmol, 1.0 eq), 1,2,3,4-tetrahydroisoquinoline (23 μ L, 0.184 mmol, 1.2 eq), and K_2CO_3 (25 mg, 0.184 mmol, 1.2 eq) to yield the product as a colorless oil (24 mg, 41%). ^1H NMR (500 MHz, CDCl_3) δ 7.19 (d, $J = 7.5$ Hz, 1H), 7.15 (s, 1H), 7.12 – 7.08 (m, 4H), 6.99 (d, $J = 7.0$ Hz, 1H), 4.57 (s, 2H), 3.66 (br s, 2H), 3.64 (s, 2H), 3.63 (s, 2H), 2.90 (t, $J = 6.0$ Hz, 2H), 2.83 (t, $J = 5.9$ Hz, 2H), 2.75 (t, $J = 5.9$ Hz, 2H), 1.49 (s, 9H).

(S)-2-amino-1-(7-((3,4-dihydroisoquinolin-2(1H)-yl)methyl)-3,4-dihydroisoquinolin-2(1H)-yl)-3-(4-hydroxy-2,6-dimethylphenyl)propan-1-one (12w).

Following General Procedure C, **11w** (24 mg, 0.063 mmol, 1.0 eq) was deprotected to yield the amine intermediate. This intermediate was coupled to diBoc-DMT (27 mg, 0.067 mmol, 1.05 eq) in the presence of PyBOP (33 mg, 0.064 mmol, 1.0 eq), and DIEA (111 μ L, 0.64 mmol, 10 eq) to yield the product. No 6CI-HOBt was used. TFA deprotection yielded the product as a white solid. ^1H NMR (500 MHz, CD_3OD , rotamers) δ 7.36 – 7.33 (m, 2H), 7.32 – 7.23 (m, 7H), 7.21 – 7.13 (m, 4H), 6.85 (s, 1H), 6.41 (s, 2H), 6.21 (s, 2H), 4.72 (d, $J = 17.3$ Hz, 1H), 4.62 (d, $J = 17.3$ Hz, 1H), 4.64 – 4.57 (m, 2H), 4.44 (s, 2H), 4.42 – 4.35 (m, 5H), 4.29 (d, $J = 16.0$ Hz, 1H), 4.10 (dt, $J = 13.0, 5.0$ Hz, 1H), 3.73 (br s, 1H), 3.57 (d, $J = 16.1$ Hz, 1H), 3.46 – 3.35 (m, 2H), 3.28 – 3.26 (m, 1H), 3.26 – 3.15 (m, 6H), 3.15 – 3.07 (m, 2H), 2.80 (t, $J = 6.0$ Hz, 2H), 2.76 – 2.67 (m, 1H), 2.62 (dt, $J = 16.5, 6.0$ Hz, 1H), 2.24 (s, 6H), 2.22 (s, 6H), 2.04 (dt, $J = 6.9, 5.0$ Hz, 1H). HPLC retention time: 21.3 min. MS calculated for $[\text{C}_{30}\text{H}_{35}\text{N}_3\text{O}_2 + \text{H}]^+$: 470.2802, found: 470.2799.

12x

Tert-butyl 7-((3,4-dihydroquinolin-1(2H)-yl)methyl)-3,4-dihydroisoquinoline-2(1H)-carboxylate (11x). **11x** was synthesized following General Procedure G from **10** (50 mg, 0.153 mmol, 1.0 eq), 1,2,3,4-tetrahydroquinoline (23 μ L, 0.184 mmol, 1.2 eq), and K_2CO_3 (25 mg, 0.184 mmol, 1.2 eq). The reaction mixture was diluted with water. The aqueous layer was extracted with several portions of ethyl acetate. Combined organic layers were dried over MgSO_4 , filtered, and concentrated under vacuum. Silica gel chromatography yielded a mixture of the desired product and 1,2,3,4-tetrahydroquinoline. The product was partitioned between ethyl acetate and 2 M NaOH. The aqueous layer was extracted with ethyl acetate. Some 1,2,3,4-tetrahydroquinoline

remained. The mixture was resubmitted to reaction conditions with additional **7** (25 mg, 0.076, 0.5 eq) and K₂CO₃ (25 mg, 0.184 mmol, 1.2 eq). Silica gel chromatography yielded the desired product as a colorless oil (24 mg, 28%). ¹H NMR (500 MHz, CDCl₃) δ 7.08 (s, 1H), 7.02 (s, 1H), 6.99 (t, *J* = 6.5 Hz, 2H), 6.59 (t, *J* = 7.3 Hz, 1H), 6.51 (d, *J* = 8.5 Hz, 1H), 4.55 (s, 2H), 4.44 (s, 2H), 3.65 (s, 2H), 3.36 (t, *J* = 5.7 Hz, 2H), 2.92 – 2.75 (m, 4H), 2.03 (p, *J* = 6.1 Hz, 2H), 1.50 (s, 9H).

(S)-2-amino-1-(7-((3,4-dihydroquinolin-1(2H)-yl)methyl)-3,4-dihydroisoquinolin-2(1H)-yl)-3-(4-hydroxy-2,6-dimethylphenyl)propan-1-one (12x). Following General Procedure C, **11x** (24 mg, 0.063 mmol, 1.0 eq) was deprotected to yield the amine intermediate. This intermediate was coupled to diBoc-DMT (27 mg, 0.067 mmol, 1.05 eq) in the presence of PyBOP (33 mg, 0.064 mmol, 1.0 eq), and DIEA (111 μL, 0.64 mmol, 10 eq) to yield the product. No 6Cl-HOBt was used. TFA deprotection yielded the product as a white solid. ¹H NMR (500 MHz, CD₃OD, rotamers) δ 7.09 (d, *J* = 7.9 Hz, 1H), 7.04 (d, *J* = 8.1 Hz, 2H), 7.01 (d, *J* = 7.9 Hz, 1H), 6.99 – 6.89 (m, 5H), 6.64 – 6.51 (m, 5H), 6.40 (s, 2H), 6.27 (s, 2H), 4.62 (d, *J* = 17.1 Hz, 1H), 4.58 – 4.53 (m, 2H), 4.51 (d, *J* = 17.0 Hz, 2H), 4.45 (s, 2H), 4.44 (s, 2H), 4.19 (d, *J* = 15.8 Hz, 1H), 3.93 (dt, *J* = 12.9, 5.4 Hz, 1H), 3.51 – 3.43 (m, 1H), 3.46 (d, *J* = 15.7 Hz, 1H), 3.40 – 3.34 (m, 4H), 3.26 – 3.19 (m, 3H), 3.11 – 3.05 (m, 2H), 2.81 (q, *J* = 5.9 Hz, 4H), 2.73 (t, *J* = 6.2 Hz, 2H), 2.69 – 2.62 (m, 1H), 2.54 (dt, *J* = 16.3, 6.1 Hz, 1H), 2.23 (s, 6H), 2.20 (s, 6H), 2.06 – 1.95 (m, 5H). HPLC retention time: 35.9 min. MS calculated for [C₃₀H₃₅N₃O₂ + H]⁺: 470.2802, found: 470.2800.

12y

Tert-butyl 7-(indolin-1-ylmethyl)-3,4-dihydroisoquinoline-2(1H)-carboxylate (11y). **11y** was synthesized following General Procedure G from **10** (50 mg, 0.153 mmol, 1.0 eq), indoline (21 μ L, 0.184 mmol, 1.2 eq), and K_2CO_3 (25 mg, 0.184 mmol, 1.2 eq) to yield the product as a brown oil (37 mg, 66%). 1H NMR (500 MHz, $CDCl_3$) δ 7.18 (d, $J = 7.9$ Hz, 1H), 7.15 – 7.08 (m, 3H), 7.07 (t, $J = 7.6$ Hz, 1H), 6.69 (t, $J = 7.3$ Hz, 1H), 6.52 (d, $J = 7.8$ Hz, 1H), 4.58 (s, 2H), 4.21 (s, 2H), 3.66 (s, 2H), 3.32 (t, $J = 8.2$ Hz, 2H), 2.99 (t, $J = 8.3$ Hz, 2H), 2.84 (t, $J = 6.0$ Hz, 2H), 1.51 (s, 9H).

(S)-2-amino-3-(4-hydroxy-2,6-dimethylphenyl)-1-(7-(indolin-1-ylmethyl)-3,4-dihydroisoquinolin-2(1H)-yl)propan-1-one (12y). Following General Procedure C, **11y** (37 mg, 0.102 mmol, 1.0 eq) was deprotected to yield the amine intermediate. This intermediate was coupled to diBoc-DMT (43 mg, 0.105 mmol, 1.05 eq) in the presence of PyBOP (52 mg, 0.100 mmol, 1.0 eq), and DIEA (174 μ L, 1.0 mmol, 10 eq) to yield the product. No 6Cl-HOBt was used. TFA deprotection yielded the product as a white solid. 1H NMR (500 MHz, CD_3OD , rotamers) δ 7.24 – 7.18 (m, 3H), 7.18 – 7.11 (m, 4H), 7.06 (d, $J = 7.9$ Hz, 1H), 7.03 – 6.94 (m, 4H), 6.89 (d, $J = 8.5$ Hz, 1H), 6.67 (s, 1H), 6.41 (s, 2H), 6.27 (s, 2H), 4.63 (d, $J = 16.9$ Hz, 1H), 4.60 – 4.56 (m, 2H), 4.53 (d, $J = 17.2$ Hz, 1H), 4.40 – 4.32 (m, 4H), 4.21 (d, $J = 15.8$ Hz, 1H), 3.89 (dt, $J = 12.7, 5.5$ Hz, 1H), 3.55 – 3.50 (m, 1H), 3.50 – 3.46 (m, 4H), 3.44 (d, $J = 15.9$ Hz, 1H), 3.28 – 3.17 (m, 3H), 3.13 – 3.06 (m, 2H), 2.99 (t, $J = 7.6$ Hz, 4H), 2.74 (t, $J = 4.7$ Hz, 2H), 2.72 – 2.65 (m, 1H), 2.56 (dt, $J = 16.3, 6.0$ Hz, 1H), 2.23 (s, 6H), 2.20 (s, 6H), 1.98 (dt, $J = 16.2, 5.9$ Hz, 1H). HPLC retention time: 30.1 min. MS calculated for $[C_{29}H_{33}N_3O_2 + H]^+$: 456.2646, found: 456.2644.

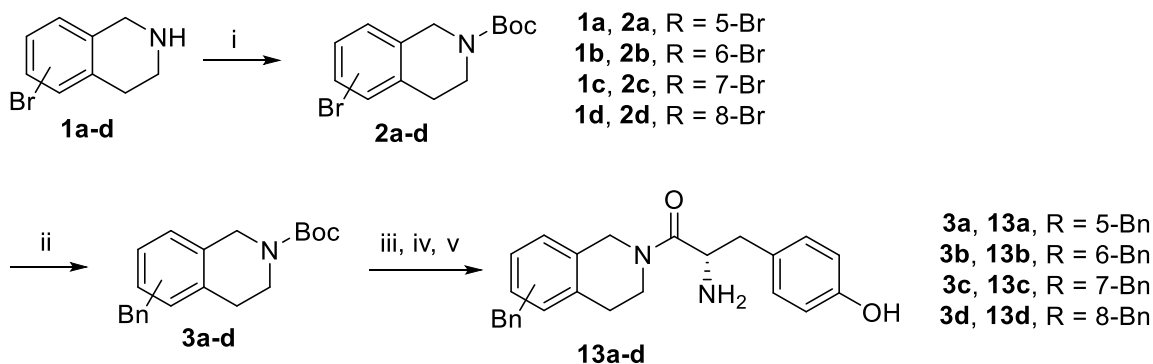
12z

Tert-butyl 7-(isoindolin-2-ylmethyl)-3,4-dihydroisoquinoline-2(1H)-carboxylate (11z). **11z** was synthesized following General Procedure G from **10** (50 mg, 0.153 mmol, 1.0 eq), isoindoline HCl (29 mg, 0.184 mmol, 1.2 eq), and K₂CO₃ (25 mg, 0.184 mmol, 1.2 eq) to yield the product as an orange oil (22 mg, 39%). ¹H NMR (500 MHz, CDCl₃) δ 7.29 (s, 1H), 7.21 (d, *J* = 7.8 Hz, 1H), 7.18 (s, 4H), 7.12 (d, *J* = 7.6 Hz, 1H), 4.58 (s, 2H), 3.93 (s, 4H), 3.88 (s, 2H), 3.65 (t, *J* = 8.2 Hz, 2H), 2.84 (t, *J* = 6.2 Hz, 2H), 1.49 (s, 9H).

(S)-2-amino-3-(4-hydroxy-2,6-dimethylphenyl)-1-(7-(isoindolin-2-ylmethyl)-3,4-dihydroisoquinolin-2(1H)-yl)propan-1-one (12z). Following General Procedure C, **11z** (22 mg, 0.060 mmol, 1.0 eq) was deprotected to yield the amine intermediate. This intermediate was coupled to diBoc-DMT (26 mg, 0.063 mmol, 1.05 eq) in the presence of PyBOP (31 mg, 0.060 mmol, 1.0 eq), and DIEA (105 μL, 0.600 mmol, 10 eq) to yield the product. No 6Cl-HOBt was used. TFA deprotection yielded the product as a white solid. ¹H NMR (500 MHz, CD₃OD, rotamers) δ 7.41 – 7.38 (m, 8H), 7.37 – 7.34 (m, 2H), 7.30 (dd, *J* = 7.9, 1.8 Hz, 1H), 7.19 (dd, *J* = 7.9, 3.5 Hz, 1H), 7.16 (dd, *J* = 8.0, 3.7 Hz, 1H), 6.86 (s, 1H), 6.42 (s, 2H), 6.24 (s, 2H), 4.72 (d, *J* = 17.2 Hz, 1H), 4.70 – 4.64 (m, 8H), 4.61 (d, *J* = 15.3 Hz, 1H), 4.65 – 4.57 (m, 2H), 4.56 (s, 2H), 4.53 (d, *J* = 10.7 Hz, 2H), 4.29 (d, *J* = 16.0 Hz, 1H), 4.09 (dt, *J* = 13.2, 4.9 Hz, 1H), 3.57 (d, *J* = 15.9 Hz, 1H), 3.44 – 3.37 (m, 1H), 3.29 – 3.25 (m, 1H), 3.24 (q, *J* = 13.0 Hz, 2H), 3.15 – 3.07 (m, 2H), 2.80 (t, *J* = 4.3 Hz, 2H), 2.75 – 2.67 (m, 1H), 2.61 (dt, *J* = 16.2, 5.6 Hz, 1H), 2.25 (s, 6H), 2.23 (s, 6H), 2.07 – 2.00 (m, 1H). HPLC retention time: 20.1 min. MS calculated for [C₂₉H₃₃N₃O₂ + H]⁺: 456.2646, found: 456.2645.

6.1.4 Procedures and Characterization for Compounds Contained in Chapter 4

Scheme 16. Synthesis of 13a-13d



13a

(S)-2-amino-1-(5-benzyl-3,4-dihydroisoquinolin-2(1H)-yl)-3-(4-hydroxyphenyl)propan-1-one (13a). Following General Procedure C, **3a** (207 mg, 0.64 mmol) was deprotected to yield the amine intermediate as a white solid. This intermediate (30 mg, 0.115 mmol, 1.0 eq) was coupled to BocTyrOH (34 mg, 0.121 mmol, 1.05 eq) in the presence of PyBOP (60 mg, 0.115 mmol, 1.0 eq), 6Cl-HOBt (20 mg, 0.115 mmol, 1.0 eq), and DIEA (161 μ L, 1.15 mmol, 10 eq). Silica gel chromatography yielded the coupled product. TFA deprotection yielded the product as a white, fluffy solid. ^1H NMR (500 MHz, CD_3OD , rotamers) δ 7.26 – 7.20 (m, 4H), 7.18 – 7.11 (m, 4H), 7.11 – 7.00 (m, 9H), 6.98 (d, J = 8.5 Hz, 2H), 6.85 (d, J = 7.7 Hz, 1H), 6.68 (d, J = 8.6 Hz, 2H), 6.59 (d, J = 8.5 Hz, 2H), 4.70 (d, J = 16.9 Hz, 1H), 4.73 – 4.55 (m, 2H), 4.60 (d, J = 17.0 Hz, 1H), 4.49 (d, J = 16.0 Hz, 1H), 4.02 (d, J = 16.2 Hz, 1H), 3.96 (s, 2H), 3.91 (s, 2H), 3.72 (dt, J = 12.3, 5.9 Hz, 1H), 3.60 (ddd, J = 16.6, 11.5, 5.3 Hz, 1H), 3.54 – 3.43 (m, 1H), 3.10 (ddd, J = 12.9, 7.6, 4.6 Hz, 1H), 3.06 – 3.00 (m, 2H), 3.00 – 2.90 (m, 2H), 2.70 – 2.59 (m, 2H), 2.53 (dt, J = 16.2, 6.2 Hz, 1H), 2.23 (dt, J =

16.6, 5.8 Hz, 1H). HPLC retention time: 36.7 min. HRMS calculated for $[C_{25}H_{26}N_2O_2 + H]^+$: 387.2067, found: 387.2073.

13b

(S)-2-amino-1-(6-benzyl-3,4-dihydroisoquinolin-2(1H)-yl)-3-(4-hydroxyphenyl)propan-1-one (13b). Following General Procedure C, **3b** (76 mg, 0.235 mmol) was deprotected to yield the amine intermediate as a white solid. This intermediate (30 mg, 0.115 mmol, 1.0 eq) was coupled to BocTyrOH (34 mg, 0.121 mmol, 1.05 eq) in the presence of PyBOP (60 mg, 0.115 mmol, 1.0 eq), 6Cl-HOBt (20 mg, 0.115 mmol, 1.0 eq), and DIEA (161 μ L, 1.15 mmol, 10 eq). Silica gel chromatography yielded the coupled product. TFA deprotection yielded the product as a white, fluffy solid. 1H NMR (500 MHz, CD_3OD , rotamers) δ 7.26 – 7.22 (m, 4H), 7.18 – 7.13 (m, 5H), 7.08 – 7.01 (m, 7H), 6.98 (d, J = 8.0 Hz, 1H), 6.94 (d, J = 7.1 Hz, 2H), 6.86 (d, J = 7.8 Hz, 1H), 6.71 (d, J = 8.5 Hz, 2H), 6.64 (d, J = 8.5 Hz, 2H), 4.75 (d, J = 17.0 Hz, 1H), 4.64 (dd, J = 8.4, 6.4 Hz, 1H), 4.60 (t, J = 7.5 Hz, 1H), 4.49 (d, J = 16.9 Hz, 1H), 4.48 (d, J = 15.9 Hz, 1H), 3.99 (d, J = 15.8 Hz, 1H), 3.90 (s, 4H), 3.78 – 3.68 (m, 2H), 3.54 (dt, J = 12.3, 5.8 Hz, 1H), 3.18 – 3.10 (m, 1H), 3.05 – 3.00 (m, 3H), 3.00 – 2.95 (m, 1H), 2.77 – 2.68 (m, 3H), 2.40 (dt, J = 16.1, 5.8 Hz, 1H). HPLC retention time: 37.7 min. MS calculated for $[C_{25}H_{26}N_2O_2 + H]^+$: 387.2, found: 387.2.

13c

(S)-2-amino-1-(7-benzyl-3,4-dihydroisoquinolin-2(1H)-yl)-3-(4-hydroxyphenyl)propan-1-one (13c). Following General Procedure C, **3c** (94 mg, 0.291 mmol) was deprotected to yield the amine intermediate as a white solid. This intermediate (25 mg, 0.096 mmol, 1.0 eq) was coupled to BocTyrOH (28 mg, 0.101

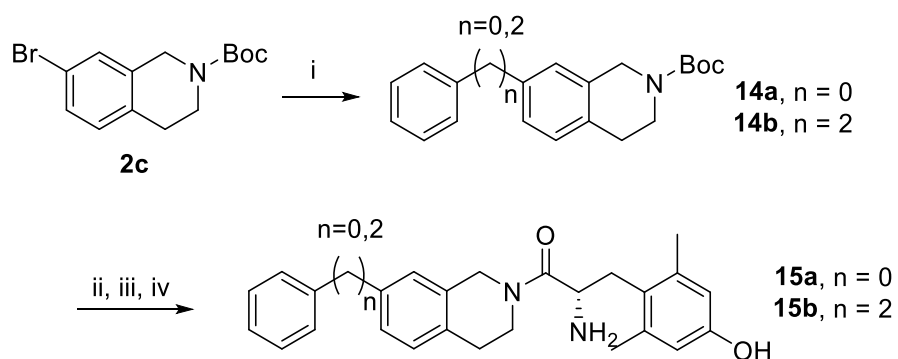
mmol, 1.05 eq) in the presence of PyBOP (50 mg, 0.096 mmol, 1.0 eq), 6Cl-HOBt (16 mg, 0.096 mmol, 1.0 eq), and DIEA (135 μ L, 0.960 mmol, 10 eq). Silica gel chromatography yielded the coupled product as a colorless oil (14 mg, 28%, 2 steps). TFA deprotection yielded the product as a white, fluffy solid. ^1H NMR (500 MHz, CD_3OD , rotamers) δ 7.27 – 7.22 (m, 4H), 7.18 – 7.14 (m, 6H), 7.05 (d, J = 8.5 Hz, 2H), 7.03 – 6.99 (m, 6H), 6.97 (s, 1H), 6.73 (s, 1H), 6.70 (d, J = 8.4 Hz, 2H), 6.62 (d, J = 8.4 Hz, 2H), 4.72 (d, J = 17.0 Hz, 1H), 4.66 – 4.59 (m, 2H), 4.49 (d, J = 17.0 Hz, 1H), 4.43 (d, J = 16.0 Hz, 1H), 3.95 (d, J = 16.0 Hz, 1H), 3.91 (s, 4H), 3.79 (dt, J = 12.1, 5.8 Hz, 1H), 3.65 (ddd, J = 12.7, 7.5, 5.1 Hz, 1H), 3.53 (ddd, J = 12.3, 6.7, 4.7 Hz, 1H), 3.13 (ddd, J = 12.7, 7.7, 4.6 Hz, 1H), 3.05 – 3.02 (m, 2H), 3.02 – 2.92 (m, 2H), 2.78 – 2.73 (m, 2H), 2.72 – 2.66 (m, 1H), 2.37 (dt, J = 16.1, 5.7 Hz, 1H). HPLC retention time: 37.5 min. MS calculated for $[\text{C}_{25}\text{H}_{26}\text{N}_2\text{O}_2 + \text{H}]^+$: 387.2, found: 387.2.

13d

(S)-2-amino-1-(8-benzyl-3,4-dihydroisoquinolin-2(1H)-yl)-3-(4-hydroxyphenyl)propan-1-one (13d). Following General Procedure C, **3d** (83 mg, 0.257 mmol) was deprotected to yield the amine intermediate as a white solid. This intermediate (16 mg, 0.062 mmol, 1.0 eq) was coupled to BocTyrOH (18 mg, 0.065 mmol, 1.05 eq) in the presence of PyBOP (32 mg, 0.062 mmol, 1.0 eq), 6Cl-HOBt (11 mg, 0.062 mmol, 1.0 eq), and DIEA (87 μ L, 0.620 mmol, 10 eq). Silica gel chromatography yielded the coupled product (20 mg, 62%, 2 steps). TFA deprotection yielded the product as a white, fluffy solid (17 mg, 100%). ^1H NMR (500 MHz, CD_3OD , rotamers) δ 7.31 (t, J = 7.6 Hz, 2H), 7.28 – 7.20 (m, 3H), 7.20 – 7.10 (m, 7H), 7.06 (dd, J = 7.5, 3.7 Hz, 1H), 7.04 – 6.96 (m, 5H), 6.86 (d, J = 8.5 Hz, 2H), 6.66 (d, J = 8.4 Hz,

2H), 6.61 (dd, $J = 8.4, 2.2$ Hz, 2H), 4.67 – 4.58 (m, 2H), 4.46 (d, $J = 17.3$ Hz, 1H), 4.24 (d, $J = 16.3$ Hz, 1H), 4.16 (td, $J = 8.8, 5.8$ Hz, 1H), 3.98 (d, $J = 3.7$ Hz, 2H), 3.88 (dd, $J = 16.0, 3.4$ Hz, 1H), 3.82 – 3.74 (m, 2H), 3.74 – 3.70 (m, 1H), 3.69 – 3.62 (m, 1H), 3.52 – 3.45 (m, 1H), 3.06 – 2.96 (m, 3H), 2.92 – 2.83 (m, 2H), 2.80 (d, $J = 7.8$ Hz, 1H), 2.78 – 2.70 (m, 2H), 2.44 – 2.35 (m, 1H). HPLC retention time: 35.5 min. MS calculated for $[C_{25}H_{26}N_2O_2 + H]^+$: 387.2, found: 387.2.

Scheme 17. Synthesis of 15a and 15b



15a

Tert-butyl 7-phenyl-3,4-dihydroisoquinoline-2(1H)-carboxylate (14a). 14a was synthesized following General Procedure B from 2c (52 mg, 0.167 mmol, 1.0 eq), phenylboronic acid (41 mg, 0.334 mmol, 2.0 eq), Pd(dppf)Cl₂ (12 mg, 0.017 mmol, 0.1 eq), and K₂CO₃ (69 mg, 0.501 mmol, 3.0 eq) to yield the product as a colorless oil (40 mg, 77%). ¹H NMR (500 MHz, CDCl₃) δ 7.59 – 7.55 (m, 2H), 7.46 – 7.39 (m, 3H), 7.37 – 7.32 (m, 2H), 7.22 (d, $J = 7.9$ Hz, 1H), 4.65 (s, 2H), 3.69 (s, 2H), 2.88 (t, $J = 5.9$ Hz, 2H), 1.51 (s, 9H).

(S)-2-amino-3-(4-hydroxy-2,6-dimethylphenyl)-1-(7-phenyl-3,4-dihydroisoquinolin-2(1H)-yl)propan-1-one (15a). Following General Procedure C, 14a (40 mg, 0.129 mmol) was deprotected to yield the amine intermediate as a white

solid. This intermediate was coupled to diBoc-DMT (56 mg, 0.136 mmol, 1.05 eq) in the presence of PyBOP (68 mg, 0.130 mmol, 1.0 eq), 6Cl-HOBt (22 mg, 0.130 mmol, 1.0 eq), and DIEA (182 μ L, 1.3 mmol, 10 eq). Silica gel chromatography yielded the coupled product as a colorless oil (44 mg, 56%, 2 steps). TFA deprotection yielded the product as a white solid. ^1H NMR (500 MHz, CD_3OD , rotamers) δ 7.59 – 7.53 (m, 4H), 7.44 – 7.35 (m, 7H), 7.34 – 7.29 (m, 2H), 7.13 (d, J = 8.0 Hz, 1H), 7.09 (d, J = 7.9 Hz, 1H), 6.95 (d, J = 1.8 Hz, 1H), 6.43 (s, 2H), 6.33 (s, 2H), 4.74 (d, J = 17.0 Hz, 1H), 4.64 (d, J = 16.9 Hz, 1H), 4.59 (ddd, J = 24.3, 11.9, 4.2 Hz, 2H), 4.32 (d, J = 15.8 Hz, 1H), 3.82 (dt, J = 12.8, 5.8 Hz, 1H), 3.70 – 3.63 (m, 1H), 3.48 (d, J = 15.8 Hz, 1H), 3.29 – 3.22 (m, 3H), 3.11 (dt, J = 13.8, 3.9 Hz, 2H), 2.83 – 2.75 (m, 2H), 2.72 (ddd, J = 12.5, 7.3, 4.6 Hz, 1H), 2.60 (dt, J = 16.2, 6.0 Hz, 1H), 2.29 (s, 6H), 2.24 (s, 6H), 2.05 (dt, J = 16.2, 5.6 Hz, 1H). HPLC retention time: 36.3 min. MS calculated for $[\text{C}_{26}\text{H}_{28}\text{N}_2\text{O}_2 + \text{H}]^+$: 401.2, found: 401.3.

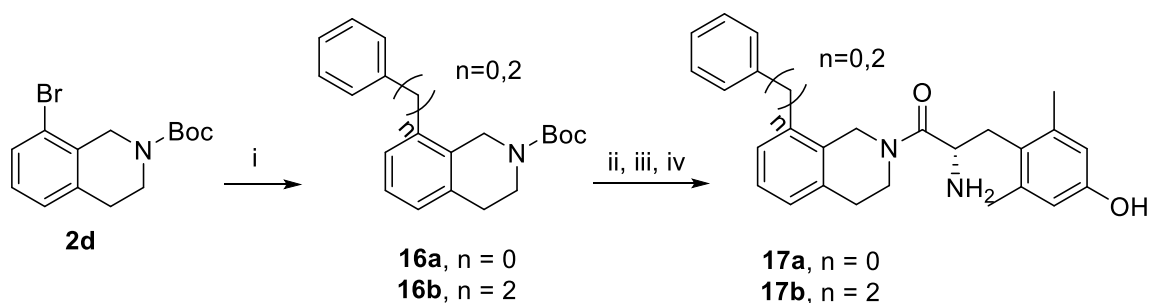
15b

Tert-butyl 7-phenethyl-3,4-dihydroisoquinoline-2(1H)-carboxylate (14b). **14b** was synthesized following General Procedure B from **2c** (62 mg, 0.199 mmol, 1.0 eq), phenethylboronic acid (60 mg, 0.398 mmol, 2.0 eq), $\text{Pd}(\text{dppf})\text{Cl}_2$ (15 mg, 0.020 mmol, 0.1 eq), and K_2CO_3 (83 mg, 0.597 mmol, 3.0 eq) to yield the product as a colorless oil (14 mg, 21%). ^1H NMR (500 MHz, CDCl_3) δ 7.32 – 7.27 (m, 2H), 7.24 – 7.17 (m, 3H), 7.08 – 7.05 (m, 1H), 7.03 – 6.99 (m, 1H), 6.95 (s, 1H), 4.55 (s, 2H), 3.65 (s, 3H), 2.90 (s, 4H), 2.81 (s, 2H), 1.50 (s, 9H).

(S)-2-amino-3-(4-hydroxy-2,6-dimethylphenyl)-1-(7-phenethyl-3,4-dihydroisoquinolin-2(1H)-yl)propan-1-one (15b). Following General Procedure C,

14b (14 mg, 0.041 mmol) was deprotected to yield the amine intermediate as a white solid. This intermediate was coupled to diBoc-DMT (17 mg, 0.042 mmol, 1.05 eq) in the presence of PyBOP (21 mg, 0.040 mmol, 1.0 eq), 6Cl-HOBt (7 mg, 0.040 mmol, 1.0 eq), and DIEA (56 μ L, 0.40 mmol, 10 eq). Silica gel chromatography yielded the coupled product as a colorless oil (12 mg, 48%, 2 steps). TFA deprotection yielded the product as a white solid (6 mg, 60%). ^1H NMR (500 MHz, CD_3OD , rotamers) δ 7.24 – 7.21 (m, 4H), 7.17 – 7.11 (m, 6H), 6.97 – 6.93 (m, 3H), 6.91 – 6.87 (m, 2H), 6.46 (s, 1H), 6.42 (s, 2H), 6.35 (s, 2H), 4.62 (d, J = 16.8 Hz, 2H), 4.58 – 4.51 (m, 2H), 4.48 (d, J = 17.0 Hz, 2H), 4.17 (d, J = 15.7 Hz, 1H), 3.70 – 3.65 (m, 2H), 3.34 (d, J = 14.9 Hz, 1H), 3.26 – 3.18 (m, 3H), 3.11 – 3.06 (m, 2H), 2.87 – 2.82 (m, 8H), 2.71 (q, J = 6.6 Hz, 2H), 2.68 – 2.62 (m, 1H), 2.51 (dt, J = 16.0, 6.3 Hz, 1H), 2.26 (s, 6H), 2.21 (s, 6H), 2.00 – 1.94 (m, 1H). HPLC retention time: 41.4 min. HRMS calculated for $[\text{C}_{28}\text{H}_{32}\text{N}_2\text{O}_2 + \text{H}]^+$: 429.2537, found: 429.2537.

Scheme 18. Synthesis of 17a and 17b



17a

Tert-butyl 8-phenyl-3,4-dihydroisoquinoline-2(1H)-carboxylate (16a). **16a** was synthesized following General Procedure B from **2d** (50 mg, 0.16 mmol, 1.0 eq), phenylboronic acid (39 mg, 0.32 mmol, 2.0 eq), $\text{Pd}(\text{dppf})\text{Cl}_2$ (12 mg, 0.016 mmol, 0.1 eq), and K_2CO_3 (66 mg, 0.48 mmol, 3.0 eq) to yield the product as a colorless oil (44

mg, 88%). ¹H NMR (500 MHz, CDCl₃) δ 7.42 (t, *J* = 7.4 Hz, 2H), 7.38 – 7.34 (m, 1H), 7.32 – 7.29 (m, 2H), 7.24 (d, *J* = 7.5 Hz, 1H), 7.17 (d, *J* = 7.6 Hz, 1H), 7.12 (d, *J* = 7.4 Hz, 1H), 4.45 (s, 2H), 3.64 (t, *J* = 6.1 Hz, 2H), 2.93 (t, *J* = 6.0 Hz, 2H), 1.44 (s, 9H).

(S)-2-amino-3-(4-hydroxy-2,6-dimethylphenyl)-1-(8-phenyl-3,4-dihydroisoquinolin-2(1H)-yl)propan-1-one (17a). Following General Procedure C, **16a** (22 mg, 0.071 mmol) was deprotected to yield the amine intermediate as a white solid. This intermediate was coupled to diBoc-DMT (30 mg, 0.072 mmol, 1.05 eq) in the presence of PyBOP (36 mg, 0.069 mmol, 1.0 eq), 6Cl-HOBt (12 mg, 0.069 mmol, 1.0 eq), and DIEA (97 μL, 0.69 mmol, 10 eq). Silica gel chromatography yielded the coupled product as a colorless oil (34 mg, 81%, 2 steps). TFA deprotection yielded the product as a white solid (23 mg, 88%). ¹H NMR (500 MHz, CD₃OD, rotamers) δ 7.54 – 7.48 (m, 3H), 7.48 – 7.42 (m, 2H), 7.41 – 7.37 (m, 1H), 7.29 – 7.26 (m, 2H), 7.21 (dt, *J* = 15.8, 7.6 Hz, 2H), 7.13 – 7.07 (m, 5H), 7.03 (d, *J* = 7.6 Hz, 1H), 6.98 (dd, *J* = 7.5, 1.3 Hz, 1H), 6.38 (s, 1H), 6.35 (s, 2H), 4.55 (d, *J* = 16.8 Hz, 1H), 4.50 – 4.44 (m, 2H), 4.06 (dd, *J* = 12.0, 4.3 Hz, 1H), 4.02 (d, *J* = 16.4 Hz, 1H), 3.94 (ddd, *J* = 12.4, 6.8, 5.2 Hz, 1H), 3.42 (ddd, *J* = 12.8, 7.8, 5.0 Hz, 1H), 3.30 – 3.26 (m, 1H), 3.20 – 3.08 (m, 2H), 3.04 (dd, *J* = 13.7, 4.1 Hz, 1H), 3.00 (d, *J* = 16.1 Hz, 1H), 2.98 – 2.93 (m, 1H), 2.91 (dd, *J* = 7.7, 5.3 Hz, 1H), 2.78 (dt, *J* = 16.2, 5.7 Hz, 1H), 2.67 (ddd, *J* = 15.5, 8.0, 5.2 Hz, 1H), 2.58 (ddd, *J* = 12.6, 7.8, 4.8 Hz, 1H), 2.20 – 2.14 (m, 1H), 2.14 (s, 6H), 2.00 (s, 6H). HPLC retention time: 34.2 min. MS calculated for [C₂₆H₂₈N₂O₂ + H]⁺: 401.2, found: 401.2.

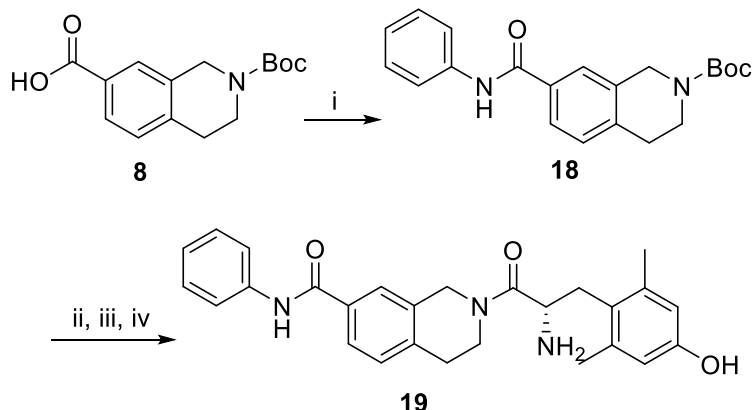
17b

Tert-butyl 8-phenethyl-3,4-dihydroisoquinoline-2(1H)-carboxylate (16b). **16b** was synthesized following General Procedure B from **2d** (90 mg, 0.288 mmol, 1.0 eq),

phenethylboronic acid (86 mg, 0.576 mmol, 2.0 eq), Pd(dppf)Cl₂ (21 mg, 0.029 mmol, 0.1 eq), and K₂CO₃ (119 mg, 0.864 mmol, 3.0 eq) to yield the product as a colorless oil (66 mg, 68%). ¹H NMR (500 MHz, CDCl₃) δ 7.35 – 7.29 (m, 2H), 7.26 – 7.21 (m, 3H), 7.15 (t, *J* = 7.6 Hz, 1H), 7.08 (d, *J* = 7.5 Hz, 1H), 7.03 (d, *J* = 7.5 Hz, 1H), 4.59 (s, 2H), 3.65 (s, 2H), 2.95 – 2.83 (m, 6H), 1.53 (s, 9H).

(S)-2-amino-3-(4-hydroxy-2,6-dimethylphenyl)-1-(8-phenethyl-3,4-dihydroisoquinolin-2(1H)-yl)propan-1-one (17b). Following General Procedure C, **16b** (33 mg, 0.098 mmol) was deprotected to yield the amine intermediate as a white solid. This intermediate was coupled to diBoc-DMT (43 mg, 0.104 mmol, 1.05 eq) in the presence of PyBOP (52 mg, 0.099 mmol, 1.0 eq), 6Cl-HOBt (17 mg, 0.099 mmol, 1.0 eq), and DIEA (139 μL, 0.99 mmol, 10 eq). Silica gel chromatography yielded the coupled product as a colorless oil (47 mg, 76%, 2 steps). TFA deprotection yielded the product as a white solid (27 mg, 73%). ¹H NMR (500 MHz, CD₃OD, rotamers) δ 7.29 (t, *J* = 7.6 Hz, 2H), 7.26 – 7.15 (m, 6H), 7.13 (d, *J* = 6.7 Hz, 2H), 7.10 – 7.01 (m, 3H), 6.95 (d, *J* = 7.6 Hz, 1H), 6.92 (d, *J* = 7.6 Hz, 1H), 6.85 (d, *J* = 7.4 Hz, 1H), 6.42 (s, 2H), 6.30 (s, 2H), 4.58 (d, *J* = 16.7 Hz, 1H), 4.55 – 4.49 (m, 2H), 4.35 (d, *J* = 16.8 Hz, 1H), 4.04 (d, *J* = 16.2 Hz, 1H), 3.91 (dt, *J* = 11.5, 5.4 Hz, 1H), 3.41 (ddd, *J* = 12.7, 8.0, 4.8 Hz, 1H), 3.27 – 3.16 (m, 3H), 3.11 – 3.05 (m, 3H), 2.90 – 2.83 (m, 5H), 2.81 – 2.72 (m, 3H), 2.64 – 2.48 (m, 4H), 2.20 (s, 6H), 2.19 (s, 6H), 2.06 (s, 1H), 2.09 – 2.03 (m, 1H). HPLC retention time: 39.1 min. MS calculated for [C₂₈H₃₂N₂O₂ + H]⁺: 429.2, found: 429.3.

Scheme 19. Synthesis of 19



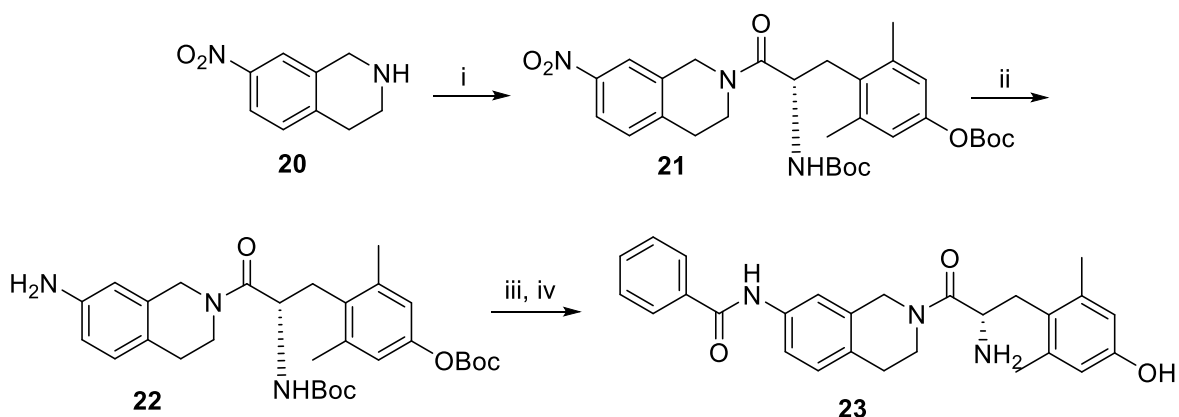
19

Tert-butyl 7-(phenylcarbamoyl)-3,4-dihydroisoquinoline-2(1H)-carboxylate (18). Carboxylic acid **5** (25 mg, 0.090 mmol, 1.0 eq) and aniline (9 μ L, 0.095 mmol, 1.05 eq) were coupled in the presence of PyBOP (47 mg, 0.090 mmol, 1.0 eq) and DIEA (123 μ L, 0.900 mmol, 10 eq) in dry DMF (2 mL). Silica gel chromatography yielded the coupled product as a colorless oil (13 mg, 41%). ^1H NMR (500 MHz, CDCl_3) δ 8.11 (s, 1H), 7.65 (dd, $J = 12.1, 8.4$ Hz, 3H), 7.39 – 7.31 (m, 2H), 7.19 (d, $J = 7.9$ Hz, 1H), 7.18 – 7.10 (m, 1H), 4.59 (s, 2H), 3.64 (t, $J = 5.9$ Hz, 2H), 2.85 (t, $J = 5.9$ Hz, 2H), 1.50 (s, 9H).

(S)-2-(2-amino-3-(4-hydroxy-2,6-dimethylphenyl)propanoyl)-N-phenyl-1,2,3,4-tetrahydroisoquinoline-7-carboxamide (19). Following General Procedure C, **18** (13 mg, 0.037 mmol) was deprotected to yield the amine intermediate as a white solid. This intermediate was coupled to diBoc-DMT (16 mg, 0.040 mmol, 1.05 eq) in the presence of PyBOP (20 mg, 0.038 mmol, 1.0 eq) and DIEA (52 μ L, 0.380 mmol, 10 eq) to yield the product as a colorless oil. No 6Cl-HOBt was used. TFA deprotection yielded the product as a white, fluffy solid. ^1H NMR (500 MHz, CD_3OD , rotamers) δ 7.75 – 7.71

(m, 2H), 7.71 – 7.66 (m, 5H), 7.36 (q, $J = 7.7$ Hz, 4H), 7.29 (s, 1H), 7.20 (d, $J = 7.7$ Hz, 1H), 7.19 – 7.11 (m, 3H), 6.41 (s, 2H), 6.29 (s, 2H), 4.71 (s, 2H), 4.60 (td, $J = 13.0, 12.2, 4.0$ Hz, 2H), 4.32 (d, $J = 16.0$ Hz, 1H), 3.99 – 3.90 (m, 1H), 3.62 – 3.56 (m, 1H), 3.52 (d, $J = 16.1$ Hz, 1H), 3.27 – 3.19 (m, 3H), 3.11 (dd, $J = 13.8, 3.9$ Hz, 2H), 2.82 (q, $J = 8.1, 7.3$ Hz, 2H), 2.75 (dt, $J = 12.9, 6.0$ Hz, 1H), 2.63 (dt, $J = 16.9, 5.9$ Hz, 1H), 2.27 (s, 6H), 2.22 (s, 6H), 2.04 (dt, $J = 17.2, 5.5$ Hz, 1H). HPLC retention time: 29.0 min. HRMS calculated for $[C_{27}H_{29}N_3O_3 + H]^+$: 444.2282, found: 444.2287.

Scheme 20. Synthesis of 23

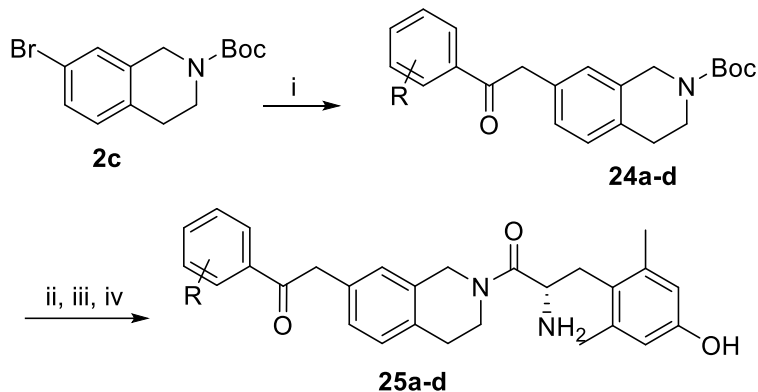


23

(S)-N-(2-(2-amino-3-(4-hydroxy-2,6-dimethylphenyl)propanoyl)-1,2,3,4-tetrahydroisoquinolin-7-yl)benzamide (23). 7-nitro-1,2,3,4-tetrahydroisoquinoline (65 mg, 0.365 mmol, 1.0 eq) was coupled to diBoc-DMT (157 mg, 0.383 mmol, 1.05 eq) in the presence of PyBOP (190 mg, 0.365 mmol, 1.0 eq), 6Cl-HOBt (62 mg, 0.365 mmol, 1.0 eq), and DIEA (512 μ L, 3.65 mmol, 10 eq). The coupled product was purified by silica gel chromatography. Remaining coupling reagents were precipitated in chloroform and filtered off. The mother liquor was concentrated to yield the pure product as a yellow solid (205 mg, 99%). The nitro intermediate (22 mg, 0.039 mmol, 1.0 eq) was

combined with NH₄Cl (83 mg, 1.56 mmol, 40 eq) and Zn dust (51 mg, 0.780 mmol, 20 eq) and dissolved in acetone (3 mL) and water (154 μL, 8.58 mmol, 220 eq). After 1 hour at room temperature, solvent was removed under vacuum, and the crude product was partitioned between ethyl acetate and water. The layers were separated, and the aqueous layer was extracted with ethyl acetate. The combined organic layers were washed with brine, dried over MgSO₄, filtered, and concentrated under vacuum to obtain the corresponding aniline as a colorless oil (18 mg, 86%). This intermediate was coupled to benzoic acid (4 mg, 0.035 mmol, 1.05 eq) in the presence of PyBOP (17 mg, 0.033 mmol, 1.0 eq) and DIEA (57 μL, 0.330 mmol, 10 eq). This intermediate was dissolved in DCM (2 mL) and TFA (2 mL), and the reaction mixture stirred at room temperature for 3 hours. Subsequent HPLC purification yielded **23** as a white solid. ¹H NMR (500 MHz, CD₃OD, rotamers) δ 7.93 (t, *J* = 7.7 Hz, 4H), 7.61 – 7.56 (m, 2H), 7.55 – 7.49 (m, 5H), 7.44 (dt, *J* = 8.4, 2.3 Hz, 1H), 7.34 (dt, *J* = 8.3, 2.6 Hz, 1H), 7.23 – 7.19 (m, 1H), 7.06 (d, *J* = 8.2 Hz, 1H), 7.02 (d, *J* = 8.3 Hz, 1H), 6.44 (s, 2H), 6.34 (s, 2H), 4.69 (d, *J* = 17.1 Hz, 1H), 4.58 (d, *J* = 15.9 Hz, 1H), 4.64 – 4.52 (m, 2H), 4.25 (d, *J* = 15.9 Hz, 1H), 3.80 (dt, *J* = 11.9, 5.7 Hz, 1H), 3.66 (ddd, *J* = 12.9, 7.6, 5.1 Hz, 1H), 3.43 (d, *J* = 15.8 Hz, 1H), 3.28 – 3.22 (m, 3H), 3.10 (dd, *J* = 14.0, 4.0 Hz, 2H), 2.78 – 2.73 (m, 2H), 2.70 (ddd, *J* = 12.5, 7.5, 4.8 Hz, 1H), 2.55 (dt, *J* = 16.2, 6.0 Hz, 1H), 2.28 (s, 6H), 2.24 (s, 6H), 2.01 (dt, *J* = 16.0, 5.8 Hz, 1H). HPLC retention time: 28.4 min. HRMS calculated for [C₂₇H₂₉N₃O₃ + H]⁺: 444.2282, found: 444.2280.

Scheme 21. Synthesis of 25a-25d



25a

Tert-Butyl 7-(2-oxo-2-phenylethyl)-3,4-dihydroisoquinoline-2(1H)-carboxylate (24a). **24a** was synthesized following General Procedure H from **2c** (75 mg, 0.240 mmol, 1.0 eq), acetophenone (58 mg, 0.480 mmol, 2.0 eq), Pd₂(dba)₃ (22 mg, 0.024 mmol, 0.1 eq), BINAP (36 mg, 0.058 mmol, 0.24 eq), and NaOtBu (30 mg, 0.312 mmol, 1.3 eq) to yield the product as a colorless oil (64 mg, 76%). ¹H NMR (500 MHz, CDCl₃) δ 8.02 (d, *J* = 7.0 Hz, 2H), 7.58 – 7.54 (m, 1H), 7.49 – 7.44 (m, 2H), 7.11 – 7.05 (m, 2H), 7.01 (s, 1H), 4.55 (s, 2H), 4.25 (s, 2H), 3.66 – 3.59 (m, 2H), 2.82 – 2.77 (m, 2H), 1.49 (s, 9H).

(S)-2-amino-3-(4-hydroxy-2,6-dimethylphenyl)-1-(7-(2-oxo-2-phenylethyl)-3,4-dihydroisoquinolin-2(1H)-yl)propan-1-one (25a). Following General Procedure C, **24a** (64 mg, 0.182 mmol) was deprotected to yield the amine intermediate as a colorless oil. This intermediate (26 mg, 0.090 mmol, 1.0 eq) was coupled to diBoc-DMT (39 mg, 0.095 mmol, 1.05 eq) in the presence of PyBOP (47 mg, 0.090 mmol, 1.0 eq) and DIEA (126 μL, 0.90 mmol, 10 eq) to yield a brown oil. No 6Cl-HOBt was used. TFA deprotection yielded the product as a dense off-white solid (43 mg, 86%, 3 steps). ¹H

NMR (500 MHz, CD₃OD, rotamers) δ 8.06 – 8.02 (m, 4H), 7.63 – 7.57 (m, 2H), 7.52 – 7.47 (m, 4H), 7.07 – 7.04 (m, 1H), 7.04 – 6.99 (m, 3H), 6.95 (d, J = 7.8 Hz, 1H), 6.57 (s, 1H), 6.39 (s, 2H), 6.31 (s, 2H), 4.64 (d, J = 17.1 Hz, 1H), 4.61 – 4.51 (m, 2H), 4.51 (d, J = 17.0 Hz, 1H), 4.32 – 4.27 (m, 4H), 4.19 (d, J = 15.8 Hz, 1H), 3.78 – 3.71 (m, 1H), 3.65 – 3.58 (m, 1H), 3.39 (d, J = 15.8 Hz, 1H), 3.25 – 3.19 (m, 3H), 3.11 – 3.06 (m, 2H), 2.74 – 2.68 (m, 2H), 2.67 – 2.60 (m, 1H), 2.57 – 2.49 (m, 1H), 2.24 (s, 6H), 2.19 (s, 6H), 2.02 – 1.95 (m, 1H). HPLC retention time: 33.4 min. HRMS calculated for [C₂₈H₃₀N₂O₃ + H]⁺: 443.2329, found: 443.2323.

25b

Tert-Butyl 7-(2-oxo-2-(*p*-tolyl)ethyl)-3,4-dihydroisoquinoline-2(1*H*)-carboxylate (24b). **24b** was synthesized following General Procedure H from **2c** (100 mg, 0.320 mmol, 1.0 eq), 1-(*p*-tolyl)ethan-1-one (86 mg, 0.640 mmol, 2.0 eq), Pd₂(dba)₃ (29 mg, 0.032 mmol, 0.1 eq), BINAP (48 mg, 0.077 mmol, 0.24 eq), and NaOtBu (40 mg, 0.416 mmol, 1.3 eq) to yield the product as a colorless oil (40 mg, 34%). ¹H NMR (400 MHz, CDCl₃) δ 7.91 (d, J = 8.0 Hz, 2H), 7.26 (d, J = 8.0 Hz, 2H), 7.09 – 7.06 (m, 2H), 7.00 (s, 1H), 4.54 (s, 2H), 4.22 (s, 2H), 3.62 (t, 2H), 2.79 (t, J = 4.9 Hz, 2H), 2.41 (s, 3H), 1.48 (s, 9H).

(S)-2-amino-3-(4-hydroxy-2,6-dimethylphenyl)-1-(7-(2-oxo-2-(*p*-tolyl)ethyl)-3,4-dihydroisoquinolin-2(1*H*)-yl)propan-1-one (25b). Following General Procedure C, **24b** (40 mg, 0.109 mmol) was deprotected to yield the amine intermediate as a white solid. This intermediate was coupled to diBoc-DMT (47 mg, 0.114 mmol, 1.05 eq) in the presence of PyBOP (57 mg, 0.109 mmol, 1.0 eq) and DIEA (152 μ L, 1.09 mmol, 10 eq) to yield a brown oil. No 6Cl-HOBt was used. TFA deprotection yielded the product as a

white, fluffy solid (34 mg, 54%, 3 steps). ¹H NMR (500 MHz, CD₃OD, rotamers) δ 7.95 – 7.91 (m, 4H), 7.32 – 7.28 (m, 4H), 7.04 (d, *J* = 8.0 Hz, 1H), 7.02 – 6.97 (m, 3H), 6.94 (d, *J* = 7.8 Hz, 1H), 6.56 (s, 1H), 6.39 (s, 2H), 6.30 (s, 2H), 4.62 (d, *J* = 17.0 Hz, 1H), 4.60 – 4.53 (m, 2H), 4.51 (d, *J* = 16.6 Hz, 1H), 4.26 – 4.22 (m, 4H), 4.18 (d, *J* = 15.8 Hz, 1H), 3.78 – 3.72 (m, 1H), 3.63 – 3.56 (m, 1H), 3.39 (d, *J* = 15.8 Hz, 1H), 3.26 – 3.18 (m, 3H), 3.11 – 3.06 (m, 2H), 2.73 – 2.68 (m, 2H), 2.66 – 2.60 (m, 1H), 2.55 – 2.48 (m, 1H), 2.40 (s, 3H), 2.39 (s, 3H), 2.24 (s, 6H), 2.18 (s, 6H), 2.00 – 1.93 (m, 1H). HPLC retention time: 36.5 min. HRMS calculated for [C₂₉H₃₂N₂O₃ + H]⁺: 457.2486, found: 457.2481.

25c

Tert-Butyl 7-(2-oxo-2-(*m*-tolyl)ethyl)-3,4-dihydroisoquinoline-2(1*H*)-carboxylate (24c). **24c** was synthesized following General Procedure H from **2c** (200 mg, 0.641 mmol, 1.0 eq), 1-(*m*-tolyl)ethan-1-one (172 mg, 1.28 mmol, 2.0 eq), Pd₂(dba)₃ (59 mg, 0.064 mmol, 0.1 eq), BINAP (96 mg, 0.154 mmol, 0.24 eq), and NaOtBu (80 mg, 0.833 mmol, 1.3 eq) to yield the product as a colorless oil (154 mg, 66%). ¹H NMR (500 MHz, CDCl₃) δ 7.85 – 7.78 (m, 2H), 7.40 – 7.33 (m, 2H), 7.13 – 7.03 (m, 2H), 7.01 (s, 1H), 4.55 (s, 2H), 4.23 (s, 2H), 3.63 (t, *J* = 7.2 Hz, 2H), 2.80 (t, *J* = 6.3 Hz, 2H), 2.41 (s, 3H), 1.49 (s, 9H).

(*S*)-2-amino-3-(4-hydroxy-2,6-dimethylphenyl)-1-(7-(2-oxo-2-(*m*-tolyl)ethyl)-3,4-dihydroisoquinolin-2(1*H*)-yl)propan-1-one (25c). Following General Procedure C, **24c** (154 mg, 0.421 mmol) was deprotected to yield the amine intermediate as a white solid. This intermediate (50 mg, 0.166 mmol, 1.0 eq) was coupled to diBoc-DMT (71 mg, 0.174 mmol, 1.05 eq) in the presence of PyBOP (86 mg, 0.166 mmol, 1.0 eq) and DIEA (233 μL, 1.66 mmol, 10 eq) to yield a brown oil. No 6Cl-HOBt was used. TFA

deprotection yielded the product as a white, fluffy solid (36 mg, 38%, 3 steps). ¹H NMR (500 MHz, CD₃OD, rotamers) δ 7.86 – 7.81 (m, 4H), 7.45 – 7.33 (m, 4H), 7.04 (d, *J* = 7.8 Hz, 1H), 7.02 – 6.97 (m, 3H), 6.94 (d, *J* = 7.8 Hz, 1H), 6.56 (s, 1H), 6.39 (s, 2H), 6.30 (s, 2H), 4.62 (d, *J* = 17.0 Hz, 1H), 4.60 – 4.54 (m, 2H), 4.52 (d, *J* = 16.9 Hz, 1H), 4.29 – 4.25 (m, 4H), 4.19 (d, *J* = 15.8 Hz, 1H), 3.78 – 3.72 (m, 1H), 3.64 – 3.56 (m, 1H), 3.40 (d, *J* = 15.8 Hz, 1H), 3.26 – 3.17 (m, 3H), 3.11 – 3.06 (m, 2H), 2.74 – 2.68 (m, 2H), 2.67 – 2.60 (m, 1H), 2.56 – 2.49 (m, 1H), 2.40 (s, 3H), 2.39 (s, 3H), 2.24 (s, 6H), 2.19 (s, 6H), 2.02 – 1.94 (m, 1H). HPLC retention time: 36.7 min. HRMS calculated for [C₂₉H₃₂N₂O₃ + H]⁺: 457.2486, found: 457.2482.

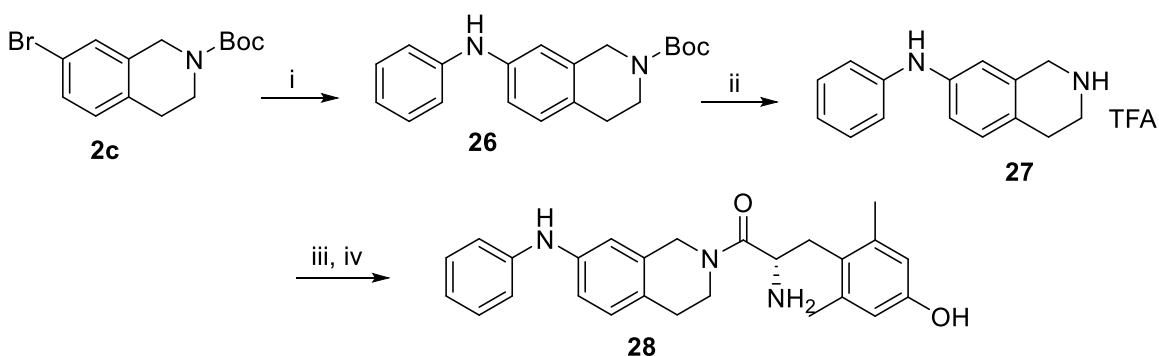
25d

Tert-Butyl 7-(2-oxo-2-(*o*-tolyl)ethyl)-3,4-dihydroisoquinoline-2(1*H*)-carboxylate (24d). **24d** was synthesized following General Procedure H from **2c** (100 mg, 0.320 mmol, 1.0 eq), 1-(*o*-tolyl)ethan-1-one (86 mg, 0.640 mmol, 2.0 eq), Pd₂(dba)₃ (29 mg, 0.032 mmol, 0.1 eq), BINAP (48 mg, 0.077 mmol, 0.24 eq), and NaOtBu (40 mg, 0.416 mmol, 1.3 eq) to yield the product as a colorless oil (96 mg, 82%). ¹H NMR (500 MHz, CDCl₃) δ 7.74 (d, *J* = 7.7 Hz, 1H), 7.40 – 7.35 (m, 1H), 7.27 – 7.22 (m, 2H), 7.09 (d, *J* = 7.8 Hz, 1H), 7.05 – 7.01 (m, 1H), 6.98 (s, 1H), 4.56 (s, 2H), 4.18 (s, 2H), 3.63 (s, 2H), 2.80 (t, *J* = 5.9 Hz, 2H), 2.47 (s, 3H), 1.49 (s, 9H).

(*S*)-2-amino-3-(4-hydroxy-2,6-dimethylphenyl)-1-(7-(2-oxo-2-(*o*-tolyl)ethyl)-3,4-dihydroisoquinolin-2(1*H*)-yl)propan-1-one (25d). Following General Procedure C, **24d** (96 mg, 0.263 mmol) was deprotected to yield the amine intermediate as a colorless oil. This intermediate (40 mg, 0.133 mmol, 1.0 eq) was coupled to diBoc-DMT (57 mg, 0.140 mmol, 1.05 eq) in the presence of PyBOP (69 mg, 0.133 mmol, 1.0 eq)

and DIEA (186 μL , 1.33 mmol, 10 eq) to yield a brown oil. No 6Cl-HOBt was used. TFA deprotection yielded the product as a white, fluffy solid (35 mg, 47%, 3 steps). ^1H NMR (500 MHz, CD_3OD , rotamers) δ 7.80 (d, $J = 7.8$ Hz, 2H), 7.39 – 7.35 (m, 2H), 7.32 – 7.27 (m, 2H), 7.26 – 7.22 (m, 2H), 7.03 – 6.99 (m, 1H), 6.99 (s, 2H), 6.93 (d, $J = 7.7$ Hz, 1H), 6.53 (s, 1H), 6.39 (s, 2H), 6.31 (s, 2H), 4.61 (d, $J = 16.9$ Hz, 1H), 4.59 – 4.53 (m, 2H), 4.51 (d, $J = 16.9$ Hz, 1H), 4.21 – 4.16 (m, 5H), 3.75 – 3.69 (m, 1H), 3.66 – 3.59 (m, 1H), 3.37 (d, $J = 15.8$ Hz, 1H), 3.26 – 3.18 (m, 3H), 3.11 – 3.05 (m, 2H), 2.74 – 2.68 (m, 2H), 2.67 – 2.62 (m, 1H), 2.55 – 2.48 (m, 1H), 2.37 (s, 3H), 2.36 (s, 3H), 2.24 (s, 6H), 2.19 (s, 6H), 1.99 – 1.92 (m, 2H). HPLC retention time: 36.1 min. HRMS calculated for $[\text{C}_{29}\text{H}_{32}\text{N}_2\text{O}_3 + \text{H}]^+$: 457.2486, found: 457.2483.

Scheme 22. Synthesis of 28



28

Tert-butyl 7-(phenylamino)-3,4-dihydroisoquinoline-2(1H)-carboxylate (**26**).

Intermediate **2c** (100 mg, 0.320 mmol, 1.0 eq), NaOtBu (92 mg, 0.960 mmol, 3.0 eq), Pd(dppf)Cl₂ (47 mg, 0.064 mmol, 0.2 eq), and aniline (35 μL , 0.384 mmol, 1.2 eq) were combined in a round bottom flask equipped with a teflon stirbar. 1,4-dioxane (10 mL) was added, and the reaction mixture was degassed. The flask was attached to a reflux condenser, and the system was flushed with argon. The reaction mixture stirred at 110

°C overnight. The reaction mixture was concentrated under vacuum to remove 1,4-dioxane. The crude product was dissolved in ethyl acetate, and solids were filtered off. Silica gel chromatography in ethyl acetate/hexanes yielded a mixture containing the desired product as a brown oil. HPLC retention time: 61.0 min. MS calculated for $[C_{20}H_{24}N_2O_2 + H]^+$: 325.2, found: 325.2.

N-phenyl-1,2,3,4-tetrahydroisoquinolin-7-amine (27). **26** (19 mg, 0.059 mmol) was dissolved in DCM (1.5 mL) and TFA (1.5 mL). The reaction mixture turned from reddish-brown to dark gray-blue. The crude product was purified by semi-preparative HPLC to yield the pure product as a green-blue oil. HPLC retention time: 26.8 min. MS calculated for $[C_{15}H_{16}N_2 + H]^+$: 225.1, found: 225.1.

(S)-2-amino-3-(4-hydroxy-2,6-dimethylphenyl)-1-(7-(phenylamino)-3,4-dihydroisoquinolin-2(1H)-yl)propan-1-one (28). **27** (22 mg, 0.065 mmol, 1.0 eq) was coupled to diBoc-DMT (28 mg, 0.068 mmol, 1.05 eq) in the presence of PyBOP (34 mg, 0.065 mmol, 1.0 eq) and DIEA (113 μ L, 0.65 mmol, 10 eq) to yield a green-gray oil. The coupled intermediate was dissolved in DCM (1.5 mL) and TFA (1.5 mL). The green reaction mixture stirred at room temperature for 1 hour. Solvent was removed under vacuum, and the product was purified by semi-preparative HPLC and lyophilized to yield a gray solid (7 mg, 21%, 3 steps). 1H NMR (500 MHz, CD_3OD , rotamers) δ 7.23 – 7.17 (m, 4H), 7.04 – 7.00 (m, 4H), 6.91 (d, $J = 8.2$ Hz, 1H), 6.89 – 6.84 (m, 3H), 6.84 – 6.80 (m, 3H), 6.45 (s, 1H), 6.44 (s, 2H), 6.38 (s, 2H), 4.63 (d, $J = 16.9$ Hz, 1H), 4.55 (ddd, $J = 13.2, 11.9, 4.2$ Hz, 3H), 4.45 (d, $J = 16.9$ Hz, 1H), 4.16 (d, $J = 15.8$ Hz, 1H), 3.73 – 3.62 (m, 2H), 3.27 (d, $J = 13.9$ Hz, 1H), 3.26 – 3.19 (m, 3H), 3.09 (ddd, $J = 13.8, 4.4, 1.9$ Hz, 2H), 2.71 – 2.59 (m, 3H), 2.49 (ddd, $J = 15.8, 7.4, 4.7$ Hz, 1H), 2.27 (s, 6H), 2.23 (s,

6H), 1.96 (ddd, $J = 15.7, 6.8, 4.6$ Hz, 1H). HPLC retention time: 34.3 min. MS calculated for $[C_{26}H_{29}N_3O_2 + H]^+$: 416.2, found: 416.3.

6.2 *In Vitro* Pharmacology

Unless otherwise noted, all tissue culture reagents and radiolabeled ligands were purchased from commercial sources.

Cell Lines and Membrane Preparations. Membranes prepared from transfected C6 rat glioma cells stably expressing rat MOR or rat DOR or Chinese hamster ovary (CHO) cells stably expressing human KOR, human MOR, or human DOR were used for all assays. Cells were grown to confluence at 37 °C in 5% CO₂ in Dulbecco's Modified Eagle's Medium (DMEM) or 1:1 DMEM:F12 media containing 10% v/v fetal bovine serum and 5% v/v penicillin/streptomycin. Membranes were prepared by washing confluent cells three times with ice cold phosphate-buffered saline (0.9% NaCl, 0.61 mM Na₂HPO₄, 0.38 mM KH₂PO₄, pH 7.4). Cells were detached from the plates by incubation in warm harvesting buffer (20 mM HEPES, 150 mM NaCl, 0.68 mM EDTA, pH 7.4) and pelleted by centrifugation at 200xg for 3 minutes. The cell pellet was suspended in ice-cold 50 mM Tris-HCl buffer, pH 7.4 and homogenized with a Tissue Tearor (Biospec Products, Inc) for 20 seconds at setting 4. The homogenate was centrifuged at 20,000xg for 20 minutes at 4 °C, and the pellet was rehomogenized in 50 mM Tris-HCl pH 7.4 with a Tissue Tearor for 10 seconds at setting 2, followed by recentrifugation. The final pellet was resuspended in 50 mM Tris-HCl pH 7.4 and frozen in aliquots at -80 °C. Protein concentration was determined via Pierce BCA protein assay kit using bovine serum albumin as the standard.

Binding Affinity. Binding affinities at KOR, MOR, and DOR were determined by competitive displacement of [³H]diprenorphine as previously reported.^{80,113–115} In a 96-well plate format, cell membranes (5-20 µg of protein) and [³H]diprenorphine (0.2 nM) were incubated in Tris-HCl buffer (50 mM, pH 7.4) with various concentrations of test compound at 25 °C for 1 hour, allowing the mixture to reach equilibrium. Nonspecific binding was determined using the opioid antagonist naloxone (10 µM), and total binding was determined using vehicle in the absence of competitive ligand. After incubation, membranes were filtered through Whatman GF/C 1.2 micron glass fiber filters and washed with 50 mM Tris-HCl buffer. The radioactivity remaining on the filters was then quantified by liquid scintillation counting after saturation with EcoLume liquid scintillation cocktail in a Perkin-Elmer Microbeta 2450. Binding affinity (K_i) values were calculated using the Cheng-Prusoff equation via nonlinear regression analysis using GraphPad Prism software from at least three separate binding assays performed in duplicate unless otherwise noted.

Stimulation of [³⁵S]GTPγS Binding. Agonist stimulation of KOR, MOR, and DOR was determined by [³⁵S]guanosine 5'-O-[γ-thio]triphosphate ([³⁵S]GTPγS) binding assays as previously reported.^{80,113–115} In a 96-well plate format, membranes from cells expressing opioid receptors as described above (10 µg of protein), [³⁵S]GTPγS (0.1 nM), and guanosine diphosphate (30 µM) were incubated in GTPγS buffer (50 mM Tris-HCl, 100 mM NaCl, 5 mM MgCl₂, 1 mM EDTA, pH 7.4) with various concentrations of test compound at 25 °C for 1 hour. Basal stimulation was determined by incubation in the absence of any ligand. After incubation, membranes were filtered through Whatman GF/C 1.2 micron glass fiber filters and washed with GTPγS buffer with no EDTA. The

radioactivity remaining on the filters was then quantified by liquid scintillation counting after saturation with EcoLume liquid scintillation cocktail in a Perkin-Elmer Microbeta 2450. Data are reported as percent stimulation compared to the effects of 10 μ M standard agonist - U69,593 (KOR), DAMGO (MOR), or DPDPE (DOR). Percent stimulation and EC₅₀ values were determined via nonlinear regression analysis using GraphPad Prism software from at least three separate assays performed in duplicate unless otherwise noted. Efficacy is expressed as percent stimulation relative to standard agonist.

6.3 Computational Modeling

Modeling of three-dimensional structures of receptor-ligand complexes was based on the available X-ray structure of the human KOR in the active conformation (PDB ID: 6b73).²⁵ Structures of peptidomimetic ligands were generated using the 3D-Builder Application of QUANTA (Accelrys, Inc.) followed by Conformational Search included in the program package. Low-energy ligand conformations (within 2 kcal/mol) that demonstrated the best superposition of aromatic substituents of the tetrahydroisoquinoline core with the pharmacophore elements (Tyr¹ and Phe³) of receptor-bound conformations of cyclic tetrapeptides¹¹⁶ were selected for docking into the receptor binding pocket. Ligands were positioned inside the receptor binding cavity to reproduce the binding modes of cyclic tetrapeptides and co-crystallized ligands in MOR and KOR X-ray structures. Two conformations of peptidomimetics were tested: with the peptide bond in cis ($\omega=0^\circ$) and trans ($\omega=180^\circ$) configurations. Though ligands with a cis peptide group have slightly higher conformational energy (by ~ 1 kcal/mol), they fit better in the ligand binding pockets of the receptors, overlapping with ligands co-

crystalized with KOR and MOR. The docking pose of each ligand was subsequently refined using the solid docking module of QUANTA. Models of opioid ligand-receptor complexes are available upon request.

References

- (1) Macht, D. I. The History of Opium and Some of Its Preparations and Alkaloids. *J. Am. Med. Assoc.* **1915**, *64* (6), 477–481.
- (2) Brownstein, M. J. A Brief History of Opiates, Opioid Peptides, and Opioid Receptors. *Proc. Natl. Acad. Sci.* **1993**, *90*, 5391–5393.
- (3) Rosenblum, A.; Marsch, L. A.; Joseph, H.; Portenoy, R. K. Opioids and the Treatment of Chronic Pain: Controversies, Current Status, and Future Directions. *Exp Clin Psychopharmacol* **2008**, *16* (5), 405–416.
- (4) Levinthal, C. F. Milk of Paradise/Milk of Hell — The History of Ideas about Opium. *Perspect. Biol. Med.* **1985**, *28* (4), 561–577.
- (5) Pasternak, G. W.; Pan, Y.-X. Mu Opioids and Their Receptors: Evolution of a Concept. *Pharmacol. Rev.* **2013**, *65* (4), 1257–1317.
- (6) Pasternak, G. W. Opioids and Their Receptors: Are We There Yet? *Neuropharmacology* **2014**, *76*, 198–203.
- (7) Portoghese, P. S. A New Concept on the Mode of Interaction of Narcotic Analgesics with Receptors. *J. Med. Chem.* **1965**, *8* (5), 609–616.
- (8) Portoghese, P. S. Stereochemical Factors and Receptor Interactions Associated with Narcotic Analgesics. *J. Pharm. Sci.* **1966**, *55* (9), 865–887.
- (9) Goldstein, A.; Lowney, L. I.; Pal, B. K. Stereospecific and Nonspecific Interactions of the Morphine Congener Levorphanol in Subcellular Fractions of Mouse Brain. *Proc. Natl. Acad. Sci.* **1971**, *68* (8), 1742–1747.
- (10) Pert, C. B.; Snyder, S. H. Opiate Receptor: Demonstration in Nervous Tissue. *Science* **1973**, *179* (4077), 1011–1014.
- (11) Simon, E. J.; Hiller, J. M.; Edelman, I. Stereospecific Binding of the Potent Narcotic Analgesic [³H]Etorphine to Rat-Brain Homogenate. *Proc. Natl. Acad. Sci.* **1973**, *70* (7), 1947–1949.
- (12) Terenius, L. Stereospecific Interaction Between Narcotic Analgesics and a Synaptic Plasma Membrane Fraction of Rat Cerebral Cortex. *Acta Pharmacol. Toxicol.* **1973**, *32*, 317–320.
- (13) Martin, W. R.; Eades, C. G.; Thompson, J. A.; Huppler, R. E.; Gilbert, P. E. The Effects of Morphine and Nalorphine-Like Drugs in the Nondependent and Morphine-Dependent Chronic Spinal Dog. *J. Pharmacol. Exp. Ther.* **1976**, *197* (3), 517–532.

- (14) Lord, J. A. H.; Waterfield, A. A.; Hughes, J.; Kosterlitz, H. W. Endogenous Opioid Peptides: Multiple Agonists and Receptors. *Nature* **1977**, *267*, 495–499.
- (15) Kieffer, B. L.; Evans, C. J. Opioid Receptors: From Binding Sites to Visible Molecules in Vivo. *Neuropharmacology* **2009**, *56*, 205–212.
- (16) Filizola, M.; Devi, L. A. Grand Opening of Structure-Guided Design for Novel Opioids. *Trends Pharmacol. Sci.* **2013**, *34* (1), 6–12.
- (17) Evans, C. J.; Keith, D. E.; Morrison, H.; Magendzo, K.; Edwards, R. H. Cloning of a Delta Opioid Receptor by Functional Expression. *Science* **1992**, *258* (5090), 1952–1955.
- (18) Kieffer, B. L.; Befort, K.; Gaveriaux-Ruff, C.; Hirth, C. G. The Delta-Opioid Receptor: Isolation of a cDNA by Expression Cloning and Pharmacological Characterization. *Proc. Natl. Acad. Sci.* **1992**, *89* (24), 12048–12052.
- (19) Dreborg, S.; Sundstrom, G.; Larsson, T. A.; Larhammar, D. Evolution of Vertebrate Opioid Receptors. *Proc. Natl. Acad. Sci.* **2008**, *105* (40), 15487–15492.
- (20) Surratt, C. K.; Adams, W. R. G Protein-Coupled Receptor Structural Motifs: Relevance to the Opioid Receptors. *Curr. Top. Med. Chem.* **2005**, *5*, 315–324.
- (21) Wu, H.; Wacker, D.; Mileni, M.; Katritch, V.; Han, G. W.; Vardy, E.; Liu, W.; Thompson, A. A.; Huang, X. P.; Carroll, F. I.; et al. Structure of the Human κ -Opioid Receptor in Complex with JDTic. *Nature* **2012**, *485* (7398), 327–332.
- (22) Manglik, A.; Kruse, A. C.; Kobilka, T. S.; Thian, F. S.; Mathiesen, J. M.; Sunahara, R. K.; Pardo, L.; Weis, W. I.; Kobilka, B. K.; Granier, S. Crystal Structure of the μ -Opioid Receptor Bound to a Morphinan Antagonist. *Nature* **2012**, *485* (7398), 321–326.
- (23) Granier, S.; Manglik, A.; Kruse, A. C.; Kobilka, T. S.; Thian, F. S.; Weis, W. I.; Kobilka, B. K. Structure of the δ -Opioid Receptor Bound to Naltrindole. *Nature* **2012**, *485* (7398), 400–404.
- (24) Fenalti, G.; Giguere, P. M.; Katritch, V.; Huang, X. P.; Thompson, A. A.; Cherezov, V.; Roth, B. L.; Stevens, R. C. Molecular Control of δ -Opioid Receptor Signalling. *Nature* **2014**, *506* (7487), 191–196.
- (25) Che, T.; Majumdar, S.; Zaidi, S. A.; Ondachi, P.; McCorvy, J. D.; Wang, S.; Mosier, P. D.; Uprety, R.; Vardy, E.; Krumm, B. E.; et al. Structure of the Nanobody-Stabilized Active State of the Kappa Opioid Receptor. *Cell* **2018**, *172* (1–2), 55–67.
- (26) Huang, W.; Manglik, A.; Venkatakrishnan, A. J.; Laeremans, T.; Feinberg, E. N.; Sanborn, A. L.; Kato, H. E.; Livingston, K. E.; Thorsen, T. S.; Kling, R. C.; et al. Structural Insights into μ -Opioid Receptor Activation. *Nature* **2015**, *524* (7565), 315–321.
- (27) Valentino, R. J.; Volkow, N. D. Untangling the Complexity of Opioid Receptor

- Function. *Neuropsychopharmacology* **2018**, *43* (13), 2514–2520.
- (28) Hanlon, C. D.; Andrew, D. J. Outside-in Signaling - a Brief Review of GPCR Signaling with a Focus on the Drosophila GPCR Family. *J. Cell Sci.* **2015**, *128* (19), 3533–3542.
- (29) Kroeze, W. K.; Sheffler, D. J.; Roth, B. L. G-Protein-Coupled Receptors at a Glance. *J. Cell Sci.* **2003**, *116* (24), 4867–4869.
- (30) Katritch, V.; Cherezov, V.; Stevens, R. C. Structure-Function of the G Protein-Coupled Receptor Superfamily. *Annu. Rev. Pharmacol. Toxicol.* **2013**, *53*, 531–556.
- (31) Erlandson, S. C.; McMahon, C.; Kruse, A. C. Structural Basis for G Protein-Coupled Receptor Signaling. *Annu. Rev. Biophys.* **2018**, *47* (1), 1–18.
- (32) Weis, W. I.; Kobilka, B. K. The Molecular Basis of G Protein-Coupled Receptor Activation. *Annu. Rev. Biochem.* **2018**, *87* (1), 897–919.
- (33) Aldrich, J. V.; McLaughlin, J. P. Opioid Peptides: Potential for Drug Development. *Drug Discov. Today Technol.* **2012**, *9* (1), e23–e31.
- (34) Chavkin, C. The Therapeutic Potential of κ -Opioids for Treatment of Pain and Addiction. *Neuropsychopharmacol. Rev.* **2011**, *36* (1), 369–370.
- (35) Janecka, A.; Perlikowska, R.; Gach, K.; Wyrebska, A.; Fichna, J. Development of Opioid Peptide Analogs for Pain Relief. *Curr. Pharm. Des.* **2010**, *16* (9), 1126–1135.
- (36) Chavkin, C.; Koob, G. F. Dynorphin, Dysphoria, and Dependence: The Stress of Addiction. *Neuropsychopharmacol. Rev.* **2016**, *41* (1), 373–374.
- (37) Lalanne, L.; Ayranci, G.; Kieffer, B. L.; Lutz, P.-E. The Kappa Opioid Receptor: From Addiction to Depression, and Back. *Front. Psychiatry* **2014**, *5*, 170.
- (38) Lutz, P. E.; Kieffer, B. L. Opioid Receptors: Distinct Roles in Mood Disorders. *Trends Neurosci.* **2013**, *36* (3), 195–206.
- (39) Le Merrer, J.; Becker, J. A. J.; Befort, K.; Kieffer, B. L. Reward Processing by the Opioid System in the Brain. *Physiol Rev* **2009**, *89*, 1379–1412.
- (40) Santiago, T. V.; Edelman, N. H. Opioids and Breathing. *J. Appl. Physiol.* **1985**, *59* (6), 1675–1685.
- (41) Boom, M.; Niesters, M.; Sarton, E.; Aarts, L.; Smith, T. W.; Dahan, A. Non-Analgesic Effects of Opioids: Opioid-Induced Respiratory Depression. *Curr. Pharm. Des.* **2012**, *18* (37), 5994–6004.
- (42) Holzer, P. Opioid Receptors in the Gastrointestinal Tract. *Regul. Pept.* **2009**, *155*, 11–17.
- (43) Camilleri, M.; Lembo, A.; Katzka, D. A. Opioids in Gastroenterology: Treating Adverse Effects and Creating Therapeutic Benefits. *Clin. Gastroenterol. Hepatol.*

2017, 15 (9), 1338–1349.

- (44) Bueno, L.; Fioramonti, J. Action of Opiates on Gastrointestinal Function. In *Bailliere's Clinical Gastroenterology*; 1988; Vol. 2, pp 123–139.
- (45) Kieffer, B. L. Recent Advances in Molecular Recognition and Signal Transduction of Active Peptides: Receptors for Opioid Peptides. *Cell. Mol. Neurobiol.* **1995**, 15 (6), 615–635.
- (46) Hughes, J.; Smith, T. W.; Kosterlitz, H. W.; Fothergill, L. A.; Morgan, B. A.; Morris, H. R. Identification of Two Related Pentapeptides from the Brain with Potent Opiate Agonist Activity. *Nature* **1975**, 258 (5536), 577–579.
- (47) Schiller, P. W. Bi- or Multifunctional Opioid Peptide Drugs. *Life Sci.* **2010**, 86, 598–603.
- (48) Egleton, R. D.; Witt, K. A.; Davis, T. P. Opioid Peptides. In *Handbook of Biologically Active Peptides (Second Edition)*; Elsevier Inc., 2016; pp 1783–1810.
- (49) Gu, Z. H.; Wang, B.; Kou, Z. Z.; Bai, Y.; Chen, T.; Dong, Y. L.; Li, H.; Li, Y. Q. Endomorphins: Promising Endogenous Opioid Peptides for the Development of Novel Analgesics. *NeuroSignals* **2018**, 25 (1), 98–116.
- (50) Handa, B. K.; Lane, A. C.; Lord, J. A. H.; Morgan, B. A.; Rance, M. J.; Smith, C. F. C. Analogues of β -LPH61-64 Possessing Selective Agonist Activity at μ -Opiate Receptors. *Eur. J. Pharmacol.* **1981**, 70 (4), 531–540.
- (51) Lahti, R. A.; Mickelson, M. M.; McCall, J. M.; Von Voigtlander, P. F. [3H]U-69593 a Highly Selective Ligand for the Opioid κ Receptor. *Eur. J. Pharmacol.* **1985**, 109 (2), 281–284.
- (52) Mosberg, H. I.; Yeomans, L.; Harland, A. A.; Bender, A. M.; Sobczyk-Kojiro, K.; Anand, J. P.; Clark, M. J.; Jutkiewicz, E. M.; Traynor, J. R. Opioid Peptidomimetics: Leads for the Design of Bioavailable Mixed Efficacy Mu Opioid Receptor (MOR) Agonist/Delta Opioid Receptor (DOR) Antagonist Ligands. *J. Med. Chem.* **2013**, 56, 2139–2149.
- (53) Dietis, N.; Guerrini, R.; Calo, G.; Salvadori, S.; Rowbotham, D. J.; Lambert, D. G. Simultaneous Targeting of Multiple Opioid Receptors: A Strategy to Improve Side-Effect Profile. *Br. J. Anaesth.* **2009**, 103 (1), 38–49.
- (54) Turnaturi, R.; Arico, G.; Ronsisvalle, G.; Parenti, C.; Pasquinucci, L. Multitarget Opioid Ligands in Pain Relief: New Players in an Old Game. *Eur. J. Med. Chem.* **2016**, 108, 211–228.
- (55) Anand, J. P.; Montgomery, D. Multifunctional Opioid Ligands. *Handb. Exp. Pharmacol.* **2018**, 247, 21–51.
- (56) Salvadori, S.; Attila, M.; Balboni, G.; Bianchi, C.; Bryant, S. D.; Crescenzi, O.; Guerrini, R.; Picone, D.; Tancredi, T.; Temussi, P. A.; et al. Delta Opioidmimetic Antagonists: Prototypes for Designing a New Generation of Ultraselective Opioid Peptides. *Mol. Med.* **1995**, 1 (6), 678–689.

- (57) Sagan, S.; Amiche, M.; Delfour, A.; Camus, A.; Mor, A.; Nicolas, P. Differential Contribution of C-Terminal Regions of Dermorphin and Dermenkephalin to Opioid-Sites Selection and Binding Potency. *Biochem. Biophys. Res. Commun.* **1989**, *163* (2), 726–732.
- (58) Sagan, S.; Amiche, M.; Delfour, A.; Mor, A.; Camus, A.; Nicolas, P. Molecular Determinants of Receptor Affinity and Selectivity of the Natural Delta-Opioid Agonist, Dermenkephalin. *J. Biol. Chem.* **1989**, *264* (29), 17100–17106.
- (59) Melchiorri, P.; Negri, L.; Falconieri-Erspamer, G.; Severini, C.; Corsi, R.; Soaje, M.; Erspamer, V.; Barra, D. Structure-Activity Relationships of the Delta-Opioid-Selective Agonists, Deltorphins. *Eur. J. Neurosci.* **1991**, *195*, 201–207.
- (60) Schiller, P. W.; Nguyen, T. M.-D.; Weltrowska, G.; Wilkes, B. C.; Marsden, B. J.; Lemieux, C.; Chung, N. N. Differential Stereochemical Requirements of Mu vs. Delta Opioid Receptors for Ligand Binding and Signal Transduction: Development of a Class of Potent and Highly Delta-Selective Peptide Antagonists. *Proc. Natl. Acad. Sci.* **1992**, *89*, 11871–11875.
- (61) Schiller, P. W.; Weltrowska, G.; Nguyen, T. M.-D.; Wilkes, B. C.; Chung, N. N.; Lemieux, C. TIPP[ψ]: A Highly Potent and Stable Pseudopeptide δ Opioid Receptor Antagonist with Extraordinary δ Selectivity. *J. Med. Chem.* **1993**, *36* (21), 3182–3187.
- (62) Temussi, P. A.; Salvadori, S.; Amodeo, P.; Bianchi, C.; Guerrini, R.; Tomatis, R.; Lazarus, L. H.; Picone, D.; Tancredi, T. Selective Opioid Dipeptides. *Biochem. Biophys. Res. Commun.* **1994**, *198* (3), 933–939.
- (63) Capasso, A.; Guerrini, R.; Balboni, G.; Sorrentino, L.; Temussi, P.; Lazarus, L. H.; Bryant, S. D.; Salvadori, S. DMT-TIC-OH, A Highly Selective and Potent Delta-Opioid Dipeptide Receptor Antagonist After Systemic Administration in the Mouse. *Pharmacol. Lett.* **1996**, *59* (8), PL 93-98.
- (64) Salvadori, S.; Balboni, G.; Guerrini, R.; Tomatis, R.; Bianchi, C.; Bryant, S. D.; Cooper, P. S.; Lazarus, L. H. Evolution of the Dmt-Tic Pharmacophore: N-Terminal Methylated Derivatives with Extraordinary Delta Opioid Antagonist Activity. *J. Med. Chem.* **1997**, *40* (19), 3100–3108.
- (65) Bryant, S. D.; Salvadori, S.; Cooper, P. S.; Lazarus, L. H. New Delta-Opioid Antagonists as Pharmacological Probes. *Trends Pharmacol. Sci.* **1998**, *19* (2), 42–46.
- (66) Pagé, D.; McClory, A.; Mischki, T.; Schmidt, R.; Butterworth, J.; St-Onge, S.; Labarre, M.; Payza, K.; Brown, W. Novel Dmt-Tic Dipeptide Analogues as Selective Delta-Opioid Receptor Antagonists. *Bioorganic Med. Chem. Lett.* **2000**, *10* (2), 167–170.
- (67) Balboni, G.; Fiorini, S.; Baldisserotto, A.; Trapella, C.; Sasaki, Y.; Ambo, A.; Marczak, E. D.; Lazarus, L. H.; Salvadori, S. Further Studies on Lead Compounds Containing the Opioid Pharmacophore Dmt-Tic. *J. Med. Chem.* **2008**, *51* (16), 5109–5117.

- (68) Labarre, M.; Butterworth, J.; St-Onge, S.; Payza, K.; Schmidhammer, H.; Salvadori, S.; Balboni, G.; Guerrini, R.; Bryant, S. D.; Lazarus, L. H. Inverse Agonism by Dmt-Tic Analogues and HS 378, a Naltrindole Analogue. *Eur. J. Pharmacol.* **2000**, *406* (1), 4–6.
- (69) Pagé, D.; Nguyen, N.; Bernard, S.; Coupal, M.; Gosselin, M.; Lepage, J.; Adam, L.; Brown, W. New Scaffolds in the Development of Mu Opioid-Receptor Ligands. *Bioorganic Med. Chem. Lett.* **2003**, *13* (9), 1585–1589.
- (70) Balboni, G.; Guerrini, R.; Salvadori, S.; Bianchi, C.; Rizzi, D.; Bryant, S. D.; Lazarus, L. H. Evaluation of the Dmt-Tic Pharmacophore: Conversion of a Potent Delta-Opioid Receptor Antagonist into a Potent Delta Agonist and Ligands with Mixed Properties. *J. Med. Chem.* **2002**, *45* (3), 713–720.
- (71) Salvadori, S.; Trapella, C.; Fiorini, S.; Negri, L.; Lattanzi, R.; Bryant, S. D.; Jinsmaa, Y.; Lazarus, L. H.; Balboni, G. A New Opioid Designed Multiple Ligand Derived from the μ Opioid Agonist Endomorphin-2 and the δ Opioid Antagonist Pharmacophore Dmt-Tic. *Bioorganic Med. Chem.* **2007**, *15* (22), 6876–6881.
- (72) Balboni, G.; Salvadori, S.; Marczak, E. D.; Knapp, B. I.; Bidlack, J. M.; Lazarus, L. H.; Peng, X.; Si, Y. G.; Neumeyer, J. L. Opioid Bifunctional Ligands from Morphine and the Opioid Pharmacophore Dmt-Tic. *Eur. J. Med. Chem.* **2011**, *46* (2), 799–803.
- (73) Balboni, G.; Salvadori, S.; Trapella, C.; Knapp, B. I.; Bidlack, J. M.; Lazarus, L. H.; Peng, X.; Neumeyer, J. L. Evolution of the Bifunctional Lead Mu Agonist/Delta Antagonist Containing the 2',6'-Dimethyl-L-Tyrosine-1,2,3,4-Tetrahydroisoquinoline-3-Carboxylic Acid (Dmt-Tic) Opioid Pharmacophore. *ACS Chem. Neurosci.* **2010**, *1* (2), 155–164.
- (74) Santagada, V.; Balboni, G.; Caliendo, G.; Guerrini, R.; Salvadori, S.; Bianchi, C.; Bryant, S. D.; Lazarus, L. H. Assessment of Substitution in the Second Pharmacophore of Dmt-Tic Analogues. *Bioorg. Med. Chem. Lett.* **2000**, *10* (24), 2745–2748.
- (75) Balboni, G.; Salvadori, S.; Guerrini, R.; Negri, L.; Giannini, E.; Bryant, S. D.; Jinsmaa, Y.; Lazarus, L. H. Direct Influence of C-Terminally Substituted Amino Acids in the Dmt-Tic Pharmacophore on Delta-Opioid Receptor Selectivity and Antagonism. *J. Med. Chem.* **2004**, *47* (16), 4066–4071.
- (76) Pagé, D.; Naismith, A.; Schmidt, R.; Coupal, M.; Labarre, M.; Gosselin, M.; Bellemare, D.; Payza, K.; Brown, W. Novel C-Terminus Modifications of the Dmt-Tic Motif: A New Class of Dipeptide Analogues Showing Altered Pharmacological Profiles toward the Opioid Receptors. *J. Med. Chem.* **2001**, *44* (15), 2387–2390.
- (77) Pogozeva, I. D.; Lomize, A. L.; Mosberg, H. I. Opioid Receptor Three-Dimensional Structures from Distance Geometry Calculations with Hydrogen Bonding Constraints. *Biophys. J.* **1998**, *75* (2), 612–634.
- (78) Fowler, C. B.; Pogozeva, I. D.; LeVine, H.; Mosberg, H. I. Refinement of a Homology Model of the μ -Opioid Receptor Using Distance Constraints from

- Intrinsic and Engineered Zinc-Binding Sites. *Biochemistry* **2004**, *43* (27), 8700–8710.
- (79) Anand, J. P.; Porter-Barrus, V. R.; Waldschmidt, H. V.; Yeomans, L.; Pogozheva, I. D.; Traynor, J. R.; Mosberg, H. I. Translation of Structure-Activity Relationships from Cyclic Mixed Efficacy Opioid Peptides to Linear Analogues. *Biopolym. Pept. Sci.* **2014**, *102* (1), 107–114.
- (80) Harland, A. A.; Bender, A. M.; Griggs, N. W.; Gao, C.; Anand, J. P.; Pogozheva, I. D.; Traynor, J. R.; Jutkiewicz, E. M.; Mosberg, H. I. Effects of N-Substitutions on the Tetrahydroquinoline (THQ) Core of Mixed-Efficacy μ -Opioid Receptor (MOR)/ δ -Opioid Receptor (DOR) Ligands. *J. Med. Chem.* **2016**, *59* (10), 4985–4998.
- (81) Bowen, C. A.; Stevens Negus, S.; Zong, R.; Neumeyer, J. L.; Bidlack, J. M.; Mello, N. K. Effects of Mixed-Action Kappa/Mu Opioids on Cocaine Self-Administration and Cocaine Discrimination by Rhesus Monkeys. *Neuropsychopharmacology* **2003**, *28*, 1125–1139.
- (82) Neumeyer, J. L.; Bidlack, J. M.; Zong, R.; Bakthavachalam, V.; Gao, P.; Cohen, D. J.; Negus, S. S.; Mello, N. K. Synthesis and Opioid Receptor Affinity of Morphinan and Benzomorphan Derivatives: Mixed Kappa Agonists and Mu Agonists/Antagonists as Potential Pharmacotherapeutics for Cocaine Dependence. *J. Med. Chem.* **2000**, *43* (1), 114–122.
- (83) Neumeyer, J. L.; Zhang, A.; Xiong, W.; Gu, X.-H.; Hilbert, J. E.; Knapp, B. I.; Negus, S. S.; Mello, N. K.; Bidlack, J. M. Design and Synthesis of Novel Dimeric Morphinan Ligands for Kappa and Mu Opioid Receptors. *J. Med. Chem.* **2003**, *46* (24), 5162–5170.
- (84) Mello, N. K.; Negus, S. S. Effects of Kappa Opioid Agonists on Cocaine- and Food-Maintained Responding by Rhesus Monkeys. *J. Pharmacol. Exp. Ther.* **1998**, *286* (2), 812–824.
- (85) Negus, S. S.; Mello, N. K.; Portoghese, P. S.; Lin, C. Effects of Kappa Opioids on Cocaine Self-Administration by Rhesus Monkeys. *J. Pharmacol. Exp. Ther.* **1997**, *282* (1), 44–55.
- (86) Zhang, A.; Xiong, W.; Bidlack, J. M.; Hilbert, J. E.; Knapp, B. I.; Wentland, M. P.; Neumeyer, J. L. 10-Ketomorphinan and 3-Substituted-3-Desoxymorphinan Analogues as Mixed Kappa and Mu Opioid Ligands: Synthesis and Biological Evaluation of Their Binding Affinity at Opioid Receptors. *J. Med. Chem.* **2004**, *47* (1), 165–174.
- (87) Bidlack, J. M.; Knapp, B. I. Chapter 14: Mixed Mu/Kappa Opioid Agonists. In *Research and Development of Opioid-Related Ligands*; 2013.
- (88) Bidlack, J. Mixed Kappa/Mu Partial Opioid Agonists as Potential Treatments for Cocaine Dependence. In *Advances in Pharmacology*; Elsevier Inc., 2014; Vol. 69, pp 387–418.

- (89) Abdelhamid, E. E.; Sultana, M.; Portoghese, P. S.; Takemori, A. E. Selective Blockage of the Delta Opioid Receptors Prevents the Development of Morphine Tolerance and Dependence in Mice. *J. Pharmacol. Exp. Ther.* **1991**, *258* (1), 299–301.
- (90) Fundytus, M. E.; Schiller, P. W.; Shapiro, M.; Weltrowska, G.; Coderre, T. J. Attenuation of Morphine Tolerance and Dependence with the Highly Selective Delta-Opioid Receptor Antagonist TIPP[ψ]. *Eur. J. Pharmacol.* **1995**, *286* (1), 105–108.
- (91) Schiller, P. W.; Fundytus, M. E.; Merovitz, L.; Weltrowska, G.; Nguyen, T. M.-D.; Lemieux, C.; Chung, N. N.; Coderre, T. J. The Opioid Mu Agonist/Delta Antagonist DIPP-NH₂[ψ] Produces a Potent Analgesic Effect, No Physical Dependence and Less Tolerance than Morphine in Rats. *J. Med. Chem.* **1999**, *42* (18), 3520–3526.
- (92) Hepburn, M. J.; Little, P. J.; Gringas, J.; Khun, C. M. Differential Effects of Naltrindole on Morphine-Induced Tolerance and Physical Dependence in Rats. *J. Pharmacol. Exp. Ther.* **1997**, *281* (3), 1350–1356.
- (93) Shippenberg, T. S.; Chefer, V. I.; Thompson, A. C. Delta-Opioid Receptor Antagonists Prevent Sensitization to the Conditioned Rewarding Effects of Morphine. *Biol. Psychiatry* **2009**, *65* (2), 169–174.
- (94) Mosberg, H. I.; Yeomans, L.; Anand, J. P.; Porter, V.; Sobczyk-Kojiro, K.; Traynor, J. R.; Jutkiewicz, E. M. Development of a Bioavailable μ Opioid Receptor (MOPr) Agonist, δ Opioid Receptor (DOPr) Antagonist Peptide That Evokes Antinociception without Development of Acute Tolerance. *J. Med. Chem.* **2014**, *57* (7), 3148–3153.
- (95) Anand, J. P.; Kochan, K. E.; Nastase, A. F.; Montgomery, D.; Griggs, N. W.; Traynor, J. R.; Mosberg, H. I.; Jutkiewicz, E. M. In Vivo Effects of μ -Opioid Receptor Agonist/ δ -Opioid Receptor Antagonist Peptidomimetics Following Acute and Repeated Administration. *Br. J. Pharmacol.* **2018**, *175* (11), 2013–2027.
- (96) Mabrouk, O. S.; Viaro, R.; Volta, M.; Ledonne, A.; Mercuri, N.; Morari, M. Stimulation of Delta Opioid Receptor and Blockade of Nociceptin/Orphanin FQ Receptor Synergistically Attenuate Parkinsonism. *J. Neurosci.* **2014**, *34* (39), 12953–12962.
- (97) Dripps, I. J.; Jutkiewicz, E. M. Delta Opioid Receptors and Modulation of Mood and Emotion. *Handb. Exp. Pharmacol.* **2017**, *247*, 179–197.
- (98) Rozenfeld, R.; Abul-Husn, N. S.; Gomes, I.; Devi, L. A. An Emerging Role for the Delta Opioid Receptor in the Regulation of Mu Opioid Receptor Function. *Sci. World J.* **2007**, *7* (S2), 64–73.
- (99) Martin, T. J.; Kim, S. A.; Cannon, D. G.; Sizemore, G. M.; Bian, D.; Porreca, F.; Smith, J. E. Antagonism of Delta(2) Opioid Receptors by Naltrindole-5'-Isothiocyanate Attenuates Heroin Self-Administration but Not Antinociception in Rats. *J. Pharmacol. Exp. Ther.* **2000**, *294* (3), 975–982.

- (100) Dick, G. R.; Woerly, E. M.; Burke, M. D. A General Solution for the 2-Pyridyl Problem. *Angew. Chemie Int. Ed.* **2012**, *51* (11), 2667–2672.
- (101) Henry, S. P.; Fernandez, T. J.; Anand, J. P.; Griggs, N. W.; Traynor, J. R.; Mosberg, H. I. Structural Simplification of a Tetrahydroquinoline-Core Peptidomimetic μ -Opioid Receptor (MOR) Agonist/ δ -Opioid Receptor (DOR) Antagonist Produces Improved Metabolic Stability. *J. Med. Chem.* **2019**, *62* (8), 4142–4157.
- (102) Nastase, A. F.; Griggs, N. W.; Anand, J. P.; Fernandez, T. J.; Harland, A. A.; Trask, T. J.; Jutkiewicz, E. M.; Traynor, J. R.; Mosberg, H. I. Synthesis and Pharmacological Evaluation of Novel C-8 Substituted Tetrahydroquinolines as Balanced-Affinity Mu/Delta Opioid Ligands for the Treatment of Pain. *ACS Chem. Neurosci.* **2018**, *9* (7), 1840–1848.
- (103) Bryant, S. D.; Jinsmaa, Y.; Salvadori, S.; Okada, Y.; Lazarus, L. H. Dmt and Opioid Peptides: A Potent Alliance. *Biopolym. (Peptide Sci.)* **2003**, *71*, 86–102.
- (104) Salvadori, S.; Guerrini, R.; Balboni, G.; Bianchi, C.; Bryant, S. D.; Cooper, P. S.; Lazarus, L. H. Further Studies on the Dmt-Tic Pharmacophore: Hydrophobic Substituents at the C-Terminus Endow Delta Antagonists to Manifest Mu Agonism or Mu Antagonism. *J. Med. Chem.* **1999**, *42* (24), 5010–5019.
- (105) Oleson, E. B.; Roberts, D. C. S. Cocaine Self-Administration in Rats: Threshold Procedures. In *Psychiatric Disorders*; 2012; Vol. 829, pp 303–319.
- (106) Panlilio, L. V.; Goldberg, S. R. Self-Administration of Drugs in Animals and Humans as a Model and an Investigative Tool. *Addiction* **2007**, *102* (12), 1863–1870.
- (107) Anderson, K. G.; Van Haaren, F. Cocaine Discrimination and Time-Course Effects in Male and Female Wistar Rats. *Eur. J. Pharmacol.* **1999**, *382* (2), 69–74.
- (108) Cunningham, C. L.; Gremel, C. M.; Groblewski, P. A. Drug-Induced Conditioned Place Preference and Aversion in Mice. *Nat. Protoc.* **2006**, *1* (4), 1662–1670.
- (109) Huston, J. P.; de Souza Silva, M. A.; Topic, B.; Müller, C. P. What's Conditioned in Conditioned Place Preference? *Trends Pharmacol. Sci.* **2013**, *34* (3), 162–166.
- (110) Bardo, M. T.; Horton, D. B.; Yates, J. R. Conditioned Place Preference as a Preclinical Model for Screening Pharmacotherapies for Drug Abuse. In *Nonclinical Assessment of Abuse Potential for New Pharmaceuticals*; Elsevier Inc., 2015; pp 151–196.
- (111) Mulder, G. B.; Pritchett, K. Rodent Analgesiometry: The Hot Plate, Tail Flick and Von Frey Hairs. *Contemp. Top. Lab. Anim. Sci.* **2004**, *43* (3), 54–55.
- (112) Montgomery, D.; Anand, J. P.; Griggs, N. W.; Fernandez, T. J.; Hartman, J. G.; Sánchez-Santiago, A. A.; Pogozheva, I. D.; Traynor, J. R.; Mosberg, H. I. Novel Dimethyltyrosine–Tetrahydroisoquinoline Peptidomimetics with Aromatic Tetrahydroisoquinoline Substitutions Show in Vitro Kappa and Mu Opioid Receptor Agonism. *ACS Chem. Neurosci.* **2019**, DOI:

10.1021/acscchemneuro.9b00250.

- (113) Traynor, J. R.; Nahorski, S. R. Modulation by Mu-Opioid Agonists of Guanosine-5'-O-(3-[35S]Thio)Triphosphate Binding to Membranes from Human Neuroblastoma SH-SY5Y Cells. *Mol. Pharmacol.* **1995**, *47* (4), 848–854.
- (114) Lee, K. O.; Akil, H.; Woods, J. H.; Traynor, J. R. Differential Binding Properties of Oripavines at Cloned Mu- and Delta-Opioid Receptors. *Eur. J. Pharmacol.* **1999**, *378* (3), 323–330.
- (115) Harrison, C.; Traynor, J. R. The [35S]GTPgammaS Binding Assay: Approaches and Applications in Pharmacology. *Life Sci.* **2003**, *74* (4), 489–508.
- (116) Pogozeva, I. D.; Przydzial, M. J.; Mosberg, H. I. Homology Modeling of Opioid Receptor-Ligand Complexes Using Experimental Constraints. *AAPS J.* **2005**, *7* (2), E434-448.